



AN ANALYSIS OF DERIVATIVE PRICES IN THE  
NORDIC POWER MARKET

A DISSERTATION SUBMITTED FOR THE DEGREE OF  
DR. OECON  
AT  
NORWEGIAN SCHOOL OF ECONOMICS AND  
BUSINESS ADMINISTRATION  
BERGEN, NORWAY

FRIDTHJOF OLLMAR  
SEPTEMBER 2003

## Acknowledgements

This work could not have been completed without the support and help from a number of people.

First of all I would like to thank my advisor Professor Jostein Lillestøl who has been very helpful and supporting. I would also like to thank the other two members of my doctoral committee; Professor Gunnar Stensland and Professor Dag Tjøstheim. A thank also go to my colleagues at NHH and my new colleagues at Skagerak Kraft. It has been instructive and motivating to work together with Steen Koekebakker and Arne-Christian Lund.

The financial support from Skagerak Kraft and the Department of Finance and Management Science at the Norwegian School of Economics and Business Administration have been crucial for carrying out the research that is the foundation for this thesis and are gratefully acknowledged.

Last but not least, I would like to thank my family and friends for their support.

Porsgrunn, September 2003

Fridthjof Ollmar



# Contents

<b>Overview</b>	<b>1</b>
Smooth forward price curves in electricity markets . . . . .	1
Forward curve dynamics in the Nordic electricity market . . . . .	2
Analyzing flexible load contracts . . . . .	2
Empirical study of the risk premium in an electricity market . . . . .	4
<b>Smooth forward price curves in electricity markets</b>	<b>7</b>
<b>Introduction</b>	<b>8</b>
<b>Market description</b>	<b>9</b>
<b>Constructing a smooth forward curve</b>	<b>9</b>
3.1 Notation . . . . .	9
3.2 Basic model . . . . .	10
3.3 Extended model . . . . .	13
<b>Numerical examples</b>	<b>15</b>
4.1 Short example . . . . .	15
4.2 Extended example . . . . .	18
4.3 Example from Nord Pool . . . . .	20
<b>Concluding remarks</b>	<b>23</b>
<b>Finding the smoothest function</b>	<b>26</b>
<b>Construction of <math>A</math> and <math>B</math> matrices</b>	<b>30</b>

<b>Forward curve dynamics in the Nordic electricity market</b>	<b>33</b>
<b>Introduction</b>	<b>34</b>
<b>The Nordic electricity market</b>	<b>37</b>
2.1 History of the Nordic Power Exchange . . . . .	37
2.2 The physical market . . . . .	37
2.3 The financial market . . . . .	38
<b>Multi-factor forward curve models</b>	<b>39</b>
<b>Descriptive analysis and data preparation</b>	<b>41</b>
4.1 Smoothed data . . . . .	42
4.2 Constructing a data set . . . . .	45
<b>Principal component analysis and volatility functions</b>	<b>48</b>
<b>Empirical results</b>	<b>52</b>
<b>Conclusions</b>	<b>58</b>
<b>Tables and figures</b>	<b>64</b>
<b>Analyzing flexible load contracts</b>	<b>67</b>
<b>Introduction</b>	<b>68</b>
<b>Mathematical formulation of the FLC</b>	<b>72</b>
2.1 FLC as an optimization problem . . . . .	72
2.2 Further observations . . . . .	73
2.3 Precise formulation . . . . .	75
2.4 The Hamilton Jacobi Bellman equation . . . . .	75
<b>Modelling the spot price</b>	<b>78</b>
3.1 Examining the spot price . . . . .	78

3.2	Selecting a model . . . . .	82
3.3	Parameter estimation method . . . . .	85
	<b>Numerical solution</b>	<b>88</b>
4.1	Discretization . . . . .	88
4.2	The numerical scheme . . . . .	90
4.3	The boundaries of the price space . . . . .	93
	4.3.1 Absorption . . . . .	94
	4.3.2 Reflection . . . . .	95
4.4	Implementation of the scheme . . . . .	96
4.5	The control matrix . . . . .	97
4.6	Deterministic test . . . . .	99
4.7	Remarks . . . . .	100
	<b>Data and estimation</b>	<b>101</b>
5.1	Price data . . . . .	101
5.2	FLC data . . . . .	102
5.3	Parameter estimation . . . . .	103
	<b>Results</b>	<b>108</b>
6.1	Results from the case . . . . .	108
	6.1.1 Results 1997-2002 . . . . .	110
	6.1.2 A closer look . . . . .	114
6.2	Analyzing properties of a FLC . . . . .	114
	6.2.1 Pricing . . . . .	115
	6.2.2 Flexibility . . . . .	116
	6.2.3 Sensitivity to the spot volatility and mean reversion . .	117
	6.2.4 Time between updates of the exercise program . . . . .	117
	<b>Concluding remarks</b>	<b>119</b>

<b>Empirical study of the risk premium in an electricity market</b>	<b>133</b>
<b>Introduction</b>	<b>134</b>
<b>The model</b>	<b>135</b>
<b>Estimation</b>	<b>137</b>
3.1 Discrete approximations . . . . .	138
3.2 The estimator . . . . .	139
3.3 Simulated example . . . . .	144
3.4 Data . . . . .	147
<b>Empirical results</b>	<b>149</b>
4.1 Functions of $\tau$ . . . . .	149
4.2 Functions of $\tau$ and $F$ . . . . .	156
4.3 Functions of $\tau$ and $\delta$ . . . . .	159
4.4 Functions of $\tau$ and $\kappa$ . . . . .	159
<b>Concluding remarks</b>	<b>163</b>
<b>Appendix</b>	<b>167</b>

# List of Tables

<b>Smooth forward price curves in electricity markets</b>	<b>7</b>
I    Input parameters, extended example. . . . .	18
II   Information about each iteration. . . . .	19
III  Input parameters, Nord Pool example. . . . .	21
<b>Forward curve dynamics in the Nordic electricity market</b>	<b>33</b>
I    Descriptive statistics for electricity forward prices and returns.	44
II   Descriptive statistics of daily forward price returns from the smoothed term structure. . . . .	49
III  Principal component analysis of forward price returns. . . . .	53
IV   Most important factors across maturities for price returns . . . .	64
V    Principal component analysis of forward price returns. . . . .	65
<b>Analyzing flexible load contracts</b>	<b>67</b>
I    Deterministic test of the algorithm . . . . .	99
II   Descriptive statistics . . . . .	106
III  Estimated parameters . . . . .	107
IV   Value of exercised FLC (Summer-1997) . . . . .	109
V    Results for the period 1997 - 2001 . . . . .	113
VI   Effect of time between policy-updates, I . . . . .	118
VII  Effect of time between policy-updates, II . . . . .	118
<b>Empirical study of the risk premium in an electricity market</b>	<b>133</b>
I    Sample of the contract-data . . . . .	148





# List of Figures

<b>Smooth forward price curves in electricity markets</b>	<b>7</b>
1 Splitting of overlapping forward contracts. . . . .	10
2 The smoothed forward curve from the short example. . . . .	17
3 The smoothed forward curve from the extended example. . . . .	19
4 The smoothed forward curves from Nord Pool. . . . .	23
<b>Forward curve dynamics in the Nordic electricity market</b>	<b>33</b>
1 Power contracts and the smoothed forward curve . . . . .	43
2 Surface plots of smoothed forward curves. . . . .	46
3 Time series plots of the forward prices. . . . .	47
4 Volatility functions and overall volatility in the full sample . . .	54
5 The two first volatility functions and overall volatility. . . . .	66
<b>Analyzing flexible load contracts</b>	<b>67</b>
1 The possible values of $Q(t)$ , given the restrictions on $u_t$ . . . . .	74
2 The $(t, Q)$ projection of the parallelepiped, defining $\Omega(t)$ . . . . .	76
3 Supply and demand curves for hour 12 on 10. July 2002. . . . .	79
4 Consumption of electricity in Norway . . . . .	81
5 System price together with the hydrological balance. . . . .	82
6 The natural nodes in the $Q$ -space. . . . .	88
7 The discretization of the $(t, Q)$ -space. . . . .	89
8 The Markov chain interpretation . . . . .	93
9 The control matrix for the FLC described in the introduction. . . . .	98
10 System price . . . . .	102
11 Relationship between the $D_t$ sample and the $X_t$ sample. . . . .	104
12 Exercise policy together with a competitor's exercise program . . . . .	112
13 The value in NOK/MWh for a FLC against spotprice . . . . .	115
14 Initial value of 20 FLC's with different degrees of flexibility . . . . .	116

15	Flexible load contract: Winter 1997 . . . . .	123
16	Flexible load contract: Summer 1998 . . . . .	124
17	Flexible load contract: Winter 1998 . . . . .	125
18	Flexible load contract: Summer 1999 . . . . .	126
19	Flexible load contract: Winter 1999 . . . . .	127
20	Flexible load contract: Summer 2000 . . . . .	128
21	Flexible load contract: Winter 2000 . . . . .	129
22	Flexible load contract: Summer 2001 . . . . .	130
23	Flexible load contract: Winter 2001 . . . . .	131

**Empirical study of the risk premium in an electricity market 133**

1	Two weight functions . . . . .	141
2	Illustration of the <i>average</i> time to maturity, $\tau$ . . . . .	142
3	Simulated price data for four forward contracts. . . . .	145
4	Estimated $\mu(\tau)$ and $\sigma(\tau)$ on simulated data. . . . .	146
5	Estimated $\mu(\tau)$ on the full sample. . . . .	150
6	Estimated $\sigma(\tau)$ based on the full sample. . . . .	152
7	Estimated risk premium, $\lambda(\tau)$ , based on the full sample . . .	153
8	Estimated $\mu$ , $\sigma$ and $\lambda$ (yearly sample). . . . .	154
9	Estimated $\mu$ , $\sigma$ and $\lambda$ (seasonal sample) . . . . .	155
10	Estimated $\mu(\tau, F)$ based on full sample . . . . .	156
11	Estimated $\sigma(\tau, F)$ based on full sample . . . . .	157
12	Estimated $\lambda(\tau, F)$ based on full sample . . . . .	158
13	Estimated $\mu(\tau, \delta)$ , $\sigma(\tau, \delta)$ and $\lambda(\tau, \delta)$ . . . . .	160
14	Estimated $\mu(\tau, \kappa)$ , $\sigma(\tau, \kappa)$ and $\lambda(\tau, \kappa)$ . . . . .	162
15	Estimated $\mu(\tau, F)$ (seasonal sample) . . . . .	167
16	Estimated $\sigma(\tau, F)$ (seasonal sample) . . . . .	168
17	Estimated $\lambda(\tau, F)$ (seasonal sample) . . . . .	169
18	Estimated $\mu(\tau, F)$ (delivery seasonal sample) . . . . .	170
19	Estimated $\sigma(\tau, F)$ (delivery seasonal sample) . . . . .	171
20	Estimated $\lambda(\tau, F)$ (delivery seasonal sample) . . . . .	172

## Overview

This thesis analyzes derivative prices in the Nordic power market. The Nordic power market is chosen since it is one of the oldest and most liquid electricity markets in the world. The thesis consist of four separate papers that together analyzes the spot price, the forward price and derivatives in this market. A short resumé of each papers follows.

### **Smooth forward price curves in electricity markets**

We have in this paper derived a method for calculating a continuous forward curve from observed forward prices. The method is based on finding the smoothest possible forward curve within a bid-ask spread. We express the forward curve as a sum of a prior function and an adjustment function. The prior function can be an arbitrary function, and will typically incorporate subjective information about the forward curve. For example information from forecasts generated by “bottom-up” models. The adjustment function is a polynomial spline of order five and is used to adjust the prior function to the observed forward prices. The forward and future contracts used to construct the smoothed curve can have overlapping settlement periods.

Parameter estimation is done by solving a constrained minimization problem. This minimization problem can be solved by solving a system of linear equations. If we use bid / ask prices to construct the smoothed forward curve the algorithm iterates to find the smoothest function. As the three examples shows, the algorithm is flexible, stable and fast.

If calculation speed, continuous forward curve or closed form solution is important requirements for the forward curve model, we believe our model will be the best choice.

## **Forward curve dynamics in the Nordic electricity market**<sup>1</sup>

In this paper we conduct an exploratory investigation of the volatility dynamics in the Nordic futures and forward market in the period 1995-2001. The modelling framework is a standard lognormal spot price model similar to the one suggested by Heath, Jarrow and Morton, 1992. We use smoothed data and perform principal component analysis to reveal the factor structure of the forward price curve.

The main results are as follows: Two factors are common across all maturities. A two-factor model explains around 75% of total variation in the data. The first two factors governing the forward curve dynamics are comparable to other markets. The first factor is positive for all maturities, hence it shifts all forward prices in the same direction. The second factor causes short and long term forward prices to move in opposite directions. In contrast to other markets, more than 10 factors are needed to explain 95% of the term structure variation. Furthermore, the main sources of uncertainty affecting the movements in the long end of the forward curve, have virtually no influence on variation in the short end of the curve. We argue that this behavior may occur because electricity is a non-storable commodity. Note that the maximum maturity in our analysis is 2 years. One might suspect that contracts sold in the OTC market with maturities further into the future are even less correlated with short term contracts. These results indicate that modelling the whole forward curve has less merit in this market than others. For example, hedging long-term commitments using short-term contracts may prove disastrous.

## **Analyzing flexible load contracts**<sup>2</sup>

In this paper we have analyzed flexible load contracts by formulating the contract as a stochastic optimization problem. The value function is expressed

---

<sup>1</sup>This paper is coauthored with Steen Koekebakker.

<sup>2</sup>This paper is coauthored with Arne-Christian Lund.

as the solution of the Hamilton-Jacobi-Bellman equation in which the optimal control takes only the extreme values. By carefully examining the dynamics of the spot price in the Nordic electricity market we decided to use a time dependent mean reverting Ornstein-Uhlenbeck process. The process modelled daily, weekly and yearly price cycles. In addition it captures mean reversion due to deviations in the hydrological balance. The process has 21 parameters which was estimated from historical price data by a mixture of OLS and maximum likelihood. Estimation was conducted partly on a weekly data sample and partly on an hourly data sample. This to distinguish the short range factors from medium range factors.

To be able to solve the optimization problem we discretized the time and state space and derived an algorithm to find the value function and optimal control in each node. To dampen the effects of a truncated price space we combined absorbing and reflecting boundary conditions.

We implemented the algorithm and calculated the optimal control for the five year period 1. May 1997 to 30. April 2002. The accumulated revenue from this control was compared to the revenue for nine market participants. We find that our algorithm obtains the highest accumulated exercise revenue for this period. The model also demonstrates that it has the courage to pick many hours early if the prices are sufficiently good. This can be seen as a more risky behavior, and may be a consequence of the risk neutral assumption. Another observation is that our model seems to perform better for winter contracts than for the summer contracts. We believe the performance for the summer contracts can be improved with a more representative process.

We see several important model extensions for further research:

- The process modelling the spot price should exhibit spikes, i.e. sudden jumps. This is especially important in the European market where price spikes is common. This can be reflected in the model by introducing a nonlinear function of the OU-process. The calibration could be done with maximum likelihood as before.
- The underlying spot price process could be calibrated to the forward

and future contracts traded in the market. Since electricity is a non storable commodity, there is no clear connection between the expected future spot price and the value of these financial products. To use the financial market to predict the future spot price one first need to know the market price of risk. If this market price of risk is unknown or stochastic one may be better off calibrating the spot price partially to historical information and partial to the information from the financial market.

In our opinion this model demonstrates a great potential for utilization of contracts of this type. The methods can be developed further to improve the results even more. We stress that the methods are fully operational, and can be implemented by practitioners, for instants for benchmarking or as an aid to improve the exercise policy.

### **Empirical study of the risk premium in an electricity market**

We have in this paper conducted an explorative analysis of the risk premium in a power market. In context of our model of an electricity market the risk premium is defined as the conditional expected forward price changes pr unit risk. The discretized version of the risk premium was estimated by a Nadaraya-Watson estimator, obtaining a nonparametric estimate. We used a variable bandwidth to compensate for varying settlement period lengths in our data. The bandwidth function was heuristically defined, but as the simulation example shows, it seems to handle different lengths of settlement periods good. By organizing the data sample with respect to  $\tau$ ,  $\delta$ ,  $\kappa$  and  $F$  we estimated several versions of the risk premium. Our main findings were:

- Negative risk premium for all maturity dates (i.e. a contango market).
- Increasing volatility with increasing future price.
- Expected return is mean reverting with respect to future price in the

price range 170 NOK/MWh to 270 NOK/MWh. Outside this range the price is driven by some sort of momentum process.

- Clear seasonal patterns. The time of the year the forward is traded has a major impact on the expected return, volatility and risk premium.

We believe that the complex nature of the risk premium in the Nordic electricity market is related to the large degree of hydro-electric power production. Especially the seasonal patterns and the mean reversion properties can be linked to hydrological phenomena. Although many of our findings coincide with statements from practitioners, we can not be certain that our findings are not influenced by the estimation method. Further research should therefore focus on the estimators small and large sample properties. It would also be interesting to see if the results are changed if we extend our datasample to include the high price period that started autumn 2002.

This paper gives new insights of the forward price dynamics in the Nordic power market. Knowing the drift, volatility and thereby the risk premium, more precisely is helpful in financial engineering work. We also believe many of the results will help producers and consumers in their hedging decisions - at least it will guide the traders toward the forward contracts with the highest return / risk ration.





# Smooth forward price curves in electricity markets \*

Fridthjof Ollmar

## Abstract

In this paper we derive a method for calculating a continuous forward curve in an electricity market. Since forward and future contracts in electricity markets have settlement periods instead of settlement dates, ordinary term structure construction methods can not be used. In addition, electricity markets have strong seasonal patterns which interest rate and FX markets do not have. Our method is based on finding the smoothest possible forward curve within a bid-ask spread. The forward curve consists of a prior function and an adjustment function. The adjustment function is a polynomial spline of order 5, where the parameters are estimated by solving a constrained minimization problem. The main advantages of our method are closed form solution, handling of overlapping contracts and calculation speed.

*Key words:* Maximum smoothness, electricity market, curve fitting

---

\*I would like to thank Jørgen Haug, Arne-Christian Lund and Jostein Lillestøl for helpful comments.

# 1 Introduction

Representing forward and future prices by one continuous term structure curve is regarded as a good and an efficient way of representing market prices. A term structure curve is also required if one is to implement one of the many no-arbitrage term structure models.

Fitting a yield curve to market data in a fixed income market has been studied for many years. The seminal paper in this field was McCulloch (1971), *Measuring the Term Structure of Interest Rates*. A survey of different methods for constructing yield curves is provided in *Estimating and Interpreting the Yield Curve* by Anderson and others. The two main approaches are either to fit one function to the entire yield curve by regression or fit all observed yields by a spline. Although there remains no single definitive solution to the problem of yield curve fitting, many practitioners regard the spline-method as the better approach in a market with low liquidity.

Since forward and future contracts in an electricity market are delivered during a time interval rather than a fixed moment of time, one cannot directly apply methods used in fixed income markets. New methods for constructing term structure curves are therefore sought after. Fleten and Lemming (2003) derived a method based on optimizing a mixture of closeness to a prior function and a smoothness criteria. Although this method can be used with good results to construct a short/low-resolution forward curve, our method<sup>1</sup> focus on calculation speed and deriving a closed form solution.

---

<sup>1</sup>The approach is inspired by Adams and Deventer (1994), Forsgren (1998), Lim and Xiao (2002) and the method used by the risk management systems - Viz Risk.

## 2 Market description

By definition energy is consumed and produced continuously and not at a fixed moment of time. This difference from most other commodities is reflected in how future and forward contracts in the electricity market are designed. In addition to a *load pattern*, future and forward contracts in an electricity market consists of a start and end date for a settlement period. This is the case in the Nordic Power Exchange (Nord Pool), European Energy Exchange (EEX) and several other electricity markets. With a load pattern we mean a deterministic function of time that scale the amount delivered. In this paper we will focus on a constant load pattern, also known as “base load”. Implementing other load patterns, such as “peak-load”, into the model is possible. We will assume a constant<sup>2</sup> risk free interest rate and thereby assuming that the forward prices evolves in the same manner as future prices.

## 3 Constructing a smooth forward curve

We will first derive a simplified model for a forward function based on the last traded or a closing price. Then we will extend the model to price the forward function within a bid-ask spread.

### 3.1 Notation

Let  $\Phi = \{(T_1^s, T_1^e), (T_2^s, T_2^e), \dots, (T_m^s, T_m^e)\}$  be a list of start and end dates for the settlement period of the forward contracts. To be able to handle overlapping settlement periods we construct a new list,  $\{t_0, t_1, \dots, t_n\}$ , of dates where overlapping contracts are split into sub periods. This is illustrated in figure 1.

As we can see from figure 1 the new list is basically the elements in  $\Phi$  sorted in ascending order with any duplicated dates removed. The bid and ask price for the forward contract  $i \in \{1, \dots, m\}$  is denoted  $F_i^B$  and  $F_i^A$

---

<sup>2</sup>It is sufficient to assume a deterministic interest rate. See Cox et al. (1981)

respectively. In the simplified model we will instead use the closing price denoted by  $F_i^C$ . Next we introduce an exogenous prior function  $h(t)$ . This prior function can be interpreted as a subjective forward curve which we want to adjust according to the market price. In this paper we do not make any assumption about  $h(t)$ . Further we define the forward function as

$$f(t) = h(t) + g(t) \quad t \in [t_0, t_n]$$

where  $g(t)$  can be interpreted as an adjustment function.

### 3.2 Basic model

In this section we derive a model for a smooth forward curve based on closing prices. With “smoothness” of a function expressed as the mean square value of its second derivative, we define the smoothest possible forward curve on an interval  $[t_0, t_n]$  as one that minimizes

$$\int_{t_0}^{t_n} [g''(t)]^2 dt \quad (3.1)$$

Note that the smoothness is calculated on the adjustment function,  $g(t)$ , and not on the forward function  $f(t)$ . The reason for this is to better retain seasonal patterns. In addition to be smoothest possible we want the adjustment function to be twice continuously differentiable and horizontal at time  $t_n$ . To summarize we want the adjustment function to be:

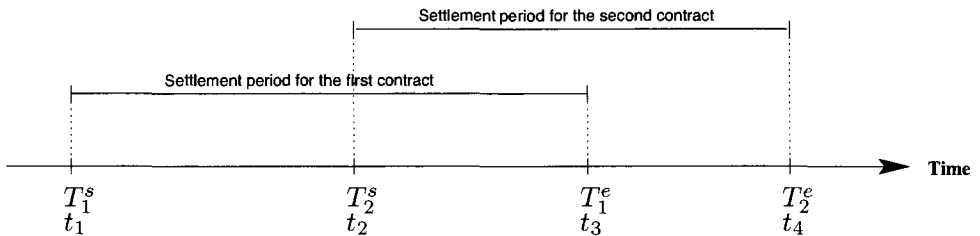


**Figure 1:** *Splitting of overlapping forward contracts.*

- Twice continuously differentiable.
- Horizontal at time  $t_n$ .
- Smoothest possible in the sense of (3.1).
- Such that the average value of the forward price function  $f(t) = g(t) + h(t)$  for contract  $i$  is equal to the closing price  $F_i^C$ .

Strictly speaking one should have that the present value of the forward price function  $f(t)$  is equal to the present value of the period based forward contracts  $F_i^C$ . We will approximate the present value with the average value. This is the same as assuming a zero interest rate. We argue that the interest rate effect is less than both the smoothing and prior function effect, and thus believe the approximation is valid. Similarly to Adam and Van Deventer and Lim and Xiao we show in Appendix A that the smoothest adjustment function with the above properties is a polynomial spline of order five. This mean that we can write the adjustment function as

$$g(t) = \begin{cases} a_1 t^4 + b_1 t^3 + c_1 t^2 + d_1 t + e_1 & t \in [t_0, t_1] \\ a_2 t^4 + b_2 t^3 + c_2 t^2 + d_2 t + e_2 & t \in [t_1, t_2] \\ \vdots & \\ a_n t^4 + b_n t^3 + c_n t^2 + d_n t + e_n & t \in [t_{n-1}, t_n] \end{cases}$$

To find the parameters,  $\mathbf{x}$ , to the adjustment function, we solve the following equality constrained convex quadratic programming problem

$$\min_{\mathbf{x}} \int_{t_0}^{t_n} [g''(t; \mathbf{x})]^2 dt \quad (3.2)$$

subject to the natural constraints in the connectivity and derivatives smoothness at the knots,  $j = 1, \dots, n - 1$ ,

$$(a_{j+1} - a_j)t_j^4 + (b_{j+1} - b_j)t_j^3 + (c_{j+1} - c_j)t_j^2 + (d_{j+1} - d_j)t_j + e_{j+1} - e_j = 0 \quad \text{C1}$$

$$4(a_{j+1} - a_j)t_j^3 + 3(b_{j+1} - b_j)t_j^2 + 2(c_{j+1} - c_j)t_j + d_{j+1} - d_j = 0 \quad \text{C2}$$

$$12(a_{j+1} - a_j)t_j^2 + 6(b_{j+1} - b_j)t_j + 2(c_{j+1} - c_j) = 0 \quad \text{C3}$$

and

$$g'(t_n; \mathbf{x}) = 0 \tag{C4}$$

$$\int_{T_i^s}^{T_i^e} e^{-rt} (g(t) + h(t)) dt = \int_{T_i^s}^{T_i^e} e^{-rt} F_i^C dt$$

for  $i = 1, \dots, m$ .  $\mathbf{x}$  is a vector of all parameters in  $g(t)$ . The last constraint ensures that the present value of the forward price function is equal to the present value of the forward contracts. We approximate this condition (by assuming  $r \approx 0$ ) with

$$F_i^C \approx \frac{1}{T_i^e - T_i^s} \int_{T_i^s}^{T_i^e} (g(t) + h(t)) dt \tag{C5}$$

This minimization problem has a total of  $3n + m - 2$  constraints. By inserting the expression for  $g''(t)$  and integrating we can write the first part of the minimization problem as

$$\min_{\mathbf{x}} \mathbf{x}^T \mathbf{H} \mathbf{x}$$

where

$$\mathbf{x}^T = [a_1 \ b_1 \ c_1 \ d_1 \ e_1 \ a_2 \ b_2 \ c_2 \ d_2 \ e_2 \ \dots \ a_n \ b_n \ c_n \ d_n \ e_n],$$

$$\mathbf{H} = \begin{bmatrix} \mathbf{h}_1 & & 0 \\ & \ddots & \\ 0 & & \mathbf{h}_n \end{bmatrix}, \quad \mathbf{h}_j = \begin{bmatrix} \frac{144}{5} \Delta_j^5 & 18 \Delta_j^4 & 8 \Delta_j^3 & 0 & 0 \\ 18 \Delta_j^4 & 12 \Delta_j^3 & 6 \Delta_j^2 & 0 & 0 \\ 8 \Delta_j^3 & 6 \Delta_j^2 & 4 \Delta_j & 0 & 0 \\ 0 & 0 & 0 & 0 & 0 \\ 0 & 0 & 0 & 0 & 0 \end{bmatrix},$$

$$\Delta_j = t_{j+1}^l - t_j^l$$

The dimensions of  $\mathbf{x}$  is  $5n \times 1$  and the dimensions of the symmetric  $\mathbf{H}$  is  $5n \times 5n$ . All the constraints in (3.2) are linear with respect to  $\mathbf{x}$ . We show in Appendix B how we can write the constraints, C1-C5, in the matrix form  $\mathbf{A}\mathbf{x} = \mathbf{B}$ , where  $\mathbf{A}$  is a  $3n+m-2 \times 5n$  matrix, and  $\mathbf{B}$  is a  $3n+m-2 \times 1$  vector. We obtain an explicit solution by the Lagrange multiplier method. Let  $\boldsymbol{\lambda}^T = [\lambda_1, \lambda_2, \dots, \lambda_{3n+m-2}]$  be the corresponding Lagrange multiplier vector to the constraints. We can now express (3.2) as the following unconstrained minimization problem

$$\min_{\mathbf{x}, \boldsymbol{\lambda}} \mathbf{x}^T \mathbf{H} \mathbf{x} + \boldsymbol{\lambda}^T (\mathbf{A}\mathbf{x} - \mathbf{B})$$

The solution  $[\mathbf{x}^*, \boldsymbol{\lambda}^*]$  is thus obtained by solving the linear equation

$$\begin{bmatrix} 2\mathbf{H} & \mathbf{A}^T \\ \mathbf{A} & \mathbf{0} \end{bmatrix} \begin{bmatrix} \mathbf{x} \\ \boldsymbol{\lambda} \end{bmatrix} = \begin{bmatrix} \mathbf{0} \\ \mathbf{B} \end{bmatrix} \quad (3.3)$$

The dimensions of the left matrix is  $8n+m-2 \times 8n+m-2$ . The solution vector and the rightmost vector have the dimensions of  $8n+m-2 \times 1$ . Numerically solving (3.3) can easily be done by using a numerical algorithm, such as Gaussian elimination, QR factorization, Cholesky factorization or Cramer's rule. Since the left matrix in (3.3) is symmetric positive definite we recommend using the faster Cholesky factorization method. If  $n$  or  $m$  is large one could improve the calculation speed further by utilizing the sparseness of the matrix.

### 3.3 Extended model

When the market is open for trading we do not observe exact prices but rather a bid-ask spread. We will now extend the previous model to handle bid-ask prices instead of fixed prices. An added feature when using bid-ask prices are that we can incorporate missing prices. This can be done by setting the missing contract's bid price as a very low value and the ask price as a very high value. By replacing constraint C5 in (3.2) with

$$\frac{1}{T_i^e - T_i^s} \int_{T_i^s}^{T_i^e} (g(t) + h(t)) dt \geq F_i^B \quad i = 1, \dots, m$$

and

$$\frac{1}{T_i^e - T_i^s} \int_{T_i^s}^{T_i^e} (g(t) + h(t)) dt \leq F_i^A \quad i = 1, \dots, m$$

we get a smooth forward function that is within the bid-ask spread. Unfortunately all of the constraints is no longer binding by equality and it is therefore not possible to use the fast and easy Lagrange multiplier method.

There exists several methods to solve this problem numerically. See Judd (1998) for a short description of some of the most commonly used algorithms.



In this paper we will use a method inspired by the “active set” approach. The strategy is to use the basic model (3.2) and change a pseudo close-price in the direction implied by the sign of the Lagrangian within the boundaries of the bid-ask spread. The algorithm is outlined as follows:

### I. Initialization

Start by solving (3.2) with a pseudo closing price,  $F_i^C = (F_i^A + F_i^B)/2$ ,  $i \in \{1, \dots, m\}$ .

### II. Start of optimization

Let the close-price-Lagrangian,  $\lambda_{3n-2}, \dots, \lambda_{3n+m-2}$ , with the largest absolute value be called  $\lambda^C$ , and adjust the pseudo closing price according to

$$F_{new}^C = \begin{cases} F^A & \text{if } \lambda^C > 0 \text{ and } \lambda^A \geq 0 \\ F^C - \frac{\lambda^C(F^A - F^C)}{\lambda^A - \lambda^C} & \text{if } \lambda^C > 0 \text{ and } \lambda^A < 0 \\ F^C - \frac{\lambda^C(F^C - F^B)}{\lambda^C - \lambda^B} & \text{if } \lambda^C < 0 \text{ and } \lambda^B > 0 \\ F^B & \text{if } \lambda^C < 0 \text{ and } \lambda^B \leq 0 \end{cases}$$

where  $\lambda^A$  denotes the contracts Lagrangian with an average price equal to the ask price  $F^A$ . Similarly  $\lambda^B$  denotes the contracts Lagrangian with the average price equal the bid price  $F^B$ .

### III. Stopping criteria

The minimization ends when one of the following two criteria are fulfilled. The first one is to stop if the following is true for each  $F_i$

- average price  $F_i^C$  is equal to  $F^B$  and  $\lambda_i^C$  is still negative or
- average price  $F_i^C$  is equal to  $F^A$  and  $\lambda_i^C$  is still positive.

This means that it is not possible to improve the smoothness by changing  $F_i^C$ . The other stopping criteria is to stop when the improvement of the smoothness is below some percentage  $\gamma$ .

$$1 - \frac{(\mathbf{x}^T \mathbf{H} \mathbf{x})_k}{(\mathbf{x}^T \mathbf{H} \mathbf{x})_{k-1}} < \gamma$$

where  $k$  is the iteration number. If neither of the stopping criteria are satisfied the algorithm continues with step II.

The main advantage of this algorithm is the calculation speed. Convergence is usually obtained in  $m$  to  $2m$  iterations. The reason for this rapid convergence is mainly due to the relative small bid-ask spread compared to the value of the adjustment function. That is a small bid-ask spread usually implies that the bid or the ask constraint is binding and thereby reducing the number of constraints with inequalities.

## 4 Numerical examples

To get a better understanding of how our model works and how we can implement it, we illustrate with three examples.

### 4.1 Short example

In this example we do not use a prior function (i.e..  $h(t) = 0$ ). We construct the forward curve from the closing prices for the following contracts,  $F^C(t, T^s, T^e)$ ,

- $F^C(0, 1, 2) = 10.00$  \$/MWh
- $F^C(0, 2, 3) = 5.00$  \$/MWh
- $F^C(0, 3, 4) = 10.00$  \$/MWh

Since the settlement periods do not overlap each other, and there are no gaps, the forward curve will consist of three polynomials ( $n = m = 3$ ). With knot points at  $t = \{1, 2, 3, 4\}$  and settlement periods at  $\Phi = \{(1, 2), (2, 3), (3, 4)\}$  we write  $\mathbf{H}$  as

$$H = \begin{bmatrix} 892.8 & 270 & 56 & 0 & 0 & 0 & 0 & 0 & 0 & 0 & 0 & 0 & 0 & 0 & 0 \\ 270 & 84 & 18 & 0 & 0 & 0 & 0 & 0 & 0 & 0 & 0 & 0 & 0 & 0 & 0 \\ 56 & 18 & 4 & 0 & 0 & 0 & 0 & 0 & 0 & 0 & 0 & 0 & 0 & 0 & 0 \\ 0 & 0 & 0 & 0 & 0 & 0 & 0 & 0 & 0 & 0 & 0 & 0 & 0 & 0 & 0 \\ 0 & 0 & 0 & 0 & 0 & 0 & 0 & 0 & 0 & 0 & 0 & 0 & 0 & 0 & 0 \\ 0 & 0 & 0 & 0 & 0 & 6076.8 & 1170 & 152 & 0 & 0 & 0 & 0 & 0 & 0 & 0 \\ 0 & 0 & 0 & 0 & 0 & 1170 & 228 & 30 & 0 & 0 & 0 & 0 & 0 & 0 & 0 \\ 0 & 0 & 0 & 0 & 0 & 152 & 30 & 4 & 0 & 0 & 0 & 0 & 0 & 0 & 0 \\ 0 & 0 & 0 & 0 & 0 & 0 & 0 & 0 & 0 & 0 & 0 & 0 & 0 & 0 & 0 \\ 0 & 0 & 0 & 0 & 0 & 0 & 0 & 0 & 0 & 0 & 0 & 0 & 0 & 0 & 0 \\ 0 & 0 & 0 & 0 & 0 & 0 & 0 & 0 & 0 & 0 & 22492.8 & 3150 & 296 & 0 & 0 \\ 0 & 0 & 0 & 0 & 0 & 0 & 0 & 0 & 0 & 0 & 3150 & 444 & 42 & 0 & 0 \\ 0 & 0 & 0 & 0 & 0 & 0 & 0 & 0 & 0 & 0 & 296 & 42 & 4 & 0 & 0 \\ 0 & 0 & 0 & 0 & 0 & 0 & 0 & 0 & 0 & 0 & 0 & 0 & 0 & 0 & 0 \\ 0 & 0 & 0 & 0 & 0 & 0 & 0 & 0 & 0 & 0 & 0 & 0 & 0 & 0 & 0 \end{bmatrix}$$

and the linear constraints  $A, B$  as

$$A^T = \begin{bmatrix} -16 & 0 & -32 & 0 & -48 & 0 & 0 & 6.20 & 0 & 0 \\ -8 & 0 & -12 & 0 & -12 & 0 & 0 & 3.75 & 0 & 0 \\ -4 & 0 & -4 & 0 & -2 & 0 & 0 & 2.33 & 0 & 0 \\ -2 & 0 & -1 & 0 & 0 & 0 & 0 & 1.50 & 0 & 0 \\ -1 & 0 & 0 & 0 & 0 & 0 & 0 & 1.00 & 0 & 0 \\ 16 & -81 & 32 & -108 & 48 & -108 & 0 & 0 & 42.20 & 0 \\ 8 & -27 & 12 & -27 & 12 & -18 & 0 & 0 & 16.25 & 0 \\ 4 & -9 & 4 & -6 & 2 & -2 & 0 & 0 & 6.33 & 0 \\ 2 & -3 & 1 & -1 & 0 & 0 & 0 & 0 & 2.50 & 0 \\ 1 & -1 & 0 & 0 & 0 & 0 & 0 & 0 & 1.00 & 0 \\ 0 & 81 & 0 & 108 & 0 & 108 & 256 & 0 & 0 & 156.20 \\ 0 & 27 & 0 & 27 & 0 & 18 & 48 & 0 & 0 & 43.75 \\ 0 & 9 & 0 & 6 & 0 & 2 & 8 & 0 & 0 & 12.33 \\ 0 & 3 & 0 & 1 & 0 & 0 & 1 & 0 & 0 & 3.50 \\ 0 & 1 & 0 & 0 & 0 & 0 & 0 & 0 & 0 & 1.00 \end{bmatrix}$$

$$B^T = [ 0 \ 0 \ 0 \ 0 \ 0 \ 0 \ 0 \ 10 \ 5 \ 10 ]$$

The construction of  $A^T$  is as follows: The two first columns ensures that  $g(t)$  is continuous at the knots and thus everywhere. Column 3 and 4 make the derivative of  $g(t)$  continuous at the knots and the next two rows makes the second derivative of  $g(t)$  continuous at the knots. Columns 7 ensures that the gradient at time  $t_n = 4$  is zero. Finally columns 8 to 10 ensures that the average value is equal to  $F^C$ .

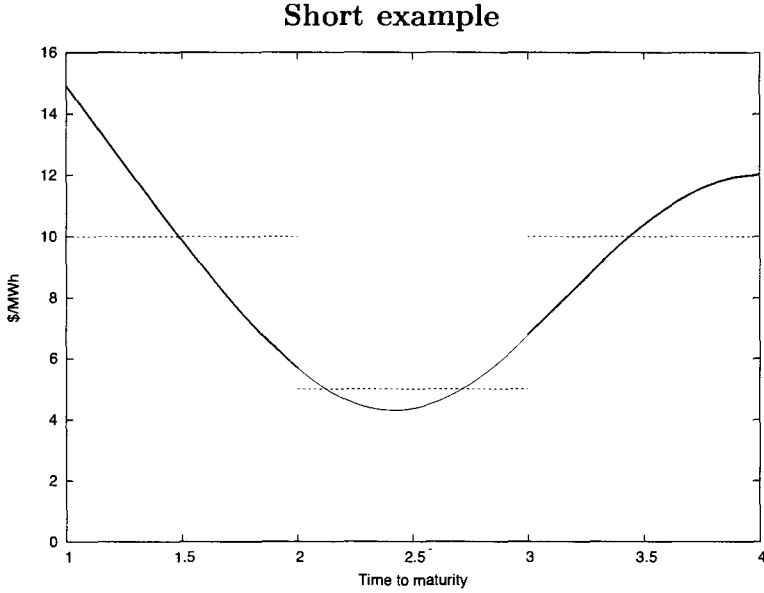


**Figure 2:** The smoothed forward curve from the short example. The forward curve consist of three polynomial functions. The closing prices are represented as horizontally lines.

With  $\mathbf{H}$ ,  $\mathbf{A}$  and  $\mathbf{B}$  we construct the set of linear equations given by (3.2). Solving the equation we get the solution  $\mathbf{x}^*, \boldsymbol{\lambda}^*$

$$\mathbf{x}^* = \begin{bmatrix} 0.987 \\ -3.949 \\ 5.924 \\ -14.168 \\ 26.118 \\ -2.536 \\ 24.237 \\ -78.636 \\ 98.578 \\ -30.255 \\ 1.549 \\ -24.780 \\ 141.943 \\ -342.579 \\ 300.613 \end{bmatrix} \quad \boldsymbol{\lambda}^* = \begin{bmatrix} -47.389 \\ 74.340 \\ 23.695 \\ 10.219 \\ 0.000 \\ 0.000 \\ 26.951 \\ -47.389 \\ 121.729 \\ -74.340 \end{bmatrix}$$

As indicated by the signs of  $\lambda_8^*$ ,  $\lambda_9^*$  and  $\lambda_{10}^*$  we can increase the smoothness by either increasing  $F^C(0, 2, 3)$  or by reducing  $F^C(0, 1, 2)$  or  $F^C(0, 3, 4)$ . Given a bid-ask spread around our fixed close prices our iterative algorithm would

have started to change  $F^C(0, 2, 3)$ . The reason for this is that this contract has the Lagrangian ( $\lambda_9^* = 121.73$ ) with the largest absolute value. But for this example, with only closing prices, the resulting smoothed forward curve is  $f(t) = g(t, \mathbf{x}^*)$  and is plotted in figure 2.

## 4.2 Extended example

In this example we construct a smooth forward curve from more realistic input parameters. For instance we use a bid-ask spread instead of a fixed closing price, and we have both missing and overlapping forward contracts. A prior function,  $h(t)$ , is also used in this example.

**Table I:** *Input parameters, extended example.*

	Bid price	Ask price
F(0, 0, 5)	200.00 NOK/MWh	205.00 NOK/MWh
F(0, 5,10)	missing	
F(0,10,12)	220.00 NOK/MWh	225.00 NOK/MWh
F(0, 0,12)	180.00 NOK/MWh	190.00 NOK/MWh

Let us assume we believe that the future expected spot price is equal to  $h(t) = 100 \cos(\frac{2\pi}{12}t) + 200$  and want to adjust it to the market prices given in table I. The time is denoted in months implying that the prior function has an annually season and a maximum at  $t = 0$ . The adjustment provided by  $g(t)$  will capture a mixture of risk premium, cost of carry and different belief about the future spot prices. The prior function we have chosen is very crude and only serves as an example. In real life one should use a function that is more able to capture seasonal patterns and long term growth.

To incorporate the missing contract into our model we introduce a contract with a low bid and a high ask. We set the bid to 100 and the ask to 200. This is approximately +/- 50 NOK from the price indicated from the one year contract and the shorter contracts. Since we have overlapping contracts we have  $t = \{0, 5, 10, 12\}$ . The first step is to calculate an initial pseudo closing

## Extended example

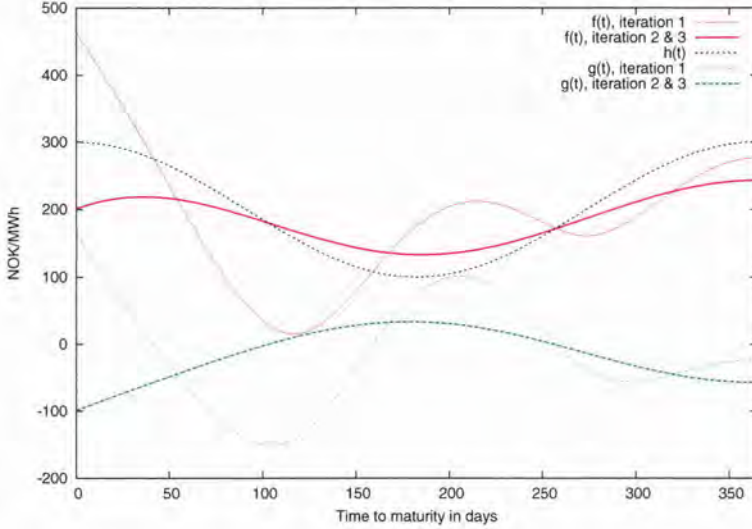


**Figure 3:** The smoothed forward curve from the extended example. The forward curve for each iteration is plotted to get an impression of the effect of the prior function and smoothness optimization.

prices and find the smoothed forward curve as described in the first example. With  $F^C = \{202.5, 150, 222.5, 185\}$  we get the following Lagrange values for the four contracts:  $\lambda_{23,24,25,26}^* = \{-0.0175, -0.0176, -0.0175, 0.0174\}$ . Since the second contract has the highest absolute Lagrange value its pseudo closing price is adjusted first. To find out how much we need to adjust the closing price we calculate  $\lambda^B$  (by solving (3.2) with  $F_2^C = F_2^B$ ). The  $\lambda^B$  was positive indicating that we could improve the smoothness by setting the new

**Table II:** Information about each iteration.

Iter.	$\lambda_{23}^*$	$\lambda_{24}^*$	$\lambda_{25}^*$	$\lambda_{26}^*$	$\mathbf{x}^T \mathbf{H} \mathbf{x}$	$F_1^C$	$F_2^C$	$F_3^C$	$F_4^C$
1	-0.0175	-0.0176	-0.0175	0.0174	1.561	202.50	150.00	222.50	185.00
2	$\approx 0$	$\approx 0$	$\approx 0$	$\approx 0$	0.025	202.50	148.86	222.50	185.00
3	$\approx 0$	$\approx 0$	$\approx 0$	$\approx 0$	0.025	202.50	148.86	222.501	185.00

close-price between  $F_2^B$  and  $F_2^C$ . According to step II of the optimization algorithm, the new close price is  $F_{new}^C = \lambda^C(F^C - F^B)/(\lambda^C - \lambda^B) = 148.86$ . With the new closing prices, the last step is repeated until the stopping criteria is met. Table II shows lambdas, the total smoothness and closing prices for each iteration. With  $\gamma = 20\%$  the stopping criteria exits the loop after three iterations. The forward curve for each iteration is illustrated in figure 3. For the first iteration the change in forward curve is substantial. This is due to the relative large bid-ask spread for the missing contract. The effect of the extra flexibility provided by using a bid-ask spread instead of a fixed price is thus clearly seen. It also illustrates how the maximum smoothness criteria affects the forward curve.

### **4.3 Example from Nord Pool**

This example feature real data from Nord Pool, the Nordic power exchange. The effect of the prior function on the smoothed forward curve is studied in this example. We will also comment on the algorithms convergence and calculation speed. The input data is from 1. August 2003 and is shown in table III.

We see from the table that we have missing and overlapping contracts. To measure the effect the prior function has on the forward function we try four different prior functions

- Zero prior function, i.e. no prior function.
- A single trigonometric function.
- A combination of six trigonometric functions.
- Spot price prognosis from a bottom-up model.

The first prior function is  $h(t) = 100 \cos\left(\frac{2\pi}{365}(t + 40)\right) + 200$ , and is constructed on the basis of a yearly season, a maximum in February and a difference between maximum and minimum of 200 NOK/MWh. The second

**Table III:** *Input parameters, Nord Pool example.*

Ticker	Start date	End date	Bid	Ask
GU32-03	04.08.2003	10.08.2003	250.00	275.00
GU33-03	11.08.2003	17.08.2003	270.00	300.00
GU34-03	18.08.2003	24.08.2003	275.00	310.00
GU35-03	25.08.2003	31.08.2003	280.25	310.00
GU36-03	01.09.2003	07.09.2003	280.25	315.00
GB10-03	08.09.2003	05.10.2003	285.25	300.00
ENOMOCT-03	01.10.2003	31.10.2003	275.00	325.00
ENOMNOV-03	01.11.2003	30.11.2003	295.00	345.00
ENOMDEC-03	01.12.2003	31.12.2003		365.00
ENOMJAN-04	01.01.2004	31.01.2004	330.00	375.00
ENOMFEB-04	01.02.2004	29.02.2004	330.00	
FWV2-03	01.10.2003	31.12.2003	317.00	319.00
FWV1-04	01.01.2004	30.04.2004	315.00	322.00
FWSO-04	01.05.2004	30.09.2004	190.00	208.00
FWV2-04	01.10.2004	31.12.2004	225.50	238.00
FWV1-05	01.01.2005	30.04.2005	235.00	250.00
FWSO-05	01.05.2005	30.09.2005	180.00	191.00
FWV2-05	01.10.2005	31.12.2005	220.00	240.00
FWYR-04	01.01.2004	31.12.2004	240.50	249.00
FWYR-05	01.01.2005	31.12.2005	214.00	220.00
FWYR-06	01.01.2006	31.12.2006	212.00	220.00

The price data is from Nord Pool 1. August 2003, 08:10. The contracts with a ticker starting with a "G" are futures and the rest of the contracts are forwards. Since the exchange at the time we collected the prices only had been open for 10 minutes, some of the contracts had no buyers or sellers. This is reflected as missing prices for ENOMDEC-03 and ENOMFEB-04.



prior function is from Lund and Ollmar's *Analysing flexible load contracts*<sup>3</sup> paper. The prior function is estimated from spot prices for the period 1993 to 2001, and is made up of six trigonometric functions. This makes it more able to capture different seasons in the spot price. The prior function is

$$h(t) = b_0 + \sum_{j=1}^6 R_j \cos(\omega_j t + \phi_j)$$

where

$$\begin{aligned} R_1 &= 27.304 & \omega_1 &= \frac{2\pi}{8760*24} & \phi_1 &= -0.110 \\ R_2 &= 5.683 & \omega_2 &= \frac{2\pi}{4380*24} & \phi_2 &= -2.275 \\ R_3 &= 6.787 & \omega_3 &= \frac{2\pi}{168*24} & \phi_3 &= -2.128 \\ R_4 &= 3.931 & \omega_4 &= \frac{2\pi}{84*24} & \phi_4 &= -1.548 \\ R_5 &= 9.595 & \omega_5 &= \frac{2\pi}{24*24} & \phi_5 &= -3.760 \\ R_6 &= 6.139 & \omega_6 &= \frac{2\pi}{12*24} & \phi_6 &= -5.093 \end{aligned}$$

and  $b_0 = 125.54$ . The third prior function is from a bottom-up model. The price prognosis is provided by Skagerak Energy AS. The prior functions are plotted together with the smoothed forward curves in figure 4. We see that the bottom-up prognosis is not as smooth as the other priors.

The smoothed forward curves are constructed from  $m = 21$  contracts and are represented by a spline consisting of  $n = 32$  polynomials. The algorithm converged after 26 to 28 iterations depending on the prior function. On an ordinary pc the computing time was about 5 seconds. As we can see from figure 4 the effect of the prior function is different for different parts of the curve. The effect of the prior function is small for the first 900 days of the forward curve. After that, the choice of prior function influence the smoothed forward function more and more. For time to maturity exceeding 900 days, there are only forward contracts with a one year settlement period. This long settlement period gives the adjustment function less structure / constraints, and thus the prior function influences the smoothed forward curve more. Overall, this example shows that the choice of prior function has little effect

---

<sup>3</sup>An extended version of this paper is included in this thesis.

on the smoothed forward curve as long as it is constructed from contracts with settlement periods shorter than one year.

### Example from Nord Pool

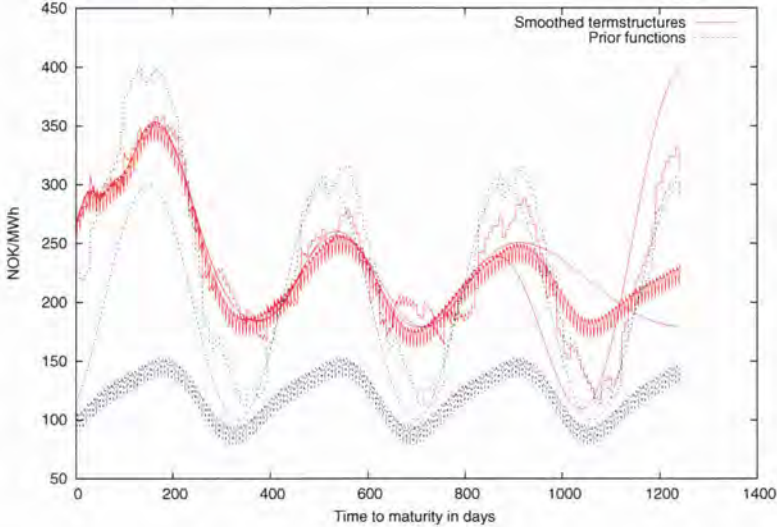


**Figure 4:** Four smoothed forward curves from Nord Pool together with three different prior functions. The effect of the prior function for forward prices with time to maturity less than 900 days is minor. Only where the smoothed curve is constructed by contracts with a one year settlement period, does the prior function play a difference.

## 5 Concluding remarks

We have in this paper derived a method for calculating a continuous forward curve from observed forward prices. The method is based on finding the smoothest possible forward curve within a bid-ask spread. We express the forward curve as a sum of a prior function and an adjustment function. The prior function can be an arbitrary function, and will typically incorporate subjective information about the forward curve. For example information from forecasts generated by “bottom-up” models. The adjustment function

is a polynomial spline of order five and is used to adjust the prior function to the observed forward prices. The forward and future contracts used to construct the smoothed curve can have overlapping settlement periods.

Parameter estimation is done by solving a constrained minimization problem. This minimization problem can be solved by solving a system of linear equations. If we use bid / ask prices to construct the smoothed forward curve the algorithm iterates to find the smoothest function. As the three examples shows, the algorithm is flexible, stable and fast.

If calculation speed, continuous forward curve or closed form solution is important requirements for the forward curve model, we believe our model will be the best choice.

## References

- [1] Adams, K. J. and D. R. van Deventer (1994), “Fitting yield curves and forward rate curves with maximum smoothness”, *Journal of Fixed Income*, pp. 52-62.
- [2] Anderson, F. B. and Deacon, M. (1996), “Estimating and Interpreting the Yield Curve”, John Wiley and Sons.
- [3] Fleten, S. E., and Lemming, J. (2003), “Constructing forward price curves in electricity markets”, *Energy Economics*, vol. 25, pp. 409-424.
- [4] Forsgren, A. (1998), “A Note on maximum-Smoothness Approximation of Forward Interest Rate”, *Technical report*, TRITA-MAT-1998-OS3, Royal Institute of Technology, Sweden.
- [5] Cox, J. C., Ingersoll, J. E. and S. A. Ross (1981), “The relation between forward prices and futures prices”, *Journal of Financial Economics*, vol. 9, pp. 321-346.
- [6] Judd, K. L (1998), “Numerical Methods in Economics”, The MIT Press, Cambridge, Massachusetts.
- [7] Lim, K. G. and Xiao, Q. (2002), “Computing Maximum Smoothness Forward Rate Curves”, *Statistics and Computing*, vol. 12, pp. 275-279.
- [8] Lund, A. C. and Ollmar, F. (2002), “Analysing Flexible Load Contracts in the Energy Market”, *Discussion paper*, No. 2002-18, Norwegian School of Economics and Business Administration, Norway.
- [9] McCulloch, J. H. (1971), “Measuring the term structure of interest rates”, *Journal of Business*, vol. 44, pp. 19-31.

## A Finding the smoothest function

We will in this section find the smoothest possible adjustment function,  $g(t)$ , that solves the following constrained minimization problem

$$\min_{\mathbf{x}} \int_{t_0}^{t_n} [g''(t; \mathbf{x})]^2 dt \quad (\text{A.1})$$

subject to

$$(a_{j+1} - a_j)t_j^4 + (b_{j+1} - b_j)t_j^3 + (c_{j+1} - c_j)t_j^2 + (d_{j+1} - d_j)t_j + e_{j+1} - e_j = 0 \quad \text{C1}$$

$$4(a_{j+1} - a_j)t_j^3 + 3(b_{j+1} - b_j)t_j^2 + 2(c_{j+1} - c_j)t_j + d_{j+1} - d_j = 0 \quad \text{C2}$$

$$12(a_{j+1} - a_j)t_j^2 + 6(b_{j+1} - b_j)t_j + 2(c_{j+1} - c_j) = 0 \quad \text{C3}$$

for  $j = 1, \dots, n - 1$ , and

$$g'(t_n; \mathbf{x}) = 0 \quad \text{C4}$$

and

$$F_i^C = \frac{1}{T_i^e - T_i^s} \int_{T_i^s}^{T_i^e} (g(t) + h(t)) dt \quad \text{C5}$$

for  $i = 1, \dots, m$ . Where  $n$  is the number of polynomial expressions and  $m$  the number of forward contracts.  $\mathbf{x}$  is the parameter vector of the adjustment function. We use a similarly approach as Adams and Van Deventer (1994) and Lim and Xiao (2002) to find the adjustment function. To shorten our notation we will use  $\alpha = T_i^s$  and  $\beta = T_i^e$ . The first step of the proof is to rewrite the minimization problem so it only contains second degree derivatives,  $g''(t)$ . Then we use the Lagrange method to find an expression for the solution, and in the last part we show that the solution is a polynomial spline of order five. By partial integration we know that

$$\begin{aligned} \int_{\alpha}^{\beta} t^2 g''(t) dt &= \beta^2 g'(\beta) - \alpha^2 g'(\alpha) - 2 \left[ \beta g(\beta) - \alpha g(\alpha) - \int_{\alpha}^{\beta} g(t) dt \right] \quad (\text{A.2}) \\ &\Downarrow \\ \int_{\alpha}^{\beta} g(t) dt &= \beta g(\beta) - \alpha g(\alpha) + \frac{1}{2} \left[ \alpha^2 g'(\alpha) - \beta^2 g'(\beta) + \int_{\alpha}^{\beta} t^2 g''(t) dt \right] \end{aligned}$$

Since  $g(t) \in C^1$  we can write  $g(x)$  as

$$g(x) = \int_{t_0}^x g'(t) dt + g(t_0)$$

and with  $g'(t_n) = 0$  we have

$$g(x) = g(t_0) - \int_{t_0}^x \int_t^{t_n} g''(v) dv dt \quad (\text{A.3})$$

Equivalently we use  $g(t) \in C^2$  to write

$$\begin{aligned} g'(x) &= g'(t_n) - \int_x^{t_n} g''(t) dt \\ &= - \int_x^{t_n} g''(t) dt \end{aligned} \quad (\text{A.4})$$

Combining (A.2), (A.3) and (A.4) we write the last condition in (A.1) as

$$\begin{aligned} (\beta - \alpha)F_i^C - \int_{\alpha}^{\beta} h(t) dt &= \int_{\alpha}^{\beta} g(t) dt \quad i = 1, \dots, m \\ &= (\alpha - \beta) \left[ \int_{t_0}^{\alpha} \int_t^{t_n} g''(v) dv dt - g(t_0) \right] \\ &\quad - \beta \int_{\alpha}^{\beta} \int_t^{t_n} g''(v) dv dt \\ &\quad + \frac{1}{2}(\beta^2 - \alpha^2) \int_{\beta}^{t_n} g''(t) dt \\ &\quad - \frac{1}{2}\alpha^2 \int_{\alpha}^{\beta} g''(t) dt \\ &\quad + \frac{1}{2} \int_{\alpha}^{\beta} t^2 g''(t) dt \end{aligned} \quad (\text{A.5})$$

Let  $q(t) = g''(t)$ . The constrained optimization problem (A.1) can now be expressed as (assuming  $g(t) \in C^2$ )

$$\begin{aligned}
 L &= \min_{q,\lambda} \int_{t_0}^{t_n} q^2(t) dt \\
 &\quad + \int_{t_0}^{t_n} \sum_{i=1}^m \lambda_i \mathbb{I}_{\{T_i^s < t < T_i^e\}} [g(t) - F_i^C + h(t)] dt \\
 &\quad \Updownarrow \\
 L &= \min_{q,\lambda} \int_{t_0}^{t_n} q^2(t) dt \\
 &\quad + \int_{t_0}^{t_n} \sum_{i=1}^m \lambda_i \left[ \mathbb{I}_{\{t > T_i^e\}} \frac{1}{2} (\beta^2 - \alpha^2) q(t) + \mathbb{I}_{\{t < T_i^s\}} (\alpha - \beta) \int_t^{t_n} q(v) dv \right. \\
 &\quad \left. + \mathbb{I}_{\{T_i^s < t < T_i^e\}} \left[ \frac{1}{2} t^2 q(t) - \frac{1}{2} \alpha^2 q(t) - \beta \int_t^{t_n} q(v) dv \right] - (\alpha - \beta) g(t_0) \right] dt \\
 &\quad + \int_{t_0}^{t_n} \sum_{i=1}^m \lambda_i \mathbb{I}_{\{T_i^s < t < T_i^e\}} [-F_i^C + h(t)] dt
 \end{aligned}$$

Suppose  $q^*$  is the solution of the optimization problem then

$$\frac{d}{d\epsilon} L(q^* + \epsilon k)|_{\epsilon=0} = 0 \tag{A.6}$$

for any continuous function  $k(\cdot)$  on the interval  $[t_0, t_n]$  such that  $k(t) = q(t) - q^*(t)$ . Solving (A.6) we get

$$\begin{aligned}
 &\frac{d}{d\epsilon} L(q^* + \epsilon k)|_{\epsilon=0} = 0 \\
 &\quad \Updownarrow \\
 &\int_{t_0}^{t_n} \left[ 2q^*(t) + \sum_{i=1}^m \lambda_i \left[ \mathbb{I}_{\{t > T_i^e\}} \frac{1}{2} (\beta^2 - \alpha^2) + \mathbb{I}_{\{T_i^s < t < T_i^e\}} \frac{1}{2} (t^2 - \alpha^2) \right] \right] k(t) dt \\
 &\quad + \int_{t_0}^{t_n} \left[ \sum_{i=1}^m \lambda_i (\mathbb{I}_{\{t < T_i^s\}} (\alpha - \beta) - \mathbb{I}_{\{T_i^s < t < T_i^e\}} \beta) \right] \left[ \int_t^{t_n} k(v) dv \right] dt = 0
 \end{aligned} \tag{A.7}$$

Next we make use of a variant of the lemma in Lim and Xiao (2002).

**Lemma A.1** *Given  $A()$  and  $h()$  are continuous functions and  $B()$  is integrable, then*

$$\int_a^b A(t)h(t) dt + \int_a^b B(t) \int_t^b h(v)dv dt = 0$$

*if and only if*

$$A(t) = - \int_a^t B(v) dv \quad \text{for all } a \leq t \leq b$$

By using the above lemma together with equation A.7 we get

$$\begin{aligned} 2q^*(t) + \sum_{i=1}^m \lambda_i \left[ \mathbb{I}_{\{t > T_i^e\}} \frac{1}{2}(\beta^2 - \alpha^2) + \mathbb{I}_{\{T_i^s < t < T_i^e\}} \frac{1}{2}(t^2 - \alpha^2) \right] = \\ - \int_{t_0}^t \sum_{i=1}^m \lambda_i \left[ \mathbb{I}_{\{v < T_i^s\}}(\alpha - \beta) - \mathbb{I}_{\{T_i^s < v < T_i^e\}}\beta \right] dv \end{aligned}$$

for all  $t \in [t_0, t_n]$ . Rearranging we get

$$q^*(t) = -\frac{1}{4} \sum_{i=1}^m \lambda_i t^2 + \frac{1}{2} \int_{t_0}^t \sum_{i=1}^m \lambda_i \beta dv + \frac{1}{4} \sum_{i=1}^m \lambda_i \alpha^2$$

for  $t \in [\alpha, \beta]$ . Proving that  $q^*(t)$  is a second-degree polynomial function. Using  $q(t) = g''(t)$  we have that the function that solves (A.1) can be written as the following fifth order polynomial spline

$$g(t) = \begin{cases} a_1 t^4 + b_1 t^3 + c_1 t^2 + d_1 t + e_1 & t \in [t_0, t_1] \\ a_2 t^4 + b_2 t^3 + c_2 t^2 + d_2 t + e_2 & t \in [t_1, t_2] \\ \vdots & \\ a_n t^4 + b_n t^3 + c_n t^2 + d_n t + e_n & t \in [t_{n-1}, t_n] \end{cases}$$



## B Construction of $A$ and $B$ matrices

In this section we show how we can write the conditions C1 to C5 on page 11 in the linear form  $\mathbf{Ax} = \mathbf{B}$ . Let  $n$  be the number of polynomials,  $m$  the number of forward contracts and  $t_0, t_1, \dots, t_n$  the knot points of the polynomials. The continuity condition C1 can then be written as the following rows in  $\mathbf{A}$

$$\begin{array}{cccccccccccccccc} -t_1^4 - t_1^3 - t_1^2 - t_1 - 1 & t_1^4 & t_1^3 & t_1^2 & t_1 & 1 & 0 & 0 & 0 & 0 & 0 & 0 & 0 & 0 & 0 & \dots \\ 0 & 0 & 0 & 0 & 0 & 0 & t_2^4 & t_2^3 & t_2^2 & t_2 & 1 & 0 & 0 & 0 & 0 & \dots \\ 0 & 0 & 0 & 0 & 0 & 0 & 0 & 0 & 0 & 0 & 0 & 0 & t_3^4 & t_3^3 & t_3^2 & \dots \\ \vdots & & & & & & & & & & & & & & & \end{array}$$

The corresponding elements in the  $\mathbf{B}$ -vector are  $n - 1$  zeros. Similarly we express the second and third constraint as the following rows in  $\mathbf{A}$

$$\begin{array}{cccccccccccccccc} -4t_1^3 - 3t_1^2 - 2t_1 - 1 & 0 & 4t_1^3 & 3t_1^2 & 2t_1 & 1 & 0 & 0 & 0 & 0 & 0 & 0 & 0 & 0 & 0 & \dots \\ 0 & 0 & 0 & 0 & 0 & 0 & -4t_2^3 - 3t_2^2 - 2t_2 - 1 & 0 & 4t_2^3 & 3t_2^2 & 2t_2 & 1 & 0 & 0 & 0 & \dots \\ 0 & 0 & 0 & 0 & 0 & 0 & 0 & 0 & 0 & 0 & 0 & 0 & -4t_3^3 - 3t_3^2 - 2t_3 - 1 & 0 & 4t_3^3 & \dots \\ \vdots & & & & & & & & & & & & & & & \end{array}$$

$$\begin{array}{cccccccccccccccc} -12t_1^2 - 6t_1 - 2 & 0 & 0 & 0 & 12t_1^2 & 6t_1 & 2 & 0 & 0 & 0 & 0 & 0 & 0 & 0 & 0 & \dots \\ 0 & 0 & 0 & 0 & 0 & 0 & -12t_2^2 - 6t_2 - 2 & 0 & 0 & 12t_2^2 & 6t_2 & 2 & 0 & 0 & 0 & \dots \\ 0 & 0 & 0 & 0 & 0 & 0 & 0 & 0 & 0 & -12t_3^2 - 6t_3 - 2 & 0 & 0 & 0 & 12t_3^2 & 6t_3 & \dots \\ \vdots & & & & & & & & & & & & & & & \end{array}$$

The corresponding elements in the  $\mathbf{B}$ -vector are  $2(n - 1)$  zeros. Next we include the terminal condition C4 as the following row in  $\mathbf{A}$

$$\dots \quad 0 \quad 0 \quad 0 \quad 0 \quad 0 \quad 0 \quad 4t_n^3 \quad 3t_n^2 \quad 2t_n \quad 1 \quad 0$$

The corresponding element in the  $\mathbf{B}$ -vector is zero.

The last constraint, C5, is

$$\begin{aligned} \frac{1}{T_j^e - T_j^s} \int_{T_j^s}^{T_j^e} f(t) dt &= F_j^C & (B.1) \\ \int_{T_j^s}^{T_j^e} g(t) dt &= F_j^C (T_j^e - T_j^s) - \int_{T_j^s}^{T_j^e} h(t) dt \end{aligned}$$

and ensures that close-price,  $F_j^C$ , is equal to the average value of the smoothed forward curve in the settlement period  $[T_j^s, T_j^e]$ . To implement this constraint we put the left side of (B.2) in the  $\mathbf{A}$ -matrix and the right side in the  $\mathbf{B}$ -vector. For overlapping contracts we need to split the integral of  $g(t)$  into

sub-periods. In the case with no overlapping contracts the sub-period is equal to the contract's settlement period. By construction of the list of knot points we have that each sub-period is equal to the domain of a polynomial. We define

$$\begin{aligned}\rho_i^1 &= [(T_j^s)^5 - (T_j^e)^5] / 5 \\ \rho_i^2 &= [(T_j^s)^4 - (T_j^e)^4] / 4 \\ \rho_i^3 &= [(T_j^s)^3 - (T_j^e)^3] / 3 \\ \rho_i^4 &= [(T_j^s)^2 - (T_j^e)^2] / 2 \\ \rho_i^5 &= T_j^s - T_j^e\end{aligned}$$

We can now implement the last constraint (assuming no overlapping contracts) by inserting the following  $m$  rows into  $\mathbf{A}$

$$\begin{array}{cccccccccccccccccccccccc} \rho_0^1 & \rho_0^2 & \rho_0^3 & \rho_0^4 & \rho_0^5 & 0 & 0 & 0 & 0 & 0 & 0 & 0 & 0 & 0 & 0 & 0 & 0 & 0 & 0 & \dots \\ 0 & 0 & 0 & 0 & 0 & \rho_1^1 & \rho_1^2 & \rho_1^3 & \rho_1^4 & \rho_1^5 & 0 & 0 & 0 & 0 & 0 & 0 & 0 & 0 & 0 & \dots \\ 0 & 0 & 0 & 0 & 0 & 0 & 0 & 0 & 0 & 0 & \rho_2^1 & \rho_2^2 & \rho_2^3 & \rho_2^4 & \rho_2^5 & 0 & 0 & 0 & 0 & \dots \\ \vdots & \dots \end{array}$$

To illustrate the splitting of the integral when we have overlapping contracts lets assume that the first contract has a settlement period equal to  $[t_0, t_2]$ . Now the last constraint can be written as

$$\begin{array}{cccccccccccccccccccccccc} \rho_0^1 & \rho_0^2 & \rho_0^3 & \rho_0^4 & \rho_0^5 & \rho_1^1 & \rho_1^2 & \rho_1^3 & \rho_1^4 & \rho_1^5 & 0 & 0 & 0 & 0 & 0 & 0 & 0 & 0 & 0 & \dots \\ 0 & 0 & 0 & 0 & 0 & \rho_1^1 & \rho_1^2 & \rho_1^3 & \rho_1^4 & \rho_1^5 & 0 & 0 & 0 & 0 & 0 & 0 & 0 & 0 & 0 & \dots \\ 0 & 0 & 0 & 0 & 0 & 0 & 0 & 0 & 0 & 0 & \rho_2^1 & \rho_2^2 & \rho_2^3 & \rho_2^4 & \rho_2^5 & 0 & 0 & 0 & 0 & \dots \\ \vdots & \dots \end{array}$$

In both cases the element in  $\mathbf{B}$  that correspond to each contract  $j$  is given by

$$F_j^C (T_j^s - T_j^e) - \int_{T_j^s}^{T_j^e} h(t) dt$$

For a numerical example please see the main text.



# Forward curve dynamics in the Nordic electricity market \*

Steen Koekebakker

Fridthjof Ollmar

## Abstract

We examine the forward curve dynamics in the Nordic electricity market. Six years of price data on futures and forward contracts traded in the Nordic electricity market are analyzed. For the forward price function of electricity, we specify a multi-factor term structure models in a Heath-Jarrow-Morton framework. Principal component analysis is used to reveal the volatility structure in the market. A two-factor model explains 75% of the price variation in our data, compared to approximately 95% in most other markets. Further investigations show that correlation between short- and long-term forward prices is lower than in other markets. We briefly discuss possible reasons why these special properties occur, and some consequences for hedging exposures in this market.

*JEL Classification Codes:* C330, G130, Q490

*Key words:* Electricity market; HJM framework; PCA analysis.

---

\*The authors would like to thank Petter Bjerksund, Svein-Arne Persson, Gunnar Stensland, Petter Osmundsen, Ellen Katrine Nyhus, Otto Andersen, Jostein Lillestøl, Jussi Keppo, an anonymous referee and seminar participants at the Norwegian School of Economics and Business Administration for helpful comments.

## 1 Introduction

With the rapid growth of derivative securities in deregulated electricity markets, the modeling and management of electricity price risk have become important topics for researchers and practitioners. In the case of electricity, contingent claims valuation and risk management were not considered important issues prior to market deregulation. Due to the special properties of this commodity, volatility in deregulated electricity markets can reach extreme levels, and a proper understanding of volatility dynamics is important for all participants in the market place.

There are two lines of research focusing on commodity contingent claims valuation and risk management. The traditional way has concentrated on modeling the stochastic process of the spot price and other state variables such as the convenience yield<sup>1</sup> (see for example Brennan and Schwartz 1985, Gibson and Schwartz 1990, Schwartz 1997 and Hilliard and Reis 1998). This approach has been adopted and modified in the recent electricity literature by, among others, Deng (2000), Kamat and Ohren (2000), Pilipović (1998) and Lucia and Schwartz (2002).

The main problem with spot price based models is that forward prices are given endogenously from the spot price dynamics. As a result, theoretical forward prices will in general not be consistent with market observed forward prices. As a response to this, a line of research has focused on modeling the evolution of the whole forward curve using only a few stochastic factors, taking the initial term structure as given. Examples of this research building on

---

<sup>1</sup>This direction is rooted in the theory of storage developed by Kaldor (1939), Working (1948) and (1949), Telser (1958) and Brennan (1958) and (1991). According to the theory of storage, the futures and spot price differential is equal to the cost of storage (including interest) and an implicit benefit that producers and consumers receive by holding inventories of a commodity. This benefit is termed the convenience yield. The most obvious benefit from holding inventory is the possibility to sell at an occurring price peak.

the modeling framework of Heath et al. (1992), are Clewlow and Strickland (1999a) and (1999b), Miltersen and Schwartz (1998) and Bjerksund et al. (2000).

Empirical investigations of forward curve models in commodity markets have been conducted by, among others, Cortazar and Schwartz (1994) and Clewlow and Strickland (2000). Cortazar and Schwartz (1994) studied the term structure of copper futures prices using principal component analysis, and found that three factors were able to explain 99% of the term structure movements. Clewlow and Strickland (2000) investigated the term structure of NYMEX oil futures and found that three factors explained 98.4% of the total price variation in the 1998-2000 period. The first factor (explaining 91% of total variation) shifted the whole curve in one direction. They termed this a "*shifting*" factor. The second factor, termed the "*tilting*" factor, influenced short and long-term contracts in opposite directions. The third factor, the "*bending*" factor, moved the short and long end in opposite direction of the mid-range of the term structure.<sup>2</sup>

In this paper we adopt the forward curve approach and perform an empirical examination of the dynamics of the forward curve in the Nordic electricity market in the period 1995-2001. Following the work of Cortazar and Schwartz (1994) and Clewlow and Strickland (2000) we use principal component analysis to analyze the volatility factor structure of the forward curve. The forward price of electricity is the price today for a delivery of electricity at some point in time in the future. This forward price function is not directly observable in the market place. Power contracts trading on Nord Pool are all written on a future average; the delivery periods of the contracts. Instead of working directly with the different financial contracts with vari-

---

<sup>2</sup>The multi-factor forward approach by Heath et al. (1992) was originally developed for interest rate markets. Empirical work on factor dynamics in fixed income securities markets have been conducted by Steely (1990), Litterman and Scheinkman (1991) and Dybvig (1997), among others. The results in these studies are quite similar to the work reported from the commodity markets. Typically, three factors explain 95%-98% of the total variation in the forward curve.

ous delivery periods, we compute a continuous forward price function from each day's futures and forward prices. This data transformation process is similar to the process of extracting a forward interest rate curve from a set of fixed income products. We apply the principle of maximum smoothness described in Adams and van Deventer (1994) and Bjerksund et al. (2000) to compute daily electricity forward curves. In the framework of Heath et al. (1992) we specify a geometric Brownian motion model for the evolution of the forward price of electricity. We construct a dataset of forward price returns. The maturities for the contracts that constitute the data set range from one week to two years. Following the work of Cortazar and Schwartz (1994) and Clewlow and Strickland (2000) we use principal component analysis to analyze the volatility factor structure of the forward curve. In the short end of the term structure, the volatility increases sharply as time to maturity decreases. In other commodity markets one typically find that a few factors are able to explain most of the variation in the forward prices. The portion of explained variance is lower in the electricity market. We find that a two-factor model explains 75% of the price variation in our data, compared to approximately 95% in most other markets. Pilipović (1998) conjectures that electricity prices exhibit "split personalities". By this she means that the correlation between short- and long term forward prices are lower in electricity markets than in other markets. We provide some empirical support for this claim. The most important factors driving the long end of the curve have very little impact on price changes in the short end. Furthermore we find some evidence of changing volatility dynamics both seasonally and from one year to another.

The rest of this paper is organized as follows: We give a short description of the Nordic electricity market in section 2. Section 3 presents the multi-factor models and section 4 describes the data set. In section 5 we show how principal component analysis can be used in order to estimate the empirical volatility functions and section 6 reports the results. Section 7 concludes the paper.

## **2 The Nordic electricity market**

### **2.1 History of the Nordic Power Exchange**

From 1971 to 1993 a market called Samkjøringen co-ordinated the Norwegian electricity production. Every week Samkjøringen set the daily or part-of-the-day price for electricity. This price was used to determine the Norwegian electricity production and the exchange with other countries. A new Energy Law was approved by the Norwegian Parliament in 1990 and came into effect in 1991. The law introduced market-based principles for production and consumption of electricity in Norway. After England and Wales in 1989, Norway was the third country to deregulate the electricity market.

In 1993 Samkjøringen merged with Statnett SF to create a new company called Statnett Marked AS. Statnett Marked AS organized the new Norwegian market place for electricity from 1993 to 1996. In 1996 the Swedish grid company, Svenska Kraftnät, bought 50% of Statnett Marked AS and became part of the power exchange area. At the same time Statnett Marked AS changed name to Nord Pool ASA. Finland joined the power exchange area in 1998, western Denmark in 1999 and eastern Denmark in 2000. The Nordic electricity market is non-mandatory and a significant share of the physical power and financial contracts are traded bilaterally.

### **2.2 The physical market**

Today Nord Pool organizes and operates Elspot, Eltermin, Eloption, and Elclearing. Elspot is a spot market for physical delivery of electricity. Each day at noon, spot prices and volumes for each hour the following day are determined in an auction. The equilibrium price is denoted the *system price*, which may be considered a one-day futures contract. The following day, the national system operators organize a *regulating-* or *balance* market, where short term up- or down regulation is handled. Since 1993 the turnover in Elspot market has increased steadily from 10.2 TWh in 1993 to 111.2 TWh



in 2001. In 1999, more than one fifth of the total consumption of electric power in the Nordic countries was traded via Nord Pool.

### **2.3 The financial market**

Eloption and Eltermin are Nord Pool's financial markets for price hedging and risk management. Financial contracts traded on Eltermin are written on the arithmetic average of the system price at a given time interval.<sup>3</sup> This time interval is termed the delivery period. The time period prior to delivery is called the trading period. Both futures and forward contracts are traded at Eltermin. The contract types differ as to how settlement is carried out during the trading period. For futures contracts, the value is calculated daily, reflecting changes in the market price of the contracts. These changes are settled financially at each participant's margin account. For forward contracts there is no cash settlement until the start of the delivery period. European options written on underlying futures and forward contracts are traded on Eloption.

The power contracts refer to a delivery rate of 1 MW during every hour for a given delivery period. Futures contracts feature daily market settlement in their trading and delivery periods. Forward contracts, on the other hand, do not have settlement of market price fluctuations during the trading period. Daily settlement is made in the delivery period. None of the contracts traded at Nord Pool are traded during the delivery period.

The contracts with the shortest delivery periods are futures contracts. Daily futures contracts with delivery period of 24 hours are available for trading within the nearest week.<sup>4</sup> Weekly futures contracts with delivery periods of 168 hours can be traded 4-8 weeks prior to delivery. Futures

---

<sup>3</sup>We only give a brief description of the different products traded at Nord Pool here. For a detailed description see [www.nordpool.no](http://www.nordpool.no) or Lucia and Schwartz (2002). Some contracts traded in the OTC market have a different underlying reference price than the system price. Such contracts are not considered in this study.

<sup>4</sup>These contracts have only a short (and illiquid) history, and will not be included in our data set when analyzing the volatility structure in the market.

contracts with 4 weeks delivery period, are termed block contracts. The forward contracts have longer delivery periods. Each year is divided into three seasons: V1 - late winter (January 1- April 30), S0 - summer (May 1 - September 30) and V2 - early winter (October 1 - December 31). Seasonal contracts<sup>5</sup> are written on each of these seasonal delivery periods. In January each year, seasonal contracts on S0 and V2 the coming year and all three seasonal contracts for the next two years are available. Furthermore, yearly forward contracts are available for the next three years. In other words, the (average based) term structure goes 3 to 4 years into the future, depending on current time of year.

In 1995 the total volume of financial contracts traded on Nord Pool and OTC was 40.9 TWh. In 2001, this number reached 2658 TWh. The most heavily traded contracts are the two seasonal contracts with shortest time to maturity. On average 100-200 weekly contracts and 200-300 seasonal contracts are traded each day.

### **3 Multi-factor forward curve models**

Our model setting is similar to the forward interest rate model of Heath et al. (1992). The model we investigate in this paper is a special case of the general multi-factor term structure models developed for commodity markets in Miltersen and Schwartz (1998). We consider a financial market where the uncertainty can be described by a  $K$ -dimensional Brownian motion  $(W_1, \dots, W_K)$  defined on an underlying probability space  $(\Omega, \mathbb{F}, \mathbb{Q})$  with the filtration  $\mathbb{F} = \{\mathcal{F}_t : t \in [0, T^*]\}$  satisfying the usual conditions and representing the revelation of information. The probability measure  $\mathbb{Q}$  represents the equivalent martingale measure. Throughout the paper we assume constant risk free interest rate, so that futures prices and forward prices with common maturity are identical (see Cox et al. (1981)).

---

<sup>5</sup>From 1995 to the end of 1999 special seasonal *futures* contract were traded. These contracts are also included in the estimation of the model.

Let the forward market be represented by a continuous forward price function, where  $f(t, T)$  denotes the forward price at date  $t$  for delivery of the commodity at time  $T$ , where  $t < T < T^*$ . Given constant interest rates the futures and forward prices are by construction martingales under the measure  $\mathbb{Q}$ . Consider a model<sup>6</sup> where the dynamics of the forward price is given by

$$\frac{df(t, T)}{f(t, T)} = \sum_{i=1}^K \sigma_i(t, T) dW_i(t) \quad (1)$$

with solution

$$f(t, T) = f(0, T) \exp \left( -\frac{1}{2} \sum_{i=1}^K \int_0^t \sigma_i(s, T)^2 ds + \sum_{i=1}^K \int_0^t \sigma_i(s, T) dW_i(s) \right)$$

Several specifications of (1) have been proposed for the Nordic electricity market. Lucia and Schwartz (2002) propose a spot price model and derive analytical expressions for futures/forward prices. They consider mean reverting spot price models both in level and log form. It is easy to show that their log based model is consistent with a forward price model with

$$\sigma_1(t, T) = \sigma e^{-\kappa(T-t)}$$

where  $\sigma$  and  $\kappa$  are positive constants. This model produce a falling volatility curve in  $T$ , approaching zero as  $T \rightarrow \infty$ . Audet et al. (2002) conduct an empirical study of the negative exponential volatility function. They generalize the one-factor model above. The volatility dynamics of futures contracts with different time to maturity are given by fixed constants of the negative exponential function above. But, different from the one-factor model of Lucia and Schwartz (2002), each contract is driven by a separate Brownian

---

<sup>6</sup>In this paper we present a standard lognormal model for the evolution of the forward curve. There is still no consensus on how the dynamic properties of electricity prices should be modeled (see discussion in Lucia and Schwartz 2002, Johnson and Bartz 1999 and Knittel and Roberts 2001). In a previous version of this paper we included a second model, the multi-dimensional arithmetic Brownian motion. Since the results from both models were qualitatively very similar, the arithmetic model was omitted to save space. These results are available from the authors upon request.

motions. Hence, there are as many Brownian motions as there are contracts in their model. These Brownian motions are given a parametric correlation structure, adding flexibility compared to the model considered by Lucia and Schwartz (2002). Bjerksund et al. (2000) propose both a one-factor and a three-factor model. The one-factor model is given by

$$\sigma_1(t, T) = \frac{a}{T - t + b} + c$$

where  $a$ ,  $b$  and  $c$  are positive constants. With realistic parameter values, this specification produces a sharply falling volatility curve in  $T$ . As  $T \rightarrow \infty$  the volatility converges to  $c$ . Bjerksund et al. (2000) also propose a three-factor model

$$\begin{aligned}\sigma_1(t, T) &= \frac{a}{T-t+b} \\ \sigma_2(t, T) &= \left(\frac{2ac}{T-t}\right)^{\frac{1}{2}} \\ \sigma_3(t, T) &= c\end{aligned}$$

with all parameters assumed positive. This three-factor model allows a richer structure of the forward price dynamics. They argue that the one factor model may be adequate for pricing contingent claims, while the three-factor model is better suited for risk management purposes. Note that in all the models above, given that all the parameters are positive, each individual Brownian motion will move forward prices of all maturities in the same direction. As we will see from the empirical analysis, this property of the proposed models is inconsistent with our empirical findings.

## 4 Descriptive analysis and data preparation

We are interested in the volatility dynamics of the forward price function described above. This forward price function, giving us today's price of a unit of electricity delivered at a specific instant in the future, is not directly observable in the market place. The power contracts trading on Nord Pool are all written on a future average; the delivery periods of the contracts. We need to pin down the relationship between the forward price function and

the average based contracts. Let  $F(t, T_1, T_2)$  be today's contract price of an average based futures contract delivering one unit of electricity at a rate of  $\frac{1}{T_2 - T_1}$  in the time period  $[T_1, T_2]$ , where  $T_1$  and  $T_2$  is the beginning and the end of the delivery period of the contract, and  $t \leq T_1 < T_2$ . Suppose that the contract price is paid as a constant cash flow during the delivery period. Then the expression for the average contract is (see Bjerk Sund et al. (2000)):

$$F(t, T_1, T_2) = \int_{T_1}^{T_2} w(r, u) f(t, u) du \quad (2)$$

where

$$w(r, u) \equiv \frac{e^{-ru}}{\int_{T_1}^{T_2} e^{-ru} du}$$

Lucia and Schwartz (2002) note that  $F(t, T_1, T_2) \approx \frac{1}{T_2 - T_1} \int_{T_1}^{T_2} f(t, u) du$  is a very good approximation of (2) for reasonable levels of interest rates. We use this approximation in the empirical analysis.

## 4.1 Smoothed data

Instead of working directly with the different financial contracts with various delivery periods, we compute a continuous forward price function from each day's futures and forward prices. The smoothing procedure is based on the principle of maximum smoothness suggested by Adams and van Deventer (1994). The smoothness criterion they state for the forward rate function is the one that minimizes the functional

$$\min \int_0^T f''(t, s)^2 ds \quad (3)$$

while at the same time fitting observed market prices.<sup>7</sup> They show, in an interest rate setting, that the yield curve with the smoothest possible forward rate function according to this criterion, is a quartic spline function

---

<sup>7</sup>Here the derivatives are taken with respect to the second time index.

## Smoothed forward curve

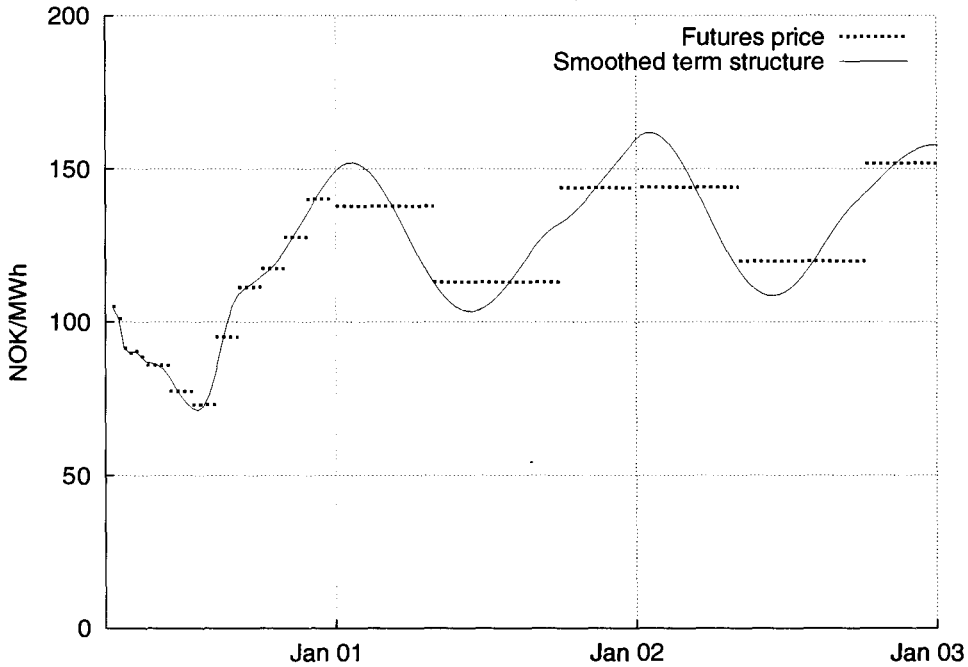


**Figure 1:** Power contracts and the smoothed forward curve on March 26, 2000. The dotted lines represent the actual market prices, and the length of the dotted lines corresponds to the delivery period on which the contracts are written. The weekly contracts (one dot) and block contracts (four dots) are futures contracts, and the seasonal contracts are forward contracts. The solid line is the smoothed term structure.

that is fitted between each knot point on the yield curve.<sup>8</sup> We use a quartic spline function to estimate a twice continuous forward function that prices all traded assets within the bid/ask spread.<sup>9</sup> The result of this smoothing procedure on March 27, 2000 is illustrated in figure 1. The horizontal dotted

<sup>8</sup>For a comprehensive description of the maximum smoothness approach see Adams and van Deventer (1994) and Lim and Xiao (2002).

<sup>9</sup>A sinusoidal prior function is defined prior to estimation to pick up the strong seasonal pattern in this market.

lines are closing prices on weekly, block and seasonal contracts. We have computed the smoothed forward price function on each of the 1340 trading days in our sample using all the contracts available each day. In figure 2 we have plotted weekly forward curves during the 1995-2001 sample period. Note the clear annual seasonal variation with high winter and low summer prices. The contract with the longest time to maturity increases from 80 weeks in 1995 to 208 weeks in 2001.

	Forward prices			Forward returns		
	W-01	W-52	W-104	W-01	W-52	W-104
Mean	145.51	159.54	163.47	-0.00297	0.00004	-0.00016
Median	130.18	153.49	158.88	-0.00228	-0.00013	-0.00000
Min	45.25	99.91	101.24	-0.38777	-0.06893	-0.25187
Max	356.00	262.03	275.75	0.21606	0.08876	0.22739
Std.dev	64.10	36.04	33.17	0.04094	0.01427	0.01471
Skewness	1.21	0.76	0.63	-0.42187	0.35750	-1.01313
Kurtosis	3.91	3.18	3.26	11.28	8.15	116.69
No. obs.	1340	1340	1279	1339	1339	1278

**Table I:** *Descriptive statistics for electricity forward prices and returns. The table reports statistics from three points on the term structure, the one week forward price (W-01), the one year forward price (W-52) and the two year forward price (W-104). The sample period is 1995-2001.*

Table I shows descriptive statistics on three different points on the term structure; W-01 (one week to maturity), W-52 (one year to maturity) and W-104 (two years to maturity). We note that the mean forward price is increasing with maturity. This means that the market on average can be

described by contango.<sup>10</sup> We note that the one-week forward price has fluctuated substantially during the sample period. The fluctuations decrease with time to maturity. To further examine the time series properties of the data, we have plotted the time series of forward prices with the same three maturities in figure 3. It is obvious that the one-week contract is much more erratic than the one- and two-year contract. Note that the short-term price varies around the long-term price indicating some sort of mean reversion. Roughly speaking the market was in normal backwardation in 1996 and in contango in the 1997-2001 period.

## 4.2 Constructing a data set

The forward price model in (1) describes the stochastic evolution under an equivalent martingale measure, and not under the real world measure where observations are made. Although there may be risk premia in the market that cause futures prices to exhibit non-zero drift terms, the diffusion terms are equal under both measures. So the volatility function in (1) can be estimated from real world data. As noted by Cortazar and Schwartz (1994), this is only strictly correct when observations are sampled continuously. In our analysis we use daily observations as a proxy to a continuously sampled data set. Let  $f(t_n, t_n + \tau_m)$  denote the forward price at date  $t_n$  with maturity at date  $t_n + \tau_m$ , where  $\tau_m = T_m - t_n$  is time to maturity for the contract. Our discrete approximations of (1) is

$$\frac{df(t_n, t_n + \tau_m)}{f(t_n, t_n + \tau_m)} \approx \frac{f(t_n, t_n + \tau_m) - f(t_{n-1}, t_n + \tau_m)}{f(t_{n-1}, t_n + \tau_m)} = x_{n,m}$$

---

<sup>10</sup>Contango is used to describe the situation when the futures price is above the expected futures spot price. The opposite situation is usually termed normal backwardation. We must be careful when using this relationship in markets with seasonal price variation. By choosing maturities exactly one year apart, forward prices on the same time of the year are compared and seasonal variation is no longer a problem.



## Data sample

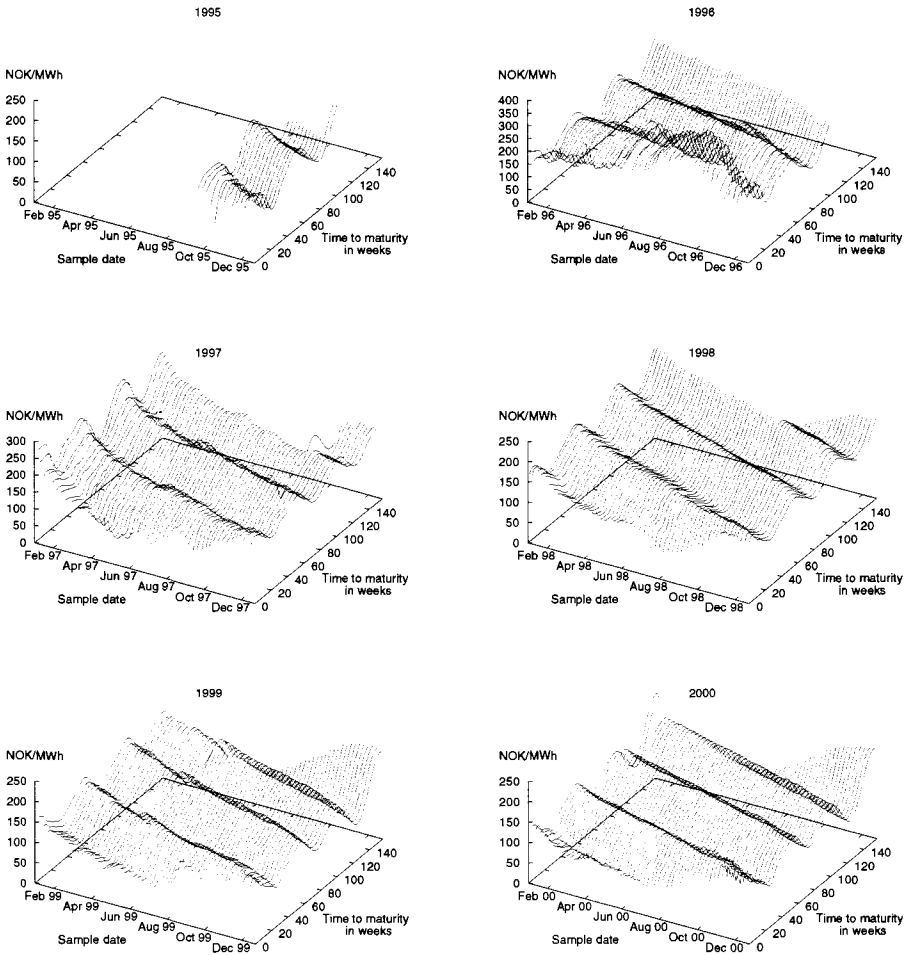


**Figure 2:** Surface plots of smoothed forward curves. Weekly surface plots (calculated from observed contracts each wednesday) for each of the years in our sample. Our data sample consists of a total of 1340 forward curves.

where  $n = 1, \dots, N$ .

## Time series of forward prices

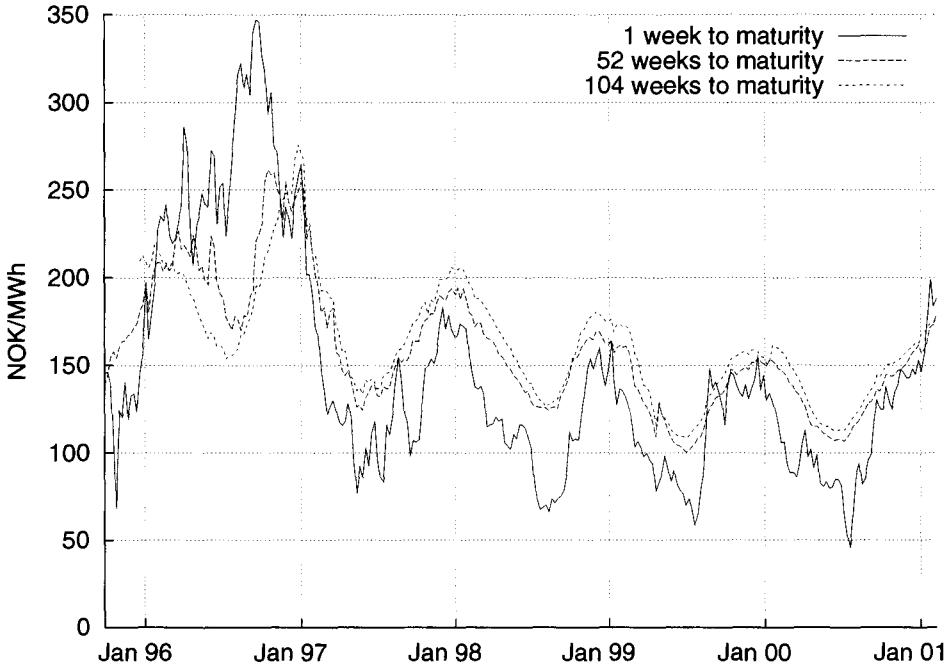


**Figure 3:** The graphs are time series plots of the forward prices with one week (solid line), one year - (dashed line) and two years (dotted line) to maturity.

For a set of maturity dates  $\{\tau_1, \dots, \tau_M\}$ , we construct a data set from the smoothed data.

$$\mathbf{X} = \begin{bmatrix} x_{1,1} & x_{1,2} & \cdots & x_{1,M} \\ x_{2,1} & x_{2,2} & \cdots & x_{2,M} \\ \vdots & \vdots & \ddots & \vdots \\ x_{N,1} & x_{N,2} & \cdots & x_{N,M} \end{bmatrix}$$

We first compute daily forward price functions from the observed market prices. From these forward functions we compute 104 weekly midpoint prices (equidistant forward prices), one price for each week along a two years term structure. Within each week these maturities are held constant. Next we

compute  $N = 1339$  time series observations on price returns. The contracts are rolled over each Friday. Let us illustrate our approach using the contract with maturity in one week: The daily returns from Monday to Friday are computed from the contracts with maturity the following week ( $\tau_1$ ). On Friday we observe the price of the contract with maturity two weeks ahead ( $\tau_2$ ). The return and difference on this contract is calculated from Friday to Monday. Reaching Monday, this contract has now become the new one-week contract. We use this approach of fixing the time to maturity to avoid problems of seasonality in prices over the year. Finally we pick  $M = 21$  price returns with different maturities among the 104 weekly prices. If we scale  $\tau_m$  in “weeks-to-maturity” the specific maturities chosen are  $\tau_1, \dots, \tau_M = [1, 2, 3, 4, 5, 6, 7, 12, 16, 20, 24, 28, 32, 36, 40, 44, 48, 52, 70, 88, 104]$ . The maturities are chosen in such a way that they reflect the actual traded contracts. In the shortest end we pick 7 maturities with weekly intervals, mimicking the weekly contracts. The next 11 maturities are 4 weeks apart. There are only three maturities in the last year of the term structure, representing seasonal contracts. In table I we report descriptive statistics on the one week-, one year- and two year forward price returns for the whole sample period. The standard deviation is sharply falling with time to maturity. We also note that kurtosis is high, and that skewness is different from zero. The sign of the skewness changes along the term structure. In table II we report descriptive statistics on semi-annual and seasonal sub-interval.

## **5 Principal component analysis and volatility functions**

Principal component analysis (PCA) is concerned with the identification of structure within a set of interrelated variables. It establishes dimensions within the data, and serves as a data reduction technique. The aim is to determine factors (i.e. principal components) in order to explain as much of the total variation in the data as possible. In order to use principal component

Panel A: Yearly sub-intervals									
	1995-1996			1997-1998			1999-2001		
	W-01	W-52	W-104	W-01	W-52	W-104	W-01	W-52	W-104
Mean	-0.0010	0.0021	0.0009	-0.0053	-0.0013	-0.0010	-0.0019	0.0001	0.0002
Median	0.0000	0.0014	0.0004	-0.0038	-0.0013	-0.0002	-0.0028	-0.0002	0.0000
Min	-0.3878	-0.0689	-0.0413	-0.1735	-0.0665	-0.2519	-0.1571	-0.0421	-0.0382
Max	0.2161	0.0888	0.0436	0.1530	0.0641	0.2274	0.1844	0.0628	0.0870
Std.dev	0.0478	0.0189	0.0128	0.0395	0.0146	0.0197	0.0377	0.0099	0.0089
Skewness	-1.3863	0.4130	0.0587	-0.2520	-0.1409	-1.2750	0.5407	0.9451	2.7326
Kurtosis	18.1721	6.2541	4.3285	5.6143	6.1021	92.5537	6.2602	11.0183	27.1745
No. obs.	315	315	254	500	500	500	524	524	524

Panel B: Seasonal sub-intervals									
	Late winter (V2)			Early winter (V1)			Summer (S0)		
	W-01	W-52	W-104	W-01	W-52	W-104	W-01	W-52	W-104
Mean	-0.0050	-0.0008	-0.0005	-0.0025	-0.0001	-0.0007	-0.0019	0.0008	0.0005
Median	-0.0037	-0.0009	-0.0003	-0.0027	0.0000	0.0000	0.0000	0.0003	0.0001
Min	-0.3878	-0.0689	-0.0413	-0.1571	-0.0592	-0.0925	-0.1735	-0.0665	-0.2519
Max	0.2161	0.0888	0.0411	0.1844	0.0640	0.0870	0.1611	0.0696	0.2274
Std.dev	0.0403	0.0125	0.0102	0.0365	0.0166	0.0135	0.0448	0.0133	0.0177
Skewness	-1.9178	0.1379	0.0753	0.5613	0.3284	-0.2259	-0.0710	0.5179	-1.3945
Kurtosis	26.9764	13.2301	5.8892	6.9858	5.8229	14.0679	4.7574	8.4175	131.6298
No. obs.	382	382	323	433	433	431	524	524	524

**Table II:** Descriptive statistics of daily forward price returns from the smoothed term structure. In panel A the analysis is performed on each two year sub-interval of the total sample. In panel B the data set is shuffled, and the analysis is performed on 3 seasonal sub-intervals, V2 (early winter), V1 (late winter) and S0 (summer) (see the text for exact period specifications). The table reports statistics from three points on the term structure, the one week forward price (W-01), the one year forward price (W-52) and the two year forward price (W-104).

analysis to estimate the volatility function in (1) we assume that the function only depend on time to maturity  $\tau_m$ . Not allowing the volatility functions to depend explicitly on  $t$  precludes seasonal variation in the volatility functions. Assume that we have a total of  $N$  observations of  $M$  different variables contained in vectors  $\mathbf{x}_1, \mathbf{x}_2, \dots, \mathbf{x}_M$  all of which dimension is  $(N \times 1)$ .<sup>11</sup> Let the data matrix,  $\mathbf{X}$ , be given by

$$\mathbf{X} = \begin{bmatrix} \mathbf{x}_1 & \mathbf{x}_2 & \cdots & \mathbf{x}_M \end{bmatrix} = \begin{bmatrix} x_{11} & x_{12} & \cdots & x_{1M} \\ x_{21} & x_{22} & \cdots & x_{2M} \\ \vdots & \vdots & \ddots & \vdots \\ x_{N1} & x_{N2} & \cdots & x_{NM} \end{bmatrix}$$

The corresponding sample covariance matrix, of order  $M$ , is denoted  $\mathbf{\Psi}$ . The orthogonal decomposition of the covariance matrix is

$$\mathbf{\Psi} = \mathbf{P}\mathbf{\Lambda}\mathbf{P}' \tag{4}$$

where

$$\mathbf{P} = \begin{bmatrix} \mathbf{p}_1 & \mathbf{p}_2 & \cdots & \mathbf{p}_M \end{bmatrix} = \begin{bmatrix} p_{11} & p_{12} & \cdots & p_{1M} \\ p_{21} & p_{22} & \cdots & p_{2M} \\ \vdots & \vdots & \ddots & \vdots \\ p_{M1} & p_{M2} & \cdots & p_{MM} \end{bmatrix}$$

and

$$\mathbf{\Lambda} = \begin{bmatrix} \lambda_{11} & 0 & \cdots & 0 \\ 0 & \lambda_{22} & \cdots & 0 \\ \vdots & \vdots & \ddots & \vdots \\ 0 & 0 & \cdots & \lambda_{MM} \end{bmatrix}$$

$\mathbf{\Lambda}$  is a diagonal matrix whose diagonal elements are the eigenvalues  $\lambda_{11}, \lambda_{22}, \dots, \lambda_{MM}$ , and where  $\mathbf{P}$  is an orthogonal matrix of order  $M$  whose  $i$ th

---

<sup>11</sup>Throughout this section we write matrices in bold upper case letters, vectors in bold lower case letters and elements in plain text. We suppress superscripts for notational convenience throughout this section.

column,  $\mathbf{p}_i$ , is the eigenvector corresponding to  $\lambda_{ii}$ .  $\mathbf{P}'$  is the transpose of  $\mathbf{P}$ . The matrix  $\mathbf{Z} = \mathbf{X}\mathbf{P}$  is called the matrix of principal components. Its columns,  $\mathbf{z}_i$ , are linear combinations of the columns of  $\mathbf{X}$  with the weights given by the elements of  $\mathbf{p}_i$ . That is, the  $i$ th principal component is

$$\mathbf{z}_i = \mathbf{X}\mathbf{p}_i = \mathbf{x}_1 p_{1i} + \mathbf{x}_2 p_{2i} + \dots + \mathbf{x}_M p_{Mi}$$

where  $p_{ij}$  is the element in the  $j$ th row and  $i$ th column of  $\mathbf{P}$ . The sample covariance matrix of  $\mathbf{Z}$  is given by

$$\text{var}(\mathbf{Z}) = \mathbf{P}'\mathbf{\Psi}\mathbf{P} = \mathbf{P}'\mathbf{P}\mathbf{\Lambda}\mathbf{P}'\mathbf{P} = \mathbf{\Lambda}$$

since  $\mathbf{P}\mathbf{P}' = \mathbf{P}'\mathbf{P} = \mathbf{I}$ , where  $\mathbf{I}$  is the identity matrix, hence the  $\mathbf{Z}$  variates are uncorrelated, and the variance of  $\mathbf{z}_i = \lambda_{ii}$ . The eigenvectors on the diagonal of  $\mathbf{\Lambda}$  are of convention ordered so that  $\lambda_{11} \geq \lambda_{22} \geq \dots \geq \lambda_{MM}$ . To explain all the variation in  $\mathbf{X}$ , we need  $M$  principal components. Since the objective of our analysis is to explain the covariance structure with just a few factors, we approximate the theoretical covariance matrix using the first  $K < M$  eigenvalues in (4). Unfortunately, we lack any solid statistical criterion to determine the number of factors that constitute the theoretical covariance matrix. Hair et al. (1995) discuss several criteria:

1. Eigenvalue criterion; only factors eigenvalues greater than 1 are considered significant.
2. Scree test criterion; the test is derived by plotting the eigenvalues against the number of factors in their order of extraction, and the shape of the curve is used to evaluate the cutoff point.
3. Percentage of variance criterion; additional factors are added until the cumulative percentage of the variance explained reach a pre-specified level.

We consider all of these criteria, but the latter criterion is the one frequently employed in the finance literature. The  $K$  factors should explain

a “big” part of the total covariance of the underlying variables (typically around 95%). The proportion of total variance accounted for by the first  $S$  factors is

$$\text{Cumulative contribution of first } S \text{ factors} = \frac{\sum_{i=1}^S \lambda_i}{\sum_{i=1}^M \lambda_i}$$

Component loadings are often computed to facilitate interpretation of the results from a principal component analysis. Here, we instead plot the empirical volatility function,  $\hat{\sigma}_i(\cdot)$ , directly from the eigenvalue decomposition as

$$\hat{\sigma}_i(t, T_m) = \sqrt{\lambda_i} p_{mi} \quad (5)$$

where  $i = 1, \dots, S$ . Here we have suppressed the time index, emphasizing the fact that the volatility is independent of calendar time. We can use (5) to plot easy-to-interpret volatility functions.

## 6 Empirical results

In table III we report the results from the PCA analysis conducted on the full sample. We note that a one factor model is able to explain 68% of the variation of price returns. The eigenvalue and scree test criteria both agree upon a two factor model with a total of 75% variation explained. This is considerably lower than in other markets. Typically two or three factors explain more than 95% of total variations in forward prices. For example, Clewlow and Strickland (2000) investigate the term structure of NYMEX oil futures and find that three-factors explain 98.4% of the total price variation. The fact that as much as 25% of the variance in the electricity market maturity specific, is, as far as we know, a feature unique to this market. If we increase the number of factors the percentage variations explained will naturally increase. We also note from table III that a target of say 95% explained variation requires more than 10 factors in our data. It is obvious that the 8 additional factors do not explain variation common to the whole

term structure. We will examine this more closely below, but first we will investigate the shape of the first two factors.

Factor	Ind.	Cum.
Fn1	0.68	0.68
Fn2	0.07	0.75
Fn3	0.05	0.80
Fn4	0.03	0.83
Fn5	0.03	0.86
Fn6	0.02	0.88
Fn7	0.02	0.89
Fn8	0.02	0.91
Fn9	0.01	0.92
Fn10	0.01	0.94

**Table III:** *Principal component analysis of forward price returns. The analysis is performed on the whole data set, 1339 observations from September 1995 to March 2001. The table reports the individual contribution (Ind.) of each factor (Fn.) of the total variance, and the cumulative effect (Cum.) of adding an additional factor.*

We now want to take a closer look at the volatility dynamics represented by the first two factors that affect the whole term structure. From the eigenvalues and the corresponding eigenvectors for the two first factors, we use (5) to plot the corresponding volatility function in figure 4 along with the overall volatility. The scaling on the vertical axes are annualized volatilities. Data for the whole sample period is used in these calculations. Note that the overall volatility is very high in the short end of the term structure, and that it falls rapidly with time to maturity. After approximately one year it stabilizes. Turning to the individual volatility functions, we see that the first factor is positive for all maturities, shifting all forward prices in the same direction. It causes much bigger movements in the short end than in the



long end. The second factor causes short and long term forward prices to move in opposite directions. These two factors are qualitatively equal to the first two factors reported in Clewlow and Strickland (2000) for NYMEX oil futures, which they denoted the *tilting* factor and *shifting* factor respectively.

## Volatility functions - full sample

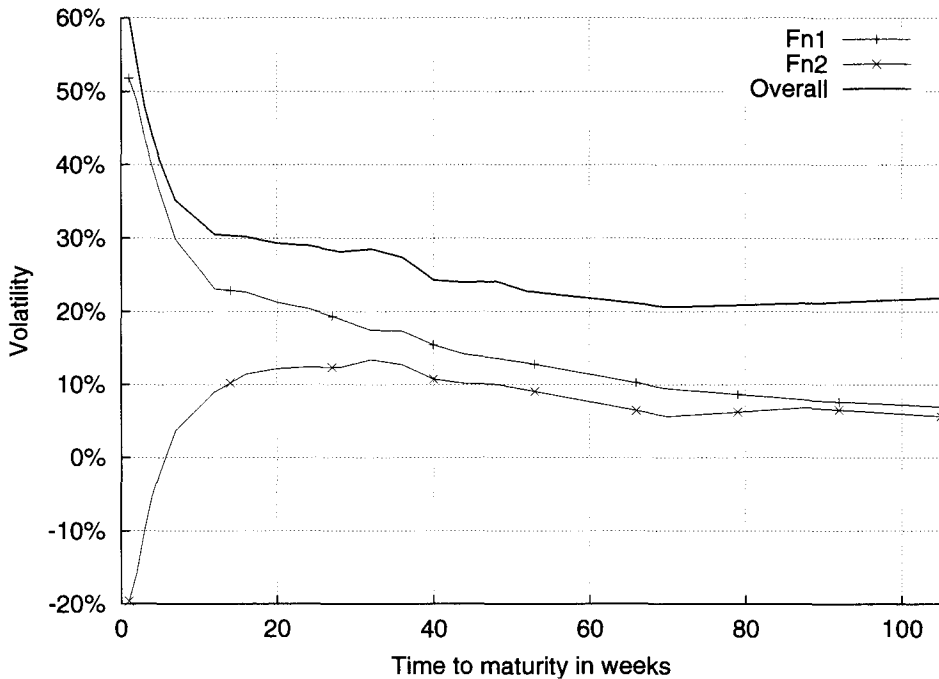


**Figure 4:** Volatility functions and overall volatility in the full sample period 1995-2001. The volatility functions are computed from price returns. The functions are annualized using a factor of square root of 250 (number of trading days).

Pilipović (1998) argues that the correlation between short-term and long-term forward prices seems to be lower in electricity markets than in other markets. If this is indeed the case, we would expect factors explaining a lot of variation in the long end of the term structure, being able to explain far less of the short term movements, and vice versa. We conducted the

PCA analysis once again to take a closer look at this. First we computed 10 principal components capturing about 95% of variation. Then all 10 factors were sorted according to size for each of the maturities. Hence for each of the 21 maturities, the 10 volatility functions resulting from the PCA analysis are sorted according to their ability to explain the overall variation for that particular maturity. The results are given in table IV.<sup>12</sup>

The first column reports the variation explained by the most important factor for that particular maturity. The number in superscript is the factor number. Hence factor number 1 is the most important factor for explaining overall volatility. The second column reports the cumulative variance explained by adding the second most important factor for that particular maturity. Again, the superscript indicates the importance of this factor in explaining total variation for all maturities. We note that factor number 1 is the factor explaining most of the variation for each maturity within the first year. Factors number 1 and 2 are among the 4 most important factors for all maturities. However, in the long end of the term structure, factors number 9 and 6 are the most important ones. In other words, the most important factors driving the long end of the curve have very little impact on price changes in the short end. On average, very little is gained in terms of percentage variation explained, by increasing the number of factors beyond 5. Combined, this evidence supports the conjecture made by Pilipović (1998) that electricity prices exhibit “split personalities”. Why do we see this kind of forward curve behavior in the electricity market? The answer possibly lies in the non-storable nature of electricity. For example, assume that the Swedish government makes a final decision to phase out their nuclear electricity production and decides to start cutting production two years from now. This would lower future supply, resulting in rising futures prices with more than 2 years to maturity. In a market where storage is possible, speculators would buy for storage (and/or producers would hold back production), as a reaction to the anticipated rise in electricity prices. This would in turn result

---

<sup>12</sup>The rest of the tables and figures are located in the appendix for space considerations.

in a positive shift in spot and short-term futures prices as well as long term futures prices. Since buying for storage is impossible<sup>13</sup> in electricity markets, the price on electricity will stay low until the date of reduced production. Consequently, only futures contracts with maturity after the production cut will react to this information. Pursuing this line of reasoning further, we are tempted to conjecture that other power markets, with less flexible hydropower than the Nordic, might experience even lower correlation between long term and short term forward prices. Temporary shocks in such a system will produce erratic spot prices to balance supply and demand. If the shocks are temporary, long term prices will be unaffected, and this will strengthen the "split personality" effect. Hydropower production offers most flexibility when it comes to smooth temporary shocks. In other words, the correlation between long term and short term forward contracts increase with the amount of hydropower in the system.

Using the whole sample period in our calculations, we implicitly assume that volatility dynamics have been constant in the 1995-2001 period. We want to investigate yearly and seasonal differences. However, our methodology does not allow calendar time dependence in the volatility functions. As a second best alternative, we repeat our PCA analysis in different sub-samples. In table V we report the results from PCA analysis on two years sub-intervals and seasonal sub-intervals. The two first volatility functions and overall volatility for each sub-sample are plotted in figure 5. From table V we see that the V1 and S0 sub-periods, fewer factors are needed to explain 95% of the variation in the data. Dividing into semi-yearly samples resulted in increased explanatory power of the 10 factors. This indicates that volatility dynamics changes both seasonally and from one year to the

---

<sup>13</sup>A large part of the electricity in the Nordic market is produced in hydropower based production units. Many of these units have reservoir facilities that, to some extent, enable them to move energy between periods. Such reservoir facilities provide a relatively high level of operating flexibility. Still, the reservoir capacity is not big enough for producers to shut down production for long periods of time without spilling water.

other<sup>14</sup>. Seasonally changing forward curve dynamics indicate that the price sensitive information is cyclical. Specifically, the results in table V seem to indicate that information released during autumn (V2 is October 1 - December 31) influences the forward curve differently than information received during the rest of the year. The rest of the year information has a stronger tendency of moving the whole curve (fewer factors produce higher explanatory power). What is special about autumn information? Autumn is the season with biggest precipitation. This is the most important variable affecting hydropower-based supply. Production decisions are made based on the level of water in the reservoir and anticipated rainfall in the future. When there is plenty of water in the reservoirs, and the producer expect heavy rainfall in the coming season, he will increase production today to give room for anticipated future precipitation. This affects spot prices and short term forward contracts. In the Nordic market, the average reservoir water level changes quite rapidly. This would indicate that prices of long term forward contracts are not very much influenced by current reservoir levels. The current reservoir situation, whether exceptionally dry, or exceptionally wet, may change many times before the long term contracts mature. This conjecture, that volatility forward curve dynamics in the Nordic market are influenced by reservoir level and expected inflow is left for future research. Also, changes in the marketplace might influence the volatility dynamics of the forward curve. Either implicitly through changes in the spot price dynamics, or explicitly through conditions affecting supply and demand of futures contracts. The most notable change is the growth of the market. In the first sub-period, Norway and Sweden constituted the whole market. In the next period sub-period, Finland was also a part of the market, and in the final sub-period Denmark joined. This means that there are more producers and consumers operating in the spot market, and hence, the equilibrium spot price dynam-

---

<sup>14</sup>We also computed the non-parametric Kolmogorov-Smirnoff test on equality of distributions across seasons and years. The test results, not reported here, showed rejections of equal distributions on 1% level in all cases.

ics may have changed as a result of this. On the other hand, neighboring countries have been affecting spot prices in Nordic market prior to formally joining the market, through exporting power from, and importing power to the market. The flow of power between the Nordic countries started long before market deregulation started. This weigh against a hypothesis of very distinct regime shifts as a result of new member countries joining the market. Both the volume of traded contracts, and the number of participants trading futures and forward contracts have grown dramatically in the time period investigated. This fact is also a possible source of changing volatility dynamics. Unfortunately, our methodology does not provide the appropriate tools to formally test the influence of new member countries, or increased volume on the volatility dynamics. This is left for future research. Still, from the volatility function in figure 5 we recognize the shifting and tilting factor as the most important factors driving the forward curve in all sub-periods.

## **7 Conclusions**

In this paper we conduct an exploratory investigation of the volatility dynamics in the Nordic futures and forward market in the period 1995-2001. The modelling framework is a standard lognormal spot price model similar to the one suggested by Heath et al. (1992). We use smoothed data and perform principal component analysis to reveal the factor structure of the forward price curve.

The main results are as follows: Two factors are common across all maturities. A two-factor model explains around 75% of total variation in the data. The first two factors governing the forward curve dynamics are comparable to other markets. The first factor is positive for all maturities, hence it shifts all forward prices in the same direction. The second factor causes short and long term forward prices to move in opposite directions. In contrast to other markets, more than 10 factors are needed to explain 95% of the term structure variation. Furthermore, the main sources of uncertainty affecting the

movements in the long end of the forward curve, have virtually no influence on variation in the short end of the curve. We argue that this behavior may occur because electricity is a non-storable commodity. Note that the maximum maturity in our analysis is 2 years. One might suspect that contracts sold in the OTC market with maturities further into the future are even less correlated with short term contracts. These results indicate that modelling the whole forward curve has less merit in this market than others. For example, hedging long-term commitments using short-term contracts may prove disastrous.

## References

- [1] Adams, K. J. and D. R. van Deventer (1994), "Fitting yield curves and forward rate curves with maximum smoothness", *Journal of Fixed Income*, pp. 52-62.
- [2] Audet, N., Heiskanen, P., Keppo, J. And I Vehvilaine (2002), "Modelling of electricity forward curve dynamics", Working paper, University of Michigan.
- [3] Bjerksund, P., Rasmussen, H. and G. Stensland (2000), "Valuation and risk management in the Nordic electricity market", Working paper, Institute of Finance and Management Science, Norwegian School of Economics and Business Administration.
- [4] Brennan, M. J. (1958), "The supply of storage", *American Economic Review*, vol. 48, pp. 50-72.
- [5] Brennan, M. J. (1991), "The price of convenience and the valuation of commodity contingent claims", in Lund, D. and B. Øksendal (eds.), *Stochastic models and option values - applications to resources, environment and investment problems*, Elsevier, Amsterdam, pp. 33-71.
- [6] Brennan, M. J. and E. S. Schwartz (1985), "Evaluating natural resource investment", *Journal of Business*, vol. 58, pp. 135-157.
- [7] Clewlow, L. and C. Strickland (2000), *Energy derivatives: Pricing and risk management*, Lacima Publications, London, England.
- [8] Clewlow, L. and C. Strickland (1999a), "A multifactor model for energy derivatives", Quantitative Finance Research Group, Working paper, University of Technology (Sydney).
- [9] Clewlow, L. and C. Strickland (1999b), "Valuing energy options in a one factor model fitted to forward prices", Quantitative Finance Research Group, Working paper, University of Technology (Sydney).

- [10] Cortazar, G. and E. S. Schwartz (1994), "The valuation of commodity contingent claims", *The Journal of Derivatives*, vol. 1 no. 4, pp. 27-39.
- [11] Cox, J. C., Ingersoll, J. E. and S. A. Ross (1981), "The relation between forward prices and futures prices", *Journal of Financial Economics*, vol. 9, pp. 321-346.
- [12] Deng, S. (2000), "Stochastic models of energy commodity prices and their applications: mean reversion with jumps and spikes", Working paper, PWP-073 of the Program on Workable Energy Regulation (POWER).
- [13] Dybvig, P. H. (1997), "Bond and bond option pricing based on the current term structure" in Dempster, M. A. H and S. Pliska (eds.), *Mathematics of Derivative Securities*, Cambridge University Press, Cambridge.
- [14] Gibson, R., and E. S. Schwartz (1990), "Stochastic convenience yield and the pricing of oil contingent claims", *Journal of Finance*, vol. 45, pp. 959-976.
- [15] Hair, J.F., Andersen R. E., Tatham R. L., and W. C. Black (1995), *Multivariate data analysis*, Fourth edition, Prentice Hall, Englewood Cliffs, New Jersey.
- [16] Heath, D., R. Jarrow and A. Morton (1992), "Bond pricing and the term structure of interest rates: A new methodology for contingent claims valuation", *Econometrica*, vol. 60, pp. 77-105.
- [17] Hilliard, J. E., and J. A. Reis (1998), "Jump processes in commodity futures pricing and option pricing", *American Journal of Agricultural Economics*, vol. 81, pp. 273-286.
- [18] Johnson, B. and G. Barz, 1999, "Selecting Stochastic Processes for Modelling Electricity Prices", in *Energy Modelling and the Management of Uncertainty - Applications in Risk Management and Investment*, Risk books, London.



- [19] Kaldor, N. (1939), "Speculation and economic stability", *The Review of Economic Studies*, vol. 7, pp. 1-7.
- [20] Kamat, R. and S. Ohren (2000), "Exotic options for interruptible electricity supply", Working paper, PWP-071 of the Program on Workable Energy Regulation (POWER).
- [21] Knittel, C. R. and M. R. Roberts, 2001, "An empirical examination of deregulated electricity prices", Working paper, PWP-087 of the Program on Workable Energy Regulation (POWER).
- [22] Lim, K. G. and Xiao, Q. (2002), "Computing Maximum Smoothness Forward Rate Curves", *Statistics and Computing*, vol. 12, pp. 275-279.
- [23] Litterman, R. and J. Scheinkman (1991), "Common factors affecting bond returns", *Journal of Fixed Income*, pp. 54-61.
- [24] Lucia, J. and E. S. Schwartz (2002), "Electricity prices and power derivatives: Evidence from the Nordic Power Exchange", *Review of Derivatives Research*, vol. 5, pp. 5-50.
- [25] Miltersen, K. R. and E. S. Schwartz (1998), "Pricing of options on commodity futures with stochastic term structures of convenience yield and interest rates", *Journal of Financial and Quantitative Analysis*, vol. 33, pp. 33-59.
- [26] Pilipović, D. (1998), *Energy risk: Valuing and managing energy derivatives*, McGraw-Hill, New York.
- [27] Schwartz, E. S. (1997), "The stochastic behavior of commodity prices: Implication for valuation and hedging", *Journal of Finance*, vol. 52, pp. 923-973.
- [28] Steeley, J. M. (1990), "Modelling the dynamics of the term structure of interest rates", *Economic and Social Review*, July, pp. 337-361.

- [29] Telser (1958), “Futures trading and the storage of cotton and wheat”, *Journal of Political Economy*, vol. 66, pp. 233-244.
- [30] Working, H. (1948), “Theory of the inverse carrying charge in futures markets”, *Journal of Farm Economics*, vol. 30, pp. 1-28.
- [31] Working, H. (1949), “Theory of the price of storage”, *American Economic Review*, vol. 39, pp. 1254-1262.

## A Tables and figures

Maturity	Cumulative variance explained									
	1 <sup>th</sup>	2 <sup>nd</sup>	3 <sup>rd</sup>	4 <sup>th</sup>	5 <sup>th</sup>	6 <sup>th</sup>	7 <sup>th</sup>	8 <sup>th</sup>	9 <sup>th</sup>	10 <sup>th</sup>
W-01	0.86 <sup>1</sup>	0.91 <sup>2</sup>	0.95 <sup>3</sup>	0.96 <sup>6</sup>	0.96 <sup>7</sup>	0.97 <sup>5</sup>	0.97 <sup>8</sup>	0.97 <sup>9</sup>	0.97 <sup>4</sup>	0.97 <sup>10</sup>
W-02	0.90 <sup>1</sup>	0.95 <sup>2</sup>	0.96 <sup>3</sup>	0.96 <sup>6</sup>	0.96 <sup>7</sup>	0.96 <sup>5</sup>	0.96 <sup>8</sup>	0.96 <sup>9</sup>	0.96 <sup>4</sup>	0.96 <sup>10</sup>
W-03	0.91 <sup>1</sup>	0.93 <sup>2</sup>	0.95 <sup>6</sup>	0.96 <sup>7</sup>	0.96 <sup>5</sup>	0.96 <sup>3</sup>	0.96 <sup>8</sup>	0.96 <sup>9</sup>	0.96 <sup>10</sup>	0.96 <sup>4</sup>
W-04	0.91 <sup>1</sup>	0.93 <sup>3</sup>	0.94 <sup>2</sup>	0.95 <sup>6</sup>	0.95 <sup>7</sup>	0.96 <sup>5</sup>	0.96 <sup>8</sup>	0.96 <sup>9</sup>	0.96 <sup>4</sup>	0.96 <sup>10</sup>
W-05	0.89 <sup>1</sup>	0.95 <sup>3</sup>	0.96 <sup>2</sup>	0.96 <sup>6</sup>	0.96 <sup>5</sup>	0.96 <sup>9</sup>	0.96 <sup>7</sup>	0.96 <sup>8</sup>	0.96 <sup>10</sup>	0.96 <sup>4</sup>
W-06	0.88 <sup>1</sup>	0.94 <sup>3</sup>	0.96 <sup>6</sup>	0.97 <sup>7</sup>	0.97 <sup>2</sup>	0.97 <sup>8</sup>	0.97 <sup>5</sup>	0.97 <sup>10</sup>	0.97 <sup>9</sup>	0.97 <sup>4</sup>
W-07	0.85 <sup>1</sup>	0.90 <sup>3</sup>	0.93 <sup>6</sup>	0.94 <sup>7</sup>	0.95 <sup>2</sup>	0.95 <sup>5</sup>	0.95 <sup>8</sup>	0.95 <sup>9</sup>	0.95 <sup>10</sup>	0.95 <sup>4</sup>
W-12	0.76 <sup>1</sup>	0.81 <sup>2</sup>	0.86 <sup>5</sup>	0.88 <sup>10</sup>	0.89 <sup>7</sup>	0.91 <sup>9</sup>	0.92 <sup>8</sup>	0.92 <sup>6</sup>	0.92 <sup>4</sup>	0.92 <sup>3</sup>
W-16	0.75 <sup>1</sup>	0.84 <sup>2</sup>	0.89 <sup>5</sup>	0.91 <sup>7</sup>	0.92 <sup>8</sup>	0.92 <sup>4</sup>	0.92 <sup>9</sup>	0.93 <sup>6</sup>	0.93 <sup>10</sup>	0.93 <sup>3</sup>
W-20	0.72 <sup>1</sup>	0.83 <sup>2</sup>	0.87 <sup>5</sup>	0.88 <sup>4</sup>	0.89 <sup>9</sup>	0.90 <sup>10</sup>	0.90 <sup>7</sup>	0.91 <sup>3</sup>	0.91 <sup>6</sup>	0.91 <sup>8</sup>
W-24	0.70 <sup>1</sup>	0.82 <sup>2</sup>	0.86 <sup>9</sup>	0.89 <sup>8</sup>	0.90 <sup>10</sup>	0.91 <sup>5</sup>	0.92 <sup>4</sup>	0.93 <sup>3</sup>	0.93 <sup>6</sup>	0.93 <sup>7</sup>
W-28	0.67 <sup>1</sup>	0.80 <sup>2</sup>	0.85 <sup>8</sup>	0.87 <sup>4</sup>	0.88 <sup>7</sup>	0.89 <sup>3</sup>	0.89 <sup>9</sup>	0.89 <sup>10</sup>	0.89 <sup>6</sup>	0.89 <sup>5</sup>
W-32	0.61 <sup>1</sup>	0.77 <sup>2</sup>	0.85 <sup>4</sup>	0.88 <sup>10</sup>	0.90 <sup>5</sup>	0.92 <sup>3</sup>	0.93 <sup>9</sup>	0.94 <sup>7</sup>	0.94 <sup>8</sup>	0.94 <sup>6</sup>
W-36	0.63 <sup>1</sup>	0.78 <sup>2</sup>	0.85 <sup>5</sup>	0.89 <sup>4</sup>	0.92 <sup>8</sup>	0.93 <sup>3</sup>	0.94 <sup>7</sup>	0.94 <sup>9</sup>	0.94 <sup>6</sup>	0.94 <sup>10</sup>
W-40	0.63 <sup>1</sup>	0.77 <sup>2</sup>	0.85 <sup>8</sup>	0.88 <sup>5</sup>	0.90 <sup>9</sup>	0.91 <sup>4</sup>	0.92 <sup>10</sup>	0.93 <sup>3</sup>	0.93 <sup>6</sup>	0.94 <sup>7</sup>
W-44	0.59 <sup>1</sup>	0.77 <sup>4</sup>	0.88 <sup>2</sup>	0.90 <sup>8</sup>	0.91 <sup>9</sup>	0.92 <sup>3</sup>	0.92 <sup>5</sup>	0.92 <sup>6</sup>	0.92 <sup>7</sup>	0.93 <sup>10</sup>
W-48	0.61 <sup>4</sup>	0.83 <sup>1</sup>	0.93 <sup>2</sup>	0.94 <sup>8</sup>	0.94 <sup>3</sup>	0.95 <sup>7</sup>	0.95 <sup>10</sup>	0.96 <sup>6</sup>	0.96 <sup>9</sup>	0.96 <sup>5</sup>
W-52	0.57 <sup>1</sup>	0.75 <sup>4</sup>	0.86 <sup>2</sup>	0.89 <sup>8</sup>	0.91 <sup>9</sup>	0.92 <sup>10</sup>	0.92 <sup>7</sup>	0.93 <sup>3</sup>	0.93 <sup>6</sup>	0.93 <sup>5</sup>
W-70	0.55 <sup>9</sup>	0.76 <sup>10</sup>	0.89 <sup>1</sup>	0.93 <sup>2</sup>	0.94 <sup>8</sup>	0.95 <sup>6</sup>	0.95 <sup>7</sup>	0.95 <sup>4</sup>	0.95 <sup>5</sup>	0.95 <sup>3</sup>
W-88	0.38 <sup>6</sup>	0.53 <sup>1</sup>	0.64 <sup>7</sup>	0.72 <sup>2</sup>	0.76 <sup>5</sup>	0.79 <sup>3</sup>	0.80 <sup>8</sup>	0.81 <sup>10</sup>	0.81 <sup>9</sup>	0.81 <sup>4</sup>
W-104	0.53 <sup>6</sup>	0.73 <sup>7</sup>	0.79 <sup>1</sup>	0.83 <sup>2</sup>	0.85 <sup>3</sup>	0.86 <sup>5</sup>	0.87 <sup>10</sup>	0.89 <sup>4</sup>	0.89 <sup>9</sup>	0.89 <sup>8</sup>
Avg.	0.71	0.83	0.88	0.90	0.92	0.92	0.93	0.93	0.93	0.93

**Table IV:** Most important factors across maturities for price returns. We have first conducted a principal component analysis using 10 factors. Then the importance of each factor is sorted for each maturity. The table reports the cumulative variance explained when adding one additional factor. The factor number is in superscript. The bottom row reports the the average cumulative variance explained.

Factor	V2		V1		S0		1995-1996		1997-1998		1999-2001	
	Ind.	Cum.	Ind.	Cum.	Ind.	Cum.	Ind.	Cum.	Ind.	Cum.	Ind.	Cum.
Fn1	0.59	0.59	0.70	0.70	0.80	0.80	0.70	0.70	0.58	0.58	0.73	0.73
Fn2	0.09	0.68	0.08	0.78	0.06	0.87	0.08	0.78	0.09	0.67	0.08	0.81
Fn3	0.05	0.73	0.05	0.83	0.04	0.91	0.06	0.83	0.07	0.74	0.05	0.86
Fn4	0.04	0.77	0.03	0.86	0.02	0.93	0.03	0.86	0.06	0.80	0.02	0.88
Fn5	0.04	0.81	0.03	0.89	0.01	0.95	0.03	0.89	0.04	0.83	0.02	0.90
Fn6	0.03	0.84	0.02	0.91	0.01	0.95	0.02	0.91	0.04	0.87	0.02	0.92
Fn7	0.02	0.86	0.02	0.93	0.01	0.96	0.02	0.92	0.02	0.89	0.01	0.93
Fn8	0.02	0.89	0.01	0.94	0.01	0.97	0.01	0.94	0.02	0.91	0.01	0.94
Fn9	0.02	0.90	0.01	0.95	0.01	0.98	0.01	0.95	0.02	0.93	0.01	0.95
Fn10	0.02	0.92	0.01	0.96	0.00	0.98	0.01	0.96	0.01	0.94	0.01	0.96

**Table V:** *Principal component analysis of forward price returns. The first three columns report the results from seasonal subintervals, V2 (early winter), V1 (late winter) and S0 (summer) (see the text for exact period specifications). The next three columns report results from each two year sub-interval of the total sample. The table reports the individual contribution (Ind.) of each factor (Fn.) of the total variance, and the cumulative effect (Cum.) of adding an additional factor.*

## Volatility functions for different samples

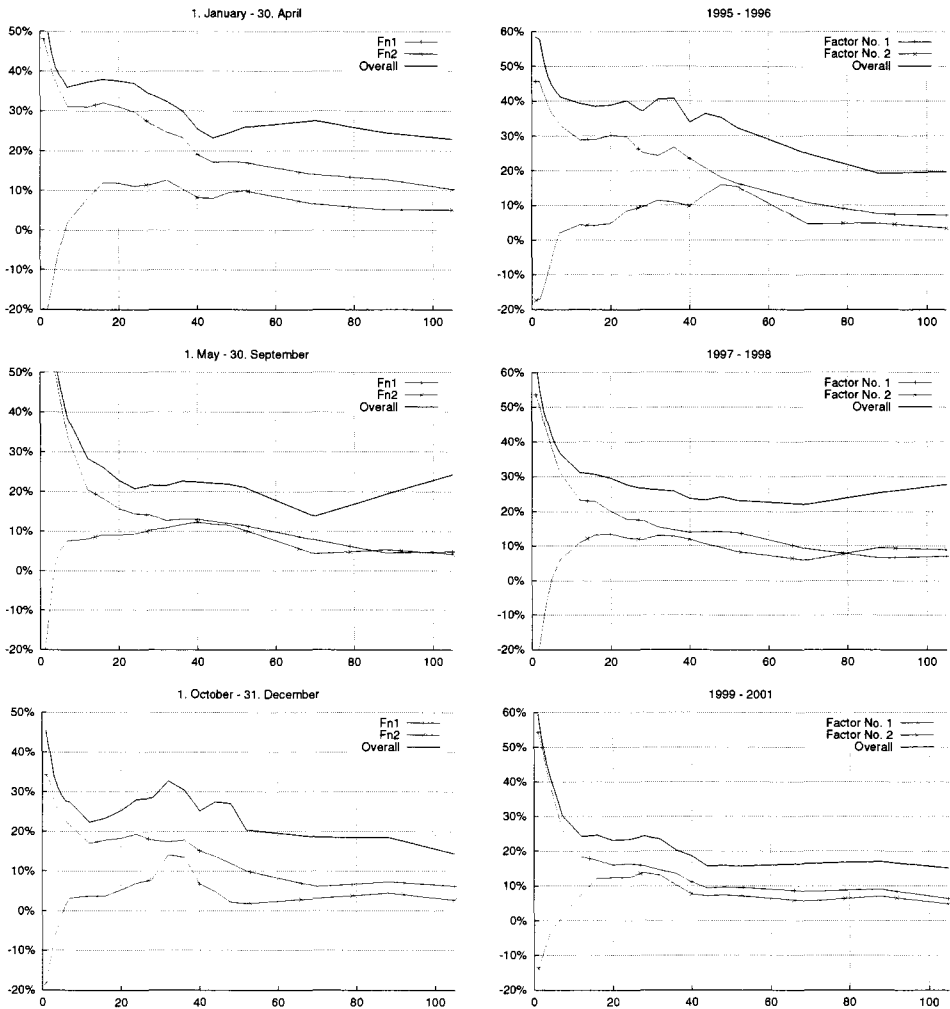


**Figure 5:** The two first volatility functions and overall volatility. The volatility functions on the left hand side are computed from different seasons corresponding to seasonal contracts traded at Nord Pool and the functions on the right hand side are computed from the time periods 1995-1996, 1997-1998 and 1999-2001. The functions are annualized using a factor of square root of 250 (number of trading days).

# Analyzing Flexible Load Contracts

Arne-Christian Lund and Fridthjof Ollmar \*

## Abstract

In this paper we analyze flexible load contracts (FLC), a type of “swing” option. This contract type has existed in energy markets for a long time and has proved to be challenging to value. The term swing refers to the flexibility in the amount of energy that the holder of the contract can receive. We formulate the FLC as a stochastic optimization problem. The price process, modelled as a time dependent Ornstein-Uhlenbeck process, is calibrated to the spot price on the Nordic electricity market. With this process the optimization problem is solved numerically. The results of the algorithm are compared with the exercise policy for nine market participants. We find that our algorithm obtain the highest accumulated exercise revenue for the five year period 1997-2002.

*Key words:* Swing options, electricity market, empirical.

---

\*We wish to thank Morten Askland, Jostein Lillestøl, Leif K. Sandal and Gunnar Stensland for valuable comments. We would also like to acknowledge helpful suggestions from the participants at the NHH’s 2001 staff seminar, FIBE’s 2003 conference and EDF’s 2003 seminar.

## 1 Introduction

The first power plants built in the first part of the previous century were built to meet the nearby industry's demand for electricity. To reduce transmission losses or the cost of transporting the raw material used to produce the electricity, the industries were often located close to the power plants. Another characteristic of this early stage was that the same firms were the owners of both the power plants and the industry that used the power. The value of electricity was consequently not exogenous calculated but endogenous valued as a part of the product costing. When it was possible to sell energy surplus, the need to formulate and value electricity contracts occurred. One of the first type of contracts to be traded was the contract that gave the owner the right to a certain amount of energy within a given period of time. To make it possible to deliver the electricity the seller restricted the maximum amount per hour (i.e. the effect) the buyer could withdraw. The buyer of the contract could then withdraw electricity, given the effect restriction, to cover his own electricity demand. This type of contract was the predecessor to a type of swing option known today as a *flexible load contract* (FLC).

Since the first flexible load contracts were traded, most electricity consumers and producers have interconnected themselves with a national or international power grid. In recent years many countries have also deregulated their electricity market. These changes have increased the possibility to utilize the flexible load contract. Earlier the owner of a flexible load contract had to withdraw the amount he consumed and any surplus energy was wasted. With a spot market the buyer of the contract can withdraw energy from the seller of the contract and sell it in the spot market. To meet his own demand for electricity he can buy it directly from the spot market instead of exercising the contract. By incorporating the spot market the owner of a flexible load contract can fully utilize the flexibility of the contract. This

effect has naturally increased the value of the contract. But it has also made the problem to value and decide when to exercise the contract more difficult.

Swing contracts have been used in several markets to hedge against frequent price and demand spiking behavior that is followed by a reversion to normal levels. More generally this type of contracts is of value in any market where the physical transfer of the underlying asset must take place through interconnected networks, and is thus subject to volume constraints. This is the case for natural gas and pipelines, electricity and cable based telecommunications and their transmission lines, wireless telecommunications and their bandwidths. Despite the long history of swing options and their importance as a risk management tool, there has been limited research regarding valuation of such contracts.

One of the first methods used to value a FLC was by modelling the contract as a hydroelectric power plant with no inflow. Optimization methods for hydroelectric power has been studied since the early 1960s. Stage and Larsson (1961) developed one of the first optimization methods for hydroelectric power plants. Their method was called incremented cost of waterpower and was based on finding the hydroelectric production that minimize the cost of the thermal power in a system where hydroelectric power is predominant. To implement this type of model one usually has to represent all hydroelectric power production as one representative hydroelectric power plant. If the individual hydroelectric power plants are significantly different from each other, representing them as one unit may be an inaccurate representation. Since there was no spot or forward market when the model was developed, they did not incorporate any information from these markets into the model. Instead they regarded the price as an endogenous function of the marginal production costs. This is a good approximation when there is no spot or forward market. If there exist a spot or forward market it is simpler to regard the price as exogenous.

Recent literature on valuing flexible load contracts/swing options is based on contingent claims and derivative theory. If there exist a forward market



with the same resolution<sup>1</sup> as the flexible load contract, Øksendal shows in his PhD thesis (2001) how it is possible to value a FLC by replicating it with a portfolio of future contracts. Similarly, Keppo (2002) shows that it is possible to hedge and thereby value a swing option if there exists an option market. The problem with these methods is that they only works when we have a forward market or an option market with equal or higher resolution than the FLC contract. If we try to use the method in practice we will discover that this assumption is not fulfilled. Typically the FLC has an hourly resolution while the forward market has a weekly or monthly resolution. This lack of completeness in the forward market will result in an erroneous valuation of the flexible load contract.

In line with Jaillet, Ronn and Tompaidis (2003), Bjørgan, Song and Liu (2000), Thompson (1995), Lavassani, Simchi and Ware (2001) we have chosen to regard the FLC as a contingent claim on the spot price and analyze it with numerical techniques. We assume there is no forward market, or that the owner of the contract is unable to participate in the forward market. This is equal to assuming that the spot price is a risk neutralized price process, obtained by the incorporation of a model of the cost-of-carry or the market-price-of-risk function. Estimation and incorporation of market risk is possible and is left for future work.

To get a better understanding of how flexible load contracts works lets assume we have a spot market for electricity and that we have just bought an 8335 MWh flexible load contract<sup>2</sup>. The contract has a maximum effect of 5 MWh per hour and a delivery period from 1. May 1997 to 30. September 1997. The price we paid for this contract was 115 NOK/MWh or 958525 NOK, and the delivery period of the contract consists of 3672 hours. Assuming profit is maximized, our target will be to exercise the contract during the

---

<sup>1</sup>With “same resolution” we mean that if the FLC is based on an hourly resolution then the forward market must have one forward contract for each hour in the delivery period of the FLC.

<sup>2</sup>We will use this contract as an example throughout the paper

1667<sup>3</sup> of the total 3672 hours with the highest spot price. Every day at 10 am we must inform the seller of the contract which hours the following day we want to exercise our right to buy for 115 NOK/MWh. The energy we buy will then be sold in the spot market, and our profit/loss will be the difference between 115 NOK/MWh and the price we manage to sell the energy in the spot market for. The flexibility of the contract is the ability to change our exercise policy during the delivery period. After buying the contract we may ask ourselves the following questions: How high should the spot price be before we start exercising the contract? What is its theoretical value? Which factors influence the value of the contracts and how do they influence the contract? This paper will answer some of these questions.

The remainder of this paper is organized as follows. In the next section we formulate the FLC as a mathematical optimization problem, and in section three we analyze the spot price and decide upon a spot price model. Then in section four we analyze how we can solve the optimization problem numerically. In section five we describe our data-set and estimate the price process. The results and concluding remarks are given in section six and seven.

---

<sup>3</sup>8335MWh/5MW=1667h

## **2 Mathematical formulation of the FLC**

We will in this section show how we can find the optimal exercise policy and corresponding contract value by formulating the FLC as an continuous stochastic optimal control problem.

### **2.1 FLC as an optimization problem**

We choose to formulate the flexible load contract as a continuous time stochastic optimal control problem. In the real world this optimization problem is a combined discrete-continuous problem. It seems natural to think of the spot price as a continuous process. The control is however chosen on an hourly basis. Still one hour is a small time interval compared to the total contract length. A continuous model formulation is therefore natural. When we later implement a numerical scheme, one hour is used as the basic discrete time interval.

We study a control problem related to the optimal delivery of electrical power. We assume that a contract for a specified amount of energy over a period  $[0, T]$  is given. The price of the electricity at a certain time  $t \in (0, T)$  is given by a specified price process  $P_t$ . We assume that the 'producer' is a small participant in the market, so the price does not depend on the amount of delivered power. Further we assume that the contract puts restrictions on the delivery; At each instant the rate of delivered energy must be in a specified interval. Let  $Q_t$  denote the amount delivered up to time  $t$ . Our goal is to find the optimal control choice at each moment  $t$ , and for all levels of  $Q$  and  $P$ . This is a feedback form of the control. With this optimal policy in hand, the controller can choose the best delivery, given the current levels of the state variables. Further, the actual value of the contract is important when such contracts are bought or sold. We now show how this problem may be formulated as a stochastic optimal control problem with a terminal condition.

Suppose that we have agreed to deliver  $M$  units of a product (e.g. power)

during the period  $[0, T]$ . The delivery rate is called  $u_t$ . Therefore

$$dQ_t = u_t dt$$

with  $Q_0 = 0$ . Obviously  $Q$  must satisfy  $Q_T = \int_0^T u_t dt = M$ . This is an *end constraint* on the variable  $Q_t$ . We assume that the control  $u_t$  must be in an interval  $[u_0, u_1]$  for all  $t$ . Further, the contract specifies that the holder of the contract is paid a spot price  $P_t$  for the delivered amount of product. We assume that  $P$  follows a process

$$dP_t = \mu dt + \sigma dW_t$$

where  $W_t$  is a Brownian motion,  $\mu$  and  $\sigma$  may be functions of  $t$  and  $P$ . At time  $t$  the price  $P_t \triangleq p$ , and the amount  $Q_t \triangleq q$  are known by observation. The objective for the producer is now to maximize the net present value. Let the function  $\Pi$  represent the instantaneous profit of the delivery, and  $\delta$  the discount factor. We want to find the *value function*

$$V(t, q, p) = \max_{u \in \mathcal{U}} E \int_t^T e^{-\delta s} \Pi(s, u_s, P_s) ds. \quad (2.1)$$

when  $t < T$  and the corresponding control under the condition that  $Q(T) = M$ . This side condition calls for a control space  $\mathcal{U}$  which is explicitly dependent of  $t$  and  $Q$ . In general such problems are hard to solve. In this case we may reformulate the problem to get a state independent control space. In subsection 2.3 we give a more precise formulation of the problem but first we need to study the structure of the problem more thoroughly.

## 2.2 Further observations

The function  $V(t, q, p)$  is the value of the remaining period, given that the time is  $t$ , the delivered amount so far is  $q$ , and the current spot price is  $p$ . As seen above, there is an intimate relationship between the control and the level of the  $Q$  variable. When the problem is solved numerically, we take advantage of this. We would expect that the value  $V$  must be found for all

$p > 0$ , all  $Q \in [0, M]$  and for all  $t \in [0, T]$ . Actually this is not necessary. Let us take a closer look on the condition  $Q(T) = M$ . The restriction limits the  $Q$ -space that must be considered. See figure 1. For this problem to be well

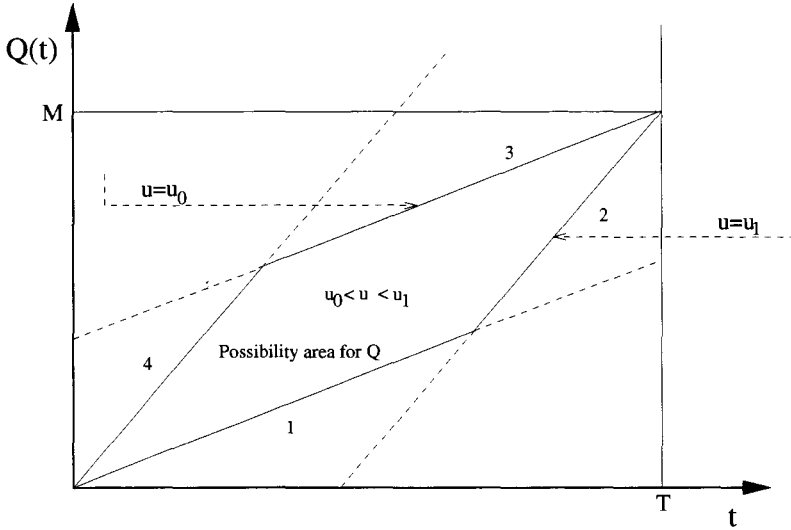


Figure 1: The possible values of  $Q(t)$ , given the restrictions on  $u_t$ .

posed we must assume that  $Tu_0 < M < Tu_1$ . The problem is trivial if one of the two extremes is binding. The upper boundaries of the parallelogram are traced out by the policy

$$\begin{aligned} u &= u_1 & \text{for } t \in [0, T_1] \\ u &= u_0 & \text{for } t \in [T_1, T] \end{aligned}$$

where

$$T_1 = \frac{M - u_0 T}{u_1 - u_0}.$$

The lower boundaries are on the other hand given by

$$\begin{aligned} u &= u_0 & \text{for } t \in [0, T_2] \\ u &= u_1 & \text{for } t \in [T_2, T] \end{aligned}$$

where

$$T_2 = \frac{u_1 T - M}{u_1 - u_0}.$$

Depending on the parameters of the problem we may have  $T_1 < T_2$ ,  $T_1 = T_2$  or  $T_2 < T_1$ .

To simplify the analysis and the numerical scheme we focus on a problem with control restrictions of the form  $[0, u_1]$ . This is no limitation since a contract with the limitation  $[u_0, u_1]$  may be modelled as a flexible load contract with  $[0, (u_1 - u_0)]$ , combined with a contract with constant delivery  $u_0$  in the same period.

### 2.3 Precise formulation

We can now formulate the optimization problem precise without a state dependent  $\mathcal{U}$ . By defining the stopping times

$$\begin{aligned}\tau_1 &= \inf\{t; Q_t = M\} \\ \tau_2 &= \inf\{t; Q_t = u_1 \cdot (t - T_2)\} \\ \tau &= \min(\tau_1, \tau_2),\end{aligned}$$

the value function can be expressed as

$$\begin{aligned}V(t, q, p) &= \max_{u \in \mathcal{U}} E_t \left\{ \int_t^\tau e^{-\delta s} \Pi(s, u_s, P_s) ds \right. \\ &\quad \left. + I_{(x=M)}(Q_\tau) F(\tau, P_\tau) + [1 - I_{(x=M)}(Q_\tau)] G(\tau, P_\tau) \right\}.\end{aligned}\tag{2.2}$$

Here the functions  $F$  and  $G$  is defined as

$$\begin{aligned}F(t, p) &= E \left[ \int_t^T e^{-\delta s} \Pi(s, u_0, P_s) ds \middle| P_t = p \right] \\ G(t, p) &= E \left[ \int_t^T e^{-\delta s} \Pi(s, u_1, P_s) ds \middle| P_t = p \right]\end{aligned}$$

Now  $\mathcal{U}$  is the space of functions taking values in  $[0, u_1]$ . It is important to keep in mind that this is not an optimal stopping problem.

### 2.4 The Hamilton Jacobi Bellman equation

First of all we assume that the instantaneous profit is given by

$$\Pi(u, P) = \alpha u P,$$

and let  $\alpha = 1$  for simplicity of notation. This turns the control problem into a problem which is completely linear in the control  $u$ . We therefore expect optimal controls of the so called 'bang-bang' type.

We want to find the value function  $V(t, q, p)$ . Define the space (see figure 2)  $\Omega(t) \subset \mathbb{R}^2$  by

$$\Omega(t) = \{(q, t) \in \{M > q > 0\} \cap \{u_1 t \geq q > u_1 \cdot (t - T_2)\}\}.$$

The function  $V : \Omega(t) \times \mathbb{R} \rightarrow \mathbb{R}$  can be found as the (viscosity) solution of the partial differential equation

$$V_t + \mu(t, p)V_p + \frac{1}{2}\sigma^2(t, p)V_{pp} + \max_{u \in \mathcal{U}}\{uV_q + e^{-\delta t}up\} = 0. \quad (2.3)$$

Here subscripts on  $V$  denotes the partial derivatives with respect to the subscript. This equation is called the Hamilton Jacobi Bellman (HJB) equation. The equation cannot be uniquely solved without proper boundary conditions.

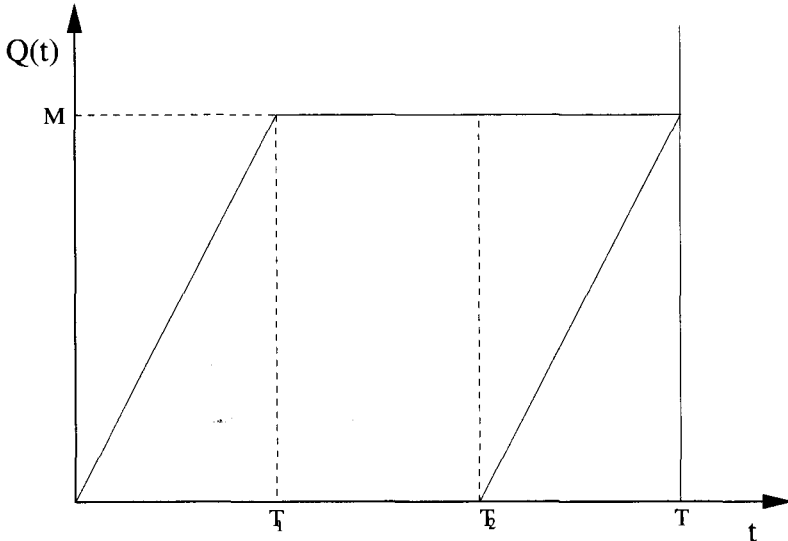


**Figure 2:** The  $(t, Q)$  projection of the parallelepiped, defining the space  $\Omega(t)$ .

We know that the value is zero at time  $T$ , i.e.

$$V(T, q, p) \equiv 0 \quad \forall \quad q, p.$$

Further,  $V(t, q, p) = F(t, p)$  when  $q = M$  and  $V(t, q, p) = G(t, p)$  when  $q = u_1 \cdot (t - T_2)$ . From the definition of  $F$  and  $G$  we see that they can be found as solutions of the following partial differential equations<sup>4</sup>

$$\begin{aligned} W_t + \mu(t, p)W_p + \frac{1}{2}\sigma^2(t, p)W_{pp} &= 0 \\ W_t + \mu(t, p)W_p + \frac{1}{2}\sigma^2(t, p)W_{pp} + u_1e^{-\delta t}p &= 0 \end{aligned} \quad (2.4)$$

both with end condition  $W(T, p) = 0$ . We see that this gives  $F(t, p) \equiv 0$ .

We now focus on the maximum operator in equation (2.3). Observe that

$$\begin{aligned} e^{-\delta t}p > -V_q &\Rightarrow u = u_1 \\ e^{-\delta t}p = -V_q &\Rightarrow u = ? \\ e^{-\delta t}p < -V_q &\Rightarrow u = u_0. \end{aligned}$$

It can be shown that the optimal control only takes the extreme values, thus a bang-bang control. This is a consequence of the risk neutral formulation.

The flexible load contract is now formulated as a stochastic control problem. Observe that the equations in this section suggests that the value function may be found by backward induction, starting at time  $T$ . To solve the problem we need to specify a reasonable spot price process. We focus on this task in the next section.

---

<sup>4</sup>Alternatively, for a price process with simple structure, the functions may be calculated directly from the definitions. We chose however to keep the presentation general with respect to the process choice.



### **3 Modelling the spot price**

We will in this chapter analyze the spot price to find a suitable stochastic differential equation that models it. After deciding upon a stochastic process we will show how we can calibrate the process parameters to data.

#### **3.1 Examining the spot price**

The Nordic spot market for electricity is a market for physical delivery of electricity. Each day at noon, spot prices and volumes for each hour the following day are determined in an auction. The spot price is the clearing price that makes the demand for a given hour match the supply. Real aggregated supply and demand curves for hour 12 on 10. July 2000 are shown in figure 3. To understand the dynamics of the spot price it helps to understand the dynamics of the aggregated supply- and demand curve. Since a high degree of all energy used for heating in the Nordic countries is electricity, the demand for electricity is closely linked to temperature. The demand for electricity is also influenced by general work activity. Due to limited choice in alternative energy forms and lack of end users that actually observe real time price movements, the demand for electricity is highly inelastic (i.e. independent of market clearing price). The inelasticity of the demand curve can be seen from the steepness of the demand curve in figure 3. From figure 4 we see that the demand follows daily, weekly and yearly cycles. We also observe a small growth in electricity demand of approximately 1% to 1.5% per year. Induced by extreme weather conditions one can on several occasions observe temporary spikes in electricity demand. These spikes are not sustainable and the demand reverts back to normal levels within a short time.

In contrast to the nearly price independent electricity demand, the supply characteristics of the electricity producers are price responsive. The supply characteristic is mainly a function of *generation technology, fuel costs, availability of generation* and the possibility of *import/export*. The supply depends, in the long run, on the production cost for electricity. In the short

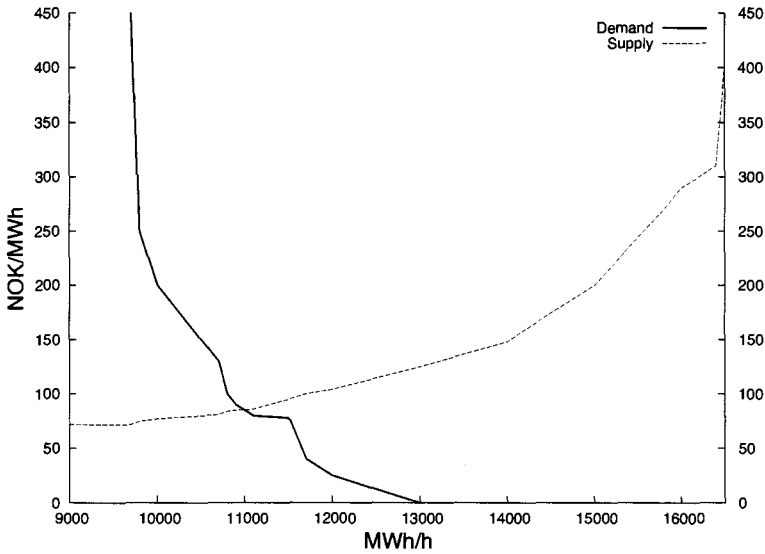


**Figure 3:** *Supply and demand curves for hour 12 on 10. July 2002.*

run the supply is influenced by production outages and constraints in the power grid. Production costs for thermal based power depends mainly on the degree of utilization and fuel costs. For hydroelectric power the production cost depends more on the reservoir filling, inflow and accumulated snow. The sum of deviation of reservoir filling and accumulated snow from the normal level is called the hydrological balance. Estimated hydrological balance together with spot price for the period 1996-2001 are shown in figure 5. From the figure we see a clear mean reversion in the hydrological balance. If we compare the hydrological balance with the spot price for the same period we see a strong negative correlation (Since we have inverted the scale in the figure it appears to be positive correlation). The empirical correlation coefficient is -0.72. The strong negative correlation is due to the fact that the hydroelectric power has a high alternative cost when the hydrological balance is below normal and a low alternative cost when the balance is above normal. The share of hydroelectric power in the Nordic electricity market is approx-

imately 60%<sup>5</sup>. It is therefore no surprise that the supply curve is strongly influenced by the hydrological balance. Since the hydrological balance is so important it is crucial that the price process we choose is able to capture its effect.

---

<sup>5</sup>The total consumption of electricity for the Nordic countries were in 2000 384 TWh, and 234 TWh of this was hydroelectric power.

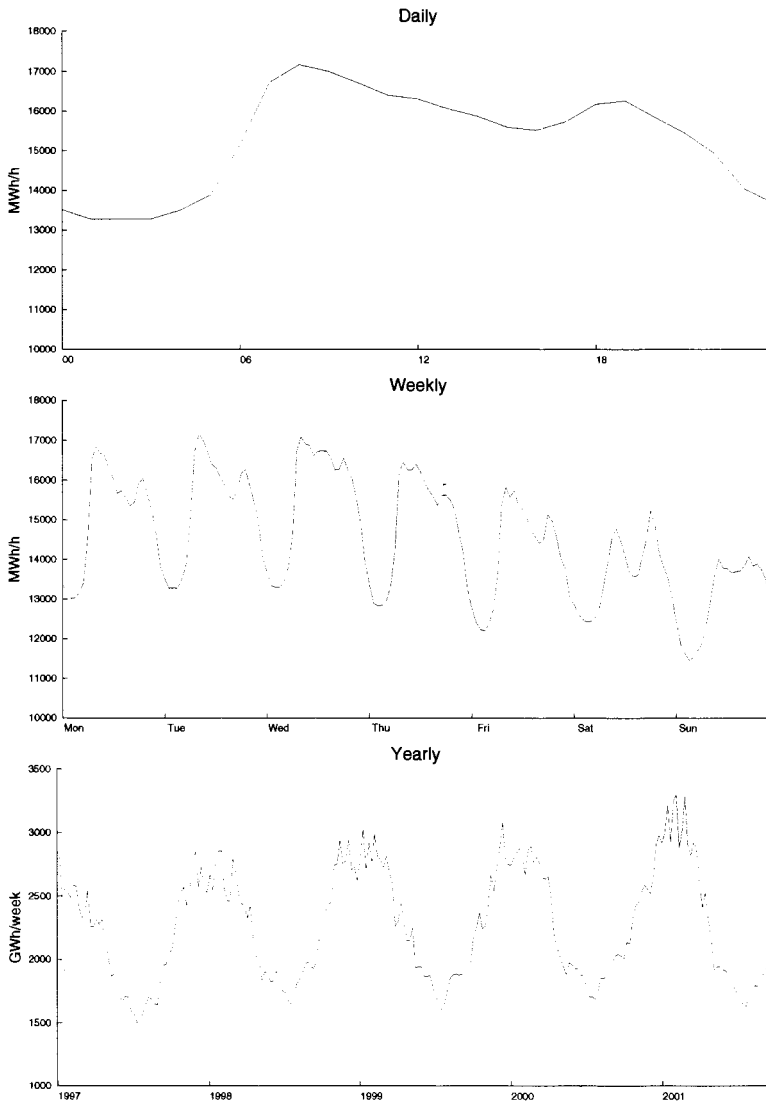


**Figure 4:** In the first figure we have total consumption of electricity in Norway during Tuesday 20. October 1998. The second figure is the total consumption during one week (19. October 1998 - 25. October 1998) and the third figure is the total consumption during a period of 4.5 years. As we can see the consumption of electricity follows daily, weekly and yearly cycles. Since the demand curve is highly inelastic we expect to find the same cycles in the electricity price.

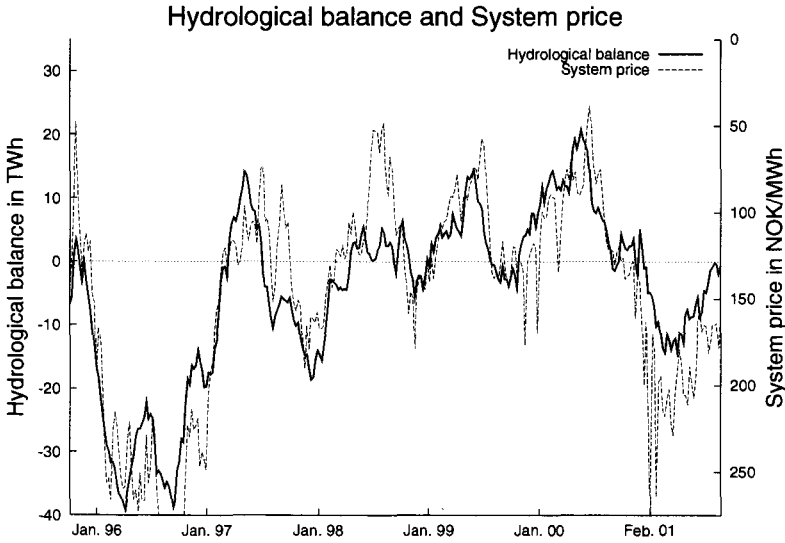


**Figure 5:** System price together with the hydrological balance. The hydrological balance is defined as the energy in snow and water minus their normal values. We have inverted the scale of the system price to illuminate the negative correlation.

### 3.2 Selecting a model

This section addresses the challenge of selecting a suitably stochastic process to model electricity prices in the Nordic electricity market. For reasons mentioned in the previous subsection the stochastic characteristics of electricity production and consumption are reflected directly in electricity prices. In addition to the lack of storability the cyclical patterns of electricity demand makes modelling the electricity price a challenge.

By analyzing the Nordic electricity market we find following important factors influencing the spot price process:

- Cyclical patterns in demand over the course of the day, week and year.
- Price spikes or fast mean reversion due to unusual load conditions.
- A slow mean reversion in price caused by mean reverting hydrological balance.

- Other factors such as fuel prices, currency exchange rates, emission costs and climate changes.

These characteristics is also found in other electricity markets, see Knittel and Roberts (2001) and Lucia and Schwartz (2002). Since we are analyzing flexible load contracts with a settlement period of approximately six to twelve months we focus on modelling the spot price dynamics within this time horizon.

In the book “Energy modelling and the management of uncertainty” (2001), B. Johnson and G. Barz analyzed how the following four stochastic differential equations managed to model the spot price for different electricity markets:

Brownian motion: 
$$dP_t = \mu_t dt + \sigma dW_t$$

Mean reversion, OU: 
$$dP_t = \kappa(\alpha_t - P_t)dt + \sigma dW_t$$

Geometric Brownian motion: 
$$dP_t = \mu_t P_t dt + \sigma P_t dW_t$$

Geometric mean reversion: 
$$dP_t = \kappa(\alpha_t + \frac{\sigma^2}{2} - \ln P_t)P_t dt + \sigma P_t dW_t$$

where  $P_t$  is the spot price of electricity,  $\mu_t$  is the drift term,  $\sigma$  is the diffusion term,  $W_t$  is a Brownian motion,  $\kappa$  is the speed of mean reversion and  $\alpha_t$  is a sort of long run mean. They tried the above models with and without jump terms. The jumps where modelled with a Poisson arrival time, Bernoulli (positive or negative) jump direction, and exponential jump magnitude. The eight models where tested on four different electricity markets. They found the best model regarding sum of log-likelihood values for the Nordic electricity market to be the mean reversion with jumps followed by the pure mean reversion model. Since we chose not to incorporate jumps into our model, we use the mean reverting Ornstein-Uhlenbeck process to model the spot price.

To model the seasonal changes in the demand curve, we need a time dependent mean. In addition we want some kind of mean reversion to capture the effect of the hydrological balance. Since this reversion is slow compared to the mean reversion generated by price spikes, we need to separate them. If we do not separate them we get a mixture of fast and slow reversion. This will result in a volatility that is so high that the daily and weekly price patterns

will vanish and a volatility that is too small to model the large deviation from the long run mean due to the hydrological balance. We specify the price process as  $P_t = X_t + D_t$ , where  $X_t$  represents the low frequent changes and  $D_t$  represents the high frequent changes. It is now possible to model the slow hydrological mean reversion together with annual seasons in  $X_t$ , and high frequent changes such as fluctuation in price over the course of the day or a week in  $D_t$ . We define the high frequent changes,  $D_t$ , as changes within one week and  $X_t$  as all other changes. Further we specify changes in  $X_t$  as

$$dX_t = a_t(b_t + \frac{b'_t}{a_t} - X_t)dt + \sigma_t dW_t, \quad X_s = x_s, \quad s < t \quad (3.1)$$

where  $a_t$  is the speed of mean reversion due to hydrological balance,  $b_t$  is the normal seasonal price,  $b'_t$  is the derivative and  $\sigma_t$  is the price volatility. We specify the normal seasonal price,  $b_t$ , and  $D_t$  as a sum of trigonometric functions.

$$\begin{aligned} b_t &= b_0 + \sum_{j=1}^k R_j^X \cos(\omega_j^X t + \phi_j^X) \\ &= b_0 + \sum_{j=1}^k \{A_j^X \cos(\omega_j^X t) + B_j^X \sin(\omega_j^X t)\} \\ D_t &= d_0 + \sum_{j=1}^l R_j^D \cos(\omega_j^D t + \phi_j^D) \\ &= d_0 + \sum_{j=1}^l \{A_j^D \cos(\omega_j^D t) + B_j^D \sin(\omega_j^D t)\} \end{aligned} \quad (3.2)$$

where  $A_j = R_j \cos(\phi_j)$ ,  $B_j = -R_j \sin(\phi_j)$ ,  $\omega$  is the frequency,  $\phi$  is the phase,  $R$  is the amplitude and  $b_0$  is a constant level. The parameter  $d_0$  will later be used to ensure that the process  $D_t$  starts at zero every week. Choosing appropriate frequencies, phases and amplitudes we can model the daily, weekly and yearly price patterns. By specifying  $b_t$  and  $D_t$  as we did in (3.2) we could alternatively simplify  $P_t$  by incorporating  $D_t$  in  $b_t$  as an extension to the sum of trigonometric functions. Since we are going to use different sampling intervals for the estimation of the parameters in  $X_t$  and  $D_t$ , we will

keep  $D_t$  separated from  $b_t$ . The explicit solution to the price process,  $P_t$ , is given by

$$P_t = (P_s - D_s - b_s)e^{-\int_s^t a_u du} + D_t + b_t + \int_s^t \sigma_u e^{-\int_u^t a_r dr} dW_u \quad (3.3)$$

If we let  $a_t = a$ ,  $\sigma_t = \sigma$  we can write  $P_t$  as

$$P_t = (P_s - D_s - b_s)e^{-a(t-s)} + D_t + b_t + \sigma\left(\frac{1 - e^{-2a(t-s)}}{2a}\right)^{1/2}\varepsilon \quad (3.4)$$

where  $\varepsilon$  is a standard normal distributed random variable. From the above equation we see that the Gaussian process,  $P_t$ , has an conditional mean equal to  $(P_s - D_s - b_s)e^{-a(t-s)} + D_t + b_t$  and a conditional standard deviation equal to  $\sigma\left(\frac{1 - e^{-2a(t-s)}}{2a}\right)^{1/2}$ . Since the expected value of  $P_t$ , when  $t \rightarrow \infty$ , is equal to  $b_t + D_t$ , we can interpret  $b_t + D_t$  as the long run mean function for the price process.

### 3.3 Parameter estimation method

In the previous section we chose a stochastic differential equation with solution given by equation (3.4) to model the spot price. In this section we will show how to estimate all the parameters in this process. Since the distribution of  $P_t$  is known, we can make use of the maximum likelihood estimation method. Let the parameter vectors  $\alpha = \{a, \sigma, \omega_1^X, \dots, \omega_k^X, \omega_1^D, \dots, \omega_l^D\}$  and  $\beta = \{b_0, A_1^X, \dots, A_k^X, B_1^X, \dots, B_k^X, A_1^D, \dots, A_l^D, B_1^D, \dots, B_l^D\}$ . The reason for collecting the parameters into two vectors is to shorten our notation and, as we see later, we can use different methods to obtain the estimates of the different parameter vectors.

Let  $\mathbf{P} = [p_{t_1}, p_{t_2}, \dots, p_{t_n}]$  be a vector of observations of  $P_t$  at  $t = t_1, t_2, \dots, t_n$ . The maximum likelihood estimates  $\tilde{\alpha}$  and  $\tilde{\beta}$  are the solution to the following maximization problem

$$(\tilde{\alpha}, \tilde{\beta}) = \arg \max_{\alpha, \beta} \Psi(\mathbf{P}, \alpha, \beta) \quad (3.5)$$



where  $P_t \sim \mathbb{N}\left(m(p_{t_i}|p_{t_{i-1}}; \alpha, \beta), s(\alpha)\right)$  and

$$\begin{aligned}\Psi(\mathbf{P}, \alpha, \beta) &= \sum_{i=1}^n \log f(p_{t_i}|p_{t_{i-1}}; \alpha, \beta), \\ f(p_{t_i}|p_{t_{i-1}}; \alpha, \beta) &= \frac{1}{\sqrt{2\pi}s(\alpha)} \exp\left\{-\frac{(p_{t_i} - m(p_{t_i}|p_{t_{i-1}}; \alpha, \beta))^2}{2s(\alpha)^2}\right\} \\ m(p_{t_i}|p_{t_{i-1}}; \alpha, \beta) &= (p_{t_{i-1}} - D_{t_{i-1}} - b_{t_{i-1}})e^{-a(t_i - t_{i-1})} + D_{t_i} + b_{t_i} \\ s(\alpha) &= \sigma\left(\frac{1 - e^{-2a(t_i - t_{i-1})}}{2a}\right)^{1/2}.\end{aligned}$$

This maximization problem has a parameter space of  $3(k + l + 1)$  dimensions.

As we discovered in the first section of this chapter the spot price has three distinct seasons. The seasons have periods of one day, one week and one year. To get a realistic representation of the spot price we need at least two trigonometric functions to represent each season. With  $k = 2$  and  $l = 4$  the maximization problem given by (3.5) has a 21 dimensional parameter space. Numerically solving a maximization problem with such a high degree of freedom can be difficult. To simplify the problem we fix the frequencies  $\omega_j^X$  and  $\omega_j^D$  to

$$\begin{aligned}\omega_1^X &= 2\pi/8760 & \omega_2^X &= 2\pi/4380 & (\text{year}) \\ \omega_1^D &= 2\pi/168 & \omega_2^D &= 2\pi/84 & (\text{week}) \\ \omega_3^D &= 2\pi/24 & \omega_4^D &= 2\pi/12 & (\text{day})\end{aligned}$$

We have here assumed an hourly sampling resolution of  $\mathbf{P}$ . The frequencies in the left column makes the long run mean follow cycles with a period of one year, one week and one day. The frequencies in the right column are set to one half of the frequencies in the left column. The reason for this is to make the long run mean able to model non-symmetric seasons. With fixed frequencies we only need to estimate 15 parameters with maximum likelihood. To further reduce the number of parameters to be estimated by

maximum likelihood we reformulate (3.4) as

$$\begin{aligned}
 Y_{t_i} = & b_0 Z_0(t_i) + \sum_{j=1}^k A_j^X Z_j^{AX}(t_i) + \sum_{j=1}^k B_j^X Z_j^{BX}(t_i) \\
 & + \sum_{j=1}^l A_j^D Z_j^{AD}(t_i) + \sum_{j=1}^l B_j^D Z_j^{BD}(t_i) + \varepsilon_{t_i}
 \end{aligned} \tag{3.6}$$

where

$$\begin{aligned}
 Y_{t_i} &= (p_{t_i} - p_{t_{i-1}} e^{-a(t_i - t_{i-1})}) / s(\alpha) \\
 Z_0(t_i) &= (1 - e^{-a(t_i - t_{i-1})}) / s(\alpha) \\
 Z_j^{AX}(t_i) &= \{\cos(\omega_j^X t_i) - e^{-a(t_i - t_{i-1})} \cos(\omega_j^X t_{i-1})\} / s(\alpha) \\
 Z_j^{BX}(t_i) &= \{\sin(\omega_j^X t_i) - e^{-a(t_i - t_{i-1})} \sin(\omega_j^X t_{i-1})\} / s(\alpha) \\
 Z_j^{AD}(t_i) &= \{\cos(\omega_j^D t_i) - e^{-a(t_i - t_{i-1})} \cos(\omega_j^D t_{i-1})\} / s(\alpha) \\
 Z_j^{BD}(t_i) &= \{\sin(\omega_j^D t_i) - e^{-a(t_i - t_{i-1})} \sin(\omega_j^D t_{i-1})\} / s(\alpha)
 \end{aligned}$$

The solution of the stochastic differential equation is now linear in the  $\beta$  parameters, and by following the principles of concentrated likelihood we can use ordinary least square to obtain an estimate of  $\beta$ . See Koopmans and Hood (1953) for more details regarding concentration of likelihood. By specifying the frequencies and reformulating (3.4) we were able to reduce the number of parameter to be estimated by maximum likelihood from 21 to 2. Solving equation (3.5) is thus equal to solving

$$(\tilde{\alpha}, \hat{\beta}) = \arg \max_{\alpha} \Psi \left( \mathbf{P}, \alpha, \hat{\beta}(\alpha) \right) \tag{3.7}$$

where  $\hat{\beta} = \{\hat{b}_0, \hat{A}_1^X, \dots, \hat{A}_k^X, \hat{B}_1^X, \dots, \hat{B}_k^X, \hat{A}_1^D, \dots, \hat{A}_l^D, \hat{B}_1^D, \dots, \hat{B}_l^D\}$  is the ordinary least squares estimate. The procedure used to solve this maximization problem is as follows: First we start with an initial guess  $\alpha$ , and find the corresponding  $\hat{\beta}(\alpha)$  by OLS. The OLS-estimates together with  $\alpha$  are then used to calculate the value of the log likelihood function. This procedure is then repeated until we find the  $\alpha$  that maximizes the log likelihood function and thereby solving the problem. We will later in section 6 use (3.7) on historical price data to estimate the parameters of the spot price process.

## 4 Numerical solution

In this section we show how the problem formulated in section 2 can be solved numerically on a discrete state space.

### 4.1 Discretization

To solve the problem on a computer we need to discretize the time and state space. In this market the natural smallest time scale is one hour, and this is chosen as the basic time discretization. In combination with the limitations on the control, this also gives the discretization of the  $Q$  space, see figure 6. The parameters of the traded contacts are typically specified such that  $T_1, T_2$  and  $T$  are all integers. The price space is truncated and divided into  $N$

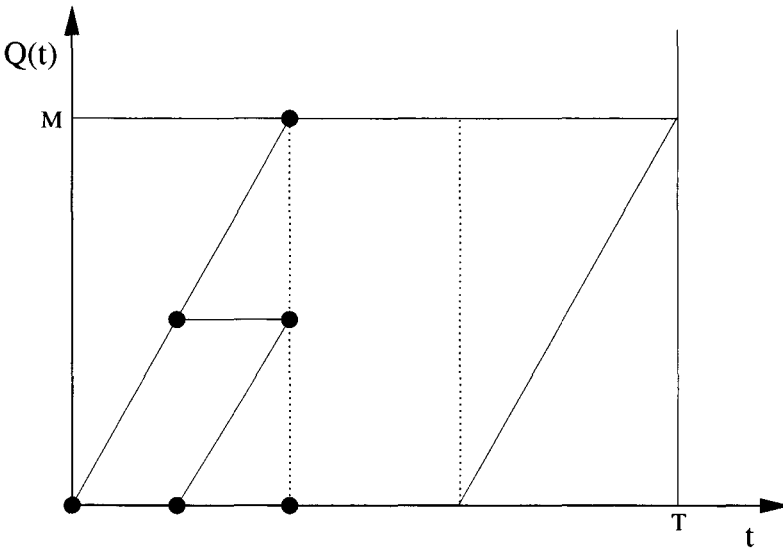


**Figure 6:** *The natural nodes in the  $Q$ -space.*

uniform intervals. The value function is found in every node of the three dimensional parallelepiped in the  $(t, q, p)$ -space. We use backward induction, starting at time  $T$ .

The time horizon  $T$  is typically measured in whole hours. If  $T_1 = \frac{M}{u_1}$  is an

integer number of hours<sup>6</sup>, it is natural to use one hour as the basic discrete time interval. In this case both  $T_1$  and  $T_2$  are reached after an integer number of periods. The initial time node is denoted 0, the last node is  $T$ , that is,

$$0 = t_0, \dots, t_T = T$$

totally  $T + 1$  nodes. The control applied in the first hour is found in time-node 0.

The time discretization combined with the control gives a natural discretization of the  $Q$  space into  $T_1 + 1$  nodes, see figure 7. Totally the  $(Q, t)$  space consists of  $(T_1 + 1)(T - T_1 + 1)$  nodes<sup>7</sup>.

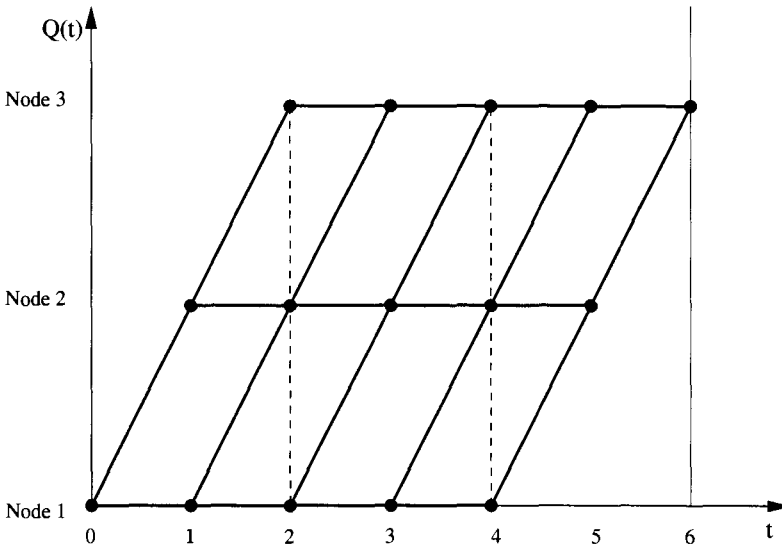


Figure 7: The discretization of the  $(t, Q)$ -space.

The price process  $P_t$  studied in section 3 is unbounded. The infinite  $P$ -space must therefore be truncated before the optimization problem can be solved numerically. Assume that the process can only take values in  $[\underline{P}, \overline{P}]$ .

<sup>6</sup>This is typically the case for the traded contracts. To increase numerical stability we may introduce e.g. four sub steps within each hour.

<sup>7</sup>For the test case we have  $T_1 = 1667$  and  $T = 3672$ . Therefore, with the  $P$  space divided into 100 intervals, we get 335 million nodes in the three dimensional parallelepiped.

This interval is represented discretely as  $\{\underline{P}, \underline{P} + \Delta P, \underline{P} + 2 \cdot \Delta P, \dots, \underline{P} + N \cdot \Delta P, \overline{P}\}$  that is,  $P_i = \underline{P} + i \cdot \Delta P$ .

## 4.2 The numerical scheme

On the grid previously stated, we define

$$V_{i,j}^k = V(t_k, q_i, p_j).$$

This is a discrete approximation to the continuous value function<sup>8</sup> in equation (2.1), see page 73. After the choice of control the HJB equation (2.3) reduces to the partial differential equation

$$V_t + \mu(t, p)V_p + \frac{1}{2}\sigma^2(t, p)V_{pp} + \hat{u}V_q + e^{-\delta t}\hat{u}p = 0 \quad (4.1)$$

where  $\hat{u}$  is either 0 or  $u_1$ .

Let us first focus on the interior of the  $P$ -space. We use finite difference to approximate the derivatives of  $V$ . At time  $t_k$  we use the known value function  $V^{k+1}$  to approximate  $V_q$  while the unknown  $V^k$  is used for  $V_p$ . Therefore the scheme is explicit in the  $q$ -variable and implicit in  $p$ . We use

$$\begin{aligned} \frac{\partial}{\partial t} \{V_{i,j}^k\} &\approx \frac{V_{i,j}^{k+1} - V_{i,j}^k}{\Delta t} \\ \frac{\partial}{\partial q} \{V_{i,j}^k\} &\approx \frac{V_{i+1,j}^{k+1} - V_{i,j}^{k+1}}{\Delta q} \\ \frac{\partial}{\partial p} \{V_{i,j}^k\} &\approx \begin{cases} \frac{V_{i,j+1}^k - V_{i,j}^k}{\Delta p} & \text{when } \mu \geq 0 \\ \frac{V_{i,j}^k - V_{i,j-1}^k}{\Delta p} & \text{when } \mu < 0. \end{cases} \\ \frac{\partial^2}{\partial p^2} \{V_{i,j}^k\} &\approx \frac{V_{i,j+1}^k - 2V_{i,j}^k + V_{i,j-1}^k}{(\Delta p)^2} \end{aligned}$$

This is a downwind-upwind discretization of  $\frac{\partial V}{\partial p}$ . Observe that the approximation is done in the flow-direction of the underlying process. Define

$$\begin{aligned} \mu^+ &= \max(\mu, 0) \\ \mu^- &= \max(-\mu, 0). \end{aligned}$$

---

<sup>8</sup>We denote the approximation and the true (continuous) function as  $V$ . When this is unclear, the continuous function is called  $\hat{V}$ .

Observe that  $\mu^+ + \mu^- = |\mu|$  and  $\mu^+ - \mu^- = \mu$ . Inserting the above approximations into (4.1) we get

$$\begin{aligned} \frac{V_{i,j}^{k+1} - V_{i,j}^k}{\Delta t} &+ (\mu_j^k)^+ \frac{V_{i,j+1}^k - V_{i,j}^k}{\Delta p} - (\mu_j^k)^- \frac{V_{i,j}^k - V_{i,j-1}^k}{\Delta p} \\ &+ \frac{1}{2}(\sigma_j^k)^2 \frac{V_{i,j+1}^k - 2V_{i,j}^k + V_{i,j-1}^k}{(\Delta p)^2} + \hat{u} \frac{V_{i+1,j}^{k+1} - V_{i,j}^{k+1}}{\Delta q} + e^{-\delta t_k} \hat{u} p_j = 0 \end{aligned}$$

Using that  $\Delta q = \Delta t u_1$ ,  $\hat{u} \in \{0, u_1\}$  and collecting the terms, we get

$$\begin{aligned} \frac{V_{i+1,j}^{k+1} - V_{i,j}^k}{\Delta t} &+ (\mu_j^k)^+ \frac{V_{i,j+1}^k - V_{i,j}^k}{\Delta p} - (\mu_j^k)^- \frac{V_{i,j}^k - V_{i,j-1}^k}{\Delta p} \\ &+ \frac{1}{2}(\sigma_j^k)^2 \frac{V_{i,j+1}^k - 2V_{i,j}^k + V_{i,j-1}^k}{(\Delta p)^2} + e^{-\delta t_k} u_1 p_j = 0 \end{aligned}$$

when  $\hat{u} = u_1$ . When  $\hat{u} = 0$  the equation is

$$\begin{aligned} \frac{V_{i,j}^{k+1} - V_{i,j}^k}{\Delta t} &+ (\mu_j^k)^+ \frac{V_{i,j+1}^k - V_{i,j}^k}{\Delta p} - (\mu_j^k)^- \frac{V_{i,j}^k - V_{i,j-1}^k}{\Delta p} \\ &+ \frac{1}{2}(\sigma_j^k)^2 \frac{V_{i,j+1}^k - 2V_{i,j}^k + V_{i,j-1}^k}{(\Delta p)^2} = 0. \end{aligned}$$

Observe that this may be seen as discrete representations of (2.4) with the convention that we move up in the  $Q$ -grid over the time step when  $u_1$  is chosen.

Since we use backward induction,  $V^{k+1}$  is completely known at time  $t_k$ . At the boundaries two and three (see figure 2 on page 76) the control must be  $u_1$  and 0 respectively, that is, there is no choice here. At these boundaries the value function is equal to the functions  $G$  and  $F$ . At the boundaries one and four, and in the interior both control choices may be used.

The above scheme can be organized as

$$a_j^k V_{i,j-1}^k + b_j^k V_{i,j}^k + c_j^k V_{i,j+1}^k = e^{-\delta t_k} u_{i,j}^k p_j \Delta t + W_{i,j}^{k+1}(u_{i,j}^k) \quad (4.2)$$

where

$$\begin{aligned} a_j^k &= - \left( (\mu_j^k)^- \frac{\Delta t}{\Delta p} + \frac{1}{2} (\sigma_j^k)^2 \frac{\Delta t}{\Delta p^2} \right) \\ b_j^k &= 1 + |\mu_j^k| \frac{\Delta t}{\Delta p} + (\sigma_j^k)^2 \frac{\Delta t}{\Delta p^2} \\ c_j^k &= - \left( (\mu_j^k)^+ \frac{\Delta t}{\Delta p} + \frac{1}{2} (\sigma_j^k)^2 \frac{\Delta t}{\Delta p^2} \right) \\ W_{i,j}^{k+1}(\hat{u}) &= \begin{cases} V_{i,j}^{k+1} & \text{when } \hat{u} = 0 \\ V_{i+1,j}^{k+1} & \text{when } \hat{u} = u_1. \end{cases} \end{aligned}$$

At the boundaries 2 and 3 of the  $(Q, t)$ -space (see figure 1 on page 74)  $\hat{u}$  is known. At each time step  $t_k$  and for each  $Q$ -node  $q_i$  away from these boundaries we find the optimal control

$$u_{i,j}^k = \arg \max_{u \in \{0, u_1\}} (e^{-\delta t_k} u p_j \Delta t + W_{i,j}^{k+1}(u)),$$

and thereby also the righthand side of the linear system of equations defined by equation (4.2).

Before we focus on the discretization on the boundaries of the  $P$ -space, we show how the above scheme may be linked to a Markov chain approximation of the underlying stochastic process.

With reference to the book by Kushner and Dupuis (2001) we note that the scheme (4.2) may be written as

$$V_{i,j}^k = \sum_{l=\{j-1, j+1\}} p(i, l; k, k) V_{i,l}^k + p(i, j; k, k+1) [W_{i,j}^{k+1}(u_{i,j}^k) + e^{-\delta t_k} u_{i,j}^k p_j \Delta t]$$

with the following definition of the ‘‘probabilities’’;

$$\begin{aligned} p(i, j-1; k, k) &= -\frac{a_j^k}{b_j^k} \\ p(i, j+1; k, k) &= -\frac{c_j^k}{b_j^k} \\ p(i, j; k, k+1) &= \frac{1}{b_j^k}. \end{aligned}$$

Observe that  $p(\cdot) \geq 0$  and  $\sum p = 1$ . With this representation we see that this scheme may be associated with a Markov chain approximation of the price process. The chain lives in the discrete  $(p, t)$  space, and time is treated as just another state variable. At each period there is only a certain probability that a time step is taken. See figure 8. This intuition proves useful when we study the boundaries of the  $P$ -space in the next subsection.

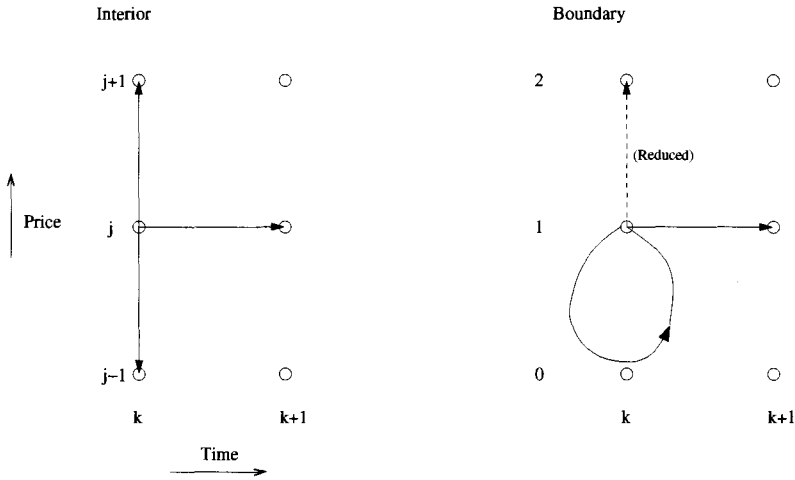


Figure 8: The Markov chain interpretation, with reflection on the boundary.

### 4.3 The boundaries of the price space

In this section we study the boundaries of the truncated  $P$ -space  $[\underline{P}, \overline{P}]$ . Two different types of boundary conditions are used. We first present the method called “Absorption”. This type of boundary conditions typically arise when a process is absorbed in a boundary node, and a specified value is known in that node. In this case conditions are put directly on the value function. In the theory of partial differential equations such boundary conditions is called “Dirichlet” conditions.

The second method is called “Reflection”, and must be used when we study a process that is reflected at a boundary. In this case it is important that the discrete Markov chain is reflected in the proper direction. This can



be seen to correspond to conditions on the derivative of the value function, so called “Neumann” conditions.

We now show in detail how these boundary conditions affects the above scheme.

### 4.3.1 Absorption

We first focus on how absorption may be implemented. Suppose that the value  $V_{i,j}^k$  is known (or approximated) for all  $k, i$  at the boundaries of the  $P$ -space, that is,

$$\begin{aligned} V_{i,0}^k &= \tilde{V}(t_k, q_i, \underline{P}) \\ V_{i,N+1}^k &= \tilde{V}(t_k, q_i, \overline{P}) \end{aligned}$$

for all  $i, k$ . Next to the lower boundary the equation (4.2) must be changed to

$$b_1^k V_{i,1}^k + c_1^k V_{i,2}^k = e^{-\delta t_k} u_{i,1}^k p_1 \Delta t + W_{i,1}^{k+1}(u_{i,1}^k) - a_1^k \tilde{V}(t_k, q_i, \underline{P})$$

and

$$b_N^k V_{i,N}^k + a_N^k V_{i,N-1}^k = e^{-\delta t_k} u_{i,N}^k p_N \Delta t + W_{i,N}^{k+1}(u_{i,N}^k) - c_N^k \tilde{V}(t_k, q_i, \overline{P})$$

at the upper. Remember that  $p_0 = \underline{P}$  and  $p_{N+1} = \overline{P}$ .

In this subsection the value function were taken as given at the boundary. The problem is that it may be hard to say anything meaningful about this value in advance. The error done in this specification typically propagate towards the center of the grid. It is damped as it gets far away from the boundary, but still this may be a problem for the scheme, especially when the volatility (modelled by  $\sigma$ ) is large. The solution is to truncate the price process at levels far away from the regions of interest. Further, we must keep an eye on the approximate solution near the boundaries, and adjust the specifications if it is clearly inconsistent with the real value function. Such methods are quite easy to implement, but is costly since the grid must be enlarged and the resulting value function inspected carefully.

### 4.3.2 Reflection

Reflection is an alternative to the method studied in the previous section. The idea is easier grasped when we think of our scheme as a (Markov chain) approximation of the movements of the price process. Instead of letting the process be absorbed at the boundaries as in the last section, we now assume that the process is reflected at the boundaries. This may be seen as a condition on the derivative of the value function, and as such, a weaker condition.

When the real process possess reflection, it is important that the reflection in the scheme is implemented in a consistent manner. The process we study has no natural reflection. We have therefore freedom to choose the approximation. What the most efficient reflection looks like is not obvious in advance, and we found a good approximation by experimentation.

At the boundaries the chain was reflected back into the grid, we here use the lower boundary as an illustration. When the chain goes from node 1 to node 0 it is immediately returned to node 1, i.e. the probability  $p(1, 1; t, t)$  is positive. Now the expected movement of the process is shifted upwards. To reduce this effect, we decrease  $p(1, 2; t, t)$  and increase  $p(1, 1; t, t)$  further. For our problem this procedure proved efficient.

We here present the chosen probabilities at node 1,

$$\begin{aligned} p(1, 1; t, t) &= -\frac{2a_1}{b_1} \\ p(1, 1; t, t+1) &= \frac{1}{b_1} \\ p(1, 2; t, t) &= -\frac{c_1 - a_1}{b_1}, \end{aligned}$$

where  $a, b$  and  $c$  (we have suppressed the time index) is defined on page 92. We see that they sum to unity. Further, if the drift is positive at node 1, they are all positive and less than one. Therefore we may interpret them as transition probabilities. The procedure is similar at node  $N$ .

#### 4.4 Implementation of the scheme

Our problem is time dependent, with very explicit periodicity on a daily, weekly and yearly scale. Further, the mean reversion effect is small. This means that the drift of the process change sign during the day. We may therefore suspect that the reflection procedure at node 1 is a good approximation when the drift is positive, but poor when the drift is very negative. Opposite in node  $N$ . We have therefore implemented absorption when the drift is smaller than a chosen level (e.g. zero). The value associated with the absorbing node is approximated as the value at the previous time step. Then the unknowns  $V_{i,1}^k, \dots, V_{i,N}^k$  may be found as the solution of the system of linear equations defined in equation (4.3). Afterwards  $V_{i,0}^k$  and  $V_{i,N+1}^k$  can be approximated with interpolation of their neighboring values.

To illustrate the above discussion we present the scheme in a situation where reflection is used on the lower boundary, and absorption on the upper. We can find  $V_{i,j}^k$  for all  $k, i, j$  by the following procedure

1.  $V_{i,j}^T = 0$  is given from the end conditions.
2. When  $V_{i,j}^{k+1}$  is given, find  $\bar{V} = [V_{i,1}^k, \dots, V_{i,N}^k]$  as the solution of the following linear system of equations (For simplicity of notation, we suppress the sub- and superscripts of  $V, A$  and  $G$ .)

$$AV = G \tag{4.3}$$

where

$$A = \begin{bmatrix} \tilde{b}_1 & \tilde{c}_1 & 0 & 0 & \dots \\ a_2 & b_2 & c_2 & 0 & \dots \\ \vdots & \ddots & \ddots & \ddots & \vdots \\ 0 & \dots & a_{N-1} & b_{N-1} & c_{N-1} \\ 0 & \dots & 0 & a_N & b_N \end{bmatrix}$$

and

$$G = \begin{bmatrix} e^{-\delta t_k} u_{i,1}^k p_1 \Delta t & + & W_{i,1}^{k+1}(u_{i,1}^k) \\ e^{-\delta t_k} u_{i,2}^k p_2 \Delta t & + & W_{i,2}^{k+1}(u_{i,2}^k) \\ & & \vdots \\ e^{-\delta t_k} u_{i,N-1}^k p_{N-1} \Delta t & + & W_{i,N-1}^{k+1}(u_{i,N-1}^k) \\ e^{-\delta t_k} u_{i,N}^k p_N \Delta t & + & W_{i,N}^{k+1}(u_{i,N}^k) - c_N V_{i,N+1}^k \end{bmatrix}$$

Here

$$\begin{aligned} \tilde{b}_1 &= b_1 + 2a_1 \\ \tilde{c}_1 &= c_1 - a_1. \end{aligned}$$

This system of equations is tridiagonal and can be solved efficiently by Gauss elimination.

3. Iterate from step 2.

Observe that the coefficients  $a, b, c$  of the  $A$  matrix are independent of the control and the  $Q$ -level. Therefore, at a given instant  $t_k$ , the  $A$  matrix is the same for all  $Q$ -levels. The three-diagonal system of equations is solved once, with a loop calculating the solutions corresponding to the different righthand sides. This improves the efficiency of the algorithm considerably. Also observe that  $b_i \geq 1.0$ , and that the matrix  $A$  is strictly diagonal dominant. This secures the stability of the scheme.

## 4.5 The control matrix

The algorithm in the previous section calculates the value and the optimal control in each node of the grid. As previously pointed out, the grid may typically have more than 300 million nodes. Consequently it is inefficient to store all the information. We chose to store the value only at the first time step. This gives an estimate for the initial value of the contract. The

value of the contract may be interesting at later time steps if the contract is re-traded, but we put this aside at the present.

The optimal control is however needed at each node of the grid. Still the structure of the problem gives a limited demand for storage. The point may be explained by the following argument.

Suppose the time is  $t_k$  and the current price is  $p_l$ . Focus on the amount delivered up to this point, i.e  $Q_t$ . If we choose to deliver  $u_1$  for  $Q_t = q_j$ , then we chose  $u_1$  for all  $q_m$  where  $m < j$ . Therefore we need only keep the critical  $q_{\hat{n}}$  such that

$$u = \begin{cases} u_1 & \text{for } n < \hat{n} \\ 0 & \text{for } n \geq \hat{n}. \end{cases}$$

This critical level must be found for all  $t_k$  and all  $p_l$ , thus giving a  $N \times T$  matrix. See figure 9. If the process parameters are fixed for the whole

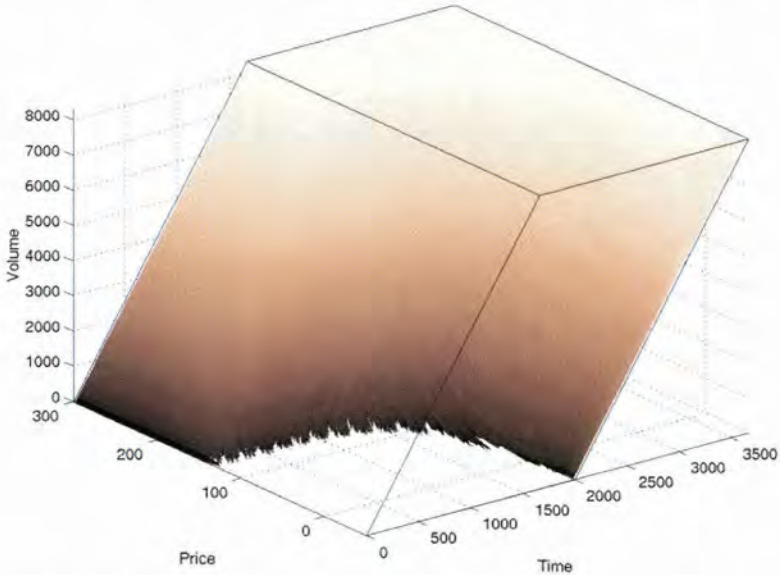


**Figure 9:** *The control matrix for the FLC described in the introduction.*

period, this matrix is generated only once. This can be quite time consuming, especially when the contract horizon is long.

The real observed price is now used to find the optimal control for each hour, and to calculate the realized value of the contract. In section 6 we use this algorithm to analyze several different contracts. The resulting control policy is compared to the strategy of competitors in the market.

## 4.6 Deterministic test

It is important to try to check the results generated by the numerical algorithm. For this problem we have no explicit solution to compare with. Still, if we let  $\sigma \equiv 0$ , we may test the algorithm by the following method.

Suppose we study a contract over the period<sup>9</sup>  $[0,168]$  and that we have to find the 100 hours with the highest price. If the price process is purely deterministic, the price is known for the whole period at time 0. It is therefore a simple task to find the hours to exercise the contract. The time 0 value we achieve (called explicit solution below) is compared with the value calculated by our algorithm. The price grid is  $[-50,300]$  with  $\Delta p = 3.846$ . In the time space we use  $\Delta t = 1$ . The results are presented in table I. Relative error is the absolute error divided by the explicit solution. Observe that

**Table I:** *Deterministic test of the algorithm*

Price time 0	Explicit solution	Algorithm	Absolute error	Relative error
-23	-14666	-6988	7678	-0.520
0	7597	8821	1224	0.160
50	55840	54311	-1529	-0.027
100	104104	102461	-1643	-0.016
150	200789	198949	-1840	-0.009
250	249205	245088	-4117	-0.017

the numerical scheme is good in the middle of the grid but worse close to the boundaries, especially at the lower boundary. The error close to the boundaries is expected. We can however not explain the asymmetry in the error.

In this version of the paper we do not include the proof for convergence

<sup>9</sup>For simplicity, we study a contract with a short settlement period.

of the algorithm. This proof is rather technical and does not give any new intuition for a reader interested in applications.

## 4.7 Remarks

The above scheme has transition only to neighboring<sup>10</sup> nodes. This limits the possible movements of the process from hour to hour. The weakness of this implementation may be dealt with in different ways. One possibility is to use non-local finite difference approximations. Another is to introduce intermediate time steps, where the control is inherited from the large time step of one hour.

An easier way to more flexible movements of the process is to introduce intermediate time steps. At each small step the optimal control is found. The control for the present hour is the accumulated controls for the sub-steps. We have promising results using this method, but the full study of this extension is left for future work.

---

<sup>10</sup>From one time step to the next the Markov chain may move to other nodes. This is because the probability that a time step is actually taken is less than 1.0. If a fully explicit scheme was used, the chain had been limited to the neighboring nodes. This motivates, from a Markov chain perspective, why implicit schemes are more stable than explicit schemes.

## 5 Data and estimation

We have chosen a stochastic process for the spot price and developed a numerical algorithm to find the value and optimal policy for a flexible load contract. The next step is to implement our algorithm. To do this we need to estimate the price process from historical prices.

### 5.1 Price data

To estimate the parameters in the price process we use historical spot prices obtained from Nord Pool. The spot price is called *system price*, and is the price in NOK for one MWh of electricity for a given hour. Our data sample consists of 76 608 hourly prices from 4. January 1993 to 1. October 2001. See figure 10 for a graphical illustration of the data sample. There were no missing data but the prices were in a standard time format. Since cyclical patterns of electricity demand over the course of a day mostly depends on the time shown by the clock and not the time implied by the sun, we need to adjust for daylight saving time. To adjust for daylight saving time we inserted one fictitious price observation in the spring and removed one in the autumn. The observation we inserted in the spring was the average of the price value before and after. If we do not adjust for daylight saving time we will get a phase shift between the daily patterns on a winter day and the daily patterns on a summer day.

Another characteristic of our data sample is that it includes several price spikes due to unusual load conditions. Since we chose a price process without a jump term we are unable to model price spikes or fast mean reversion directly. We must therefore be careful not to let the spikes influence the parameter estimation too much. By closer inspection it seems that the price spikes mainly occurs in the morning or in the afternoon, with a duration of one to six hours. Fortunately the data sample used to estimate the parameters in the weekly process,  $X_t$ , does not include many spikes. The reason for this is that the data sample consist of the first hour on every Monday and



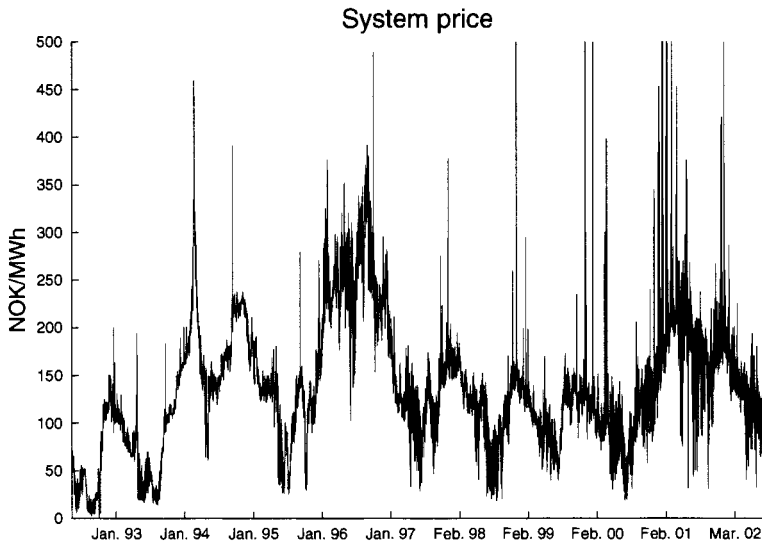


**Figure 10:** System price for the period 4. January 1993 to 1. October 2001, a total of 76 608 hours. Since we have plotted hourly prices we can more clearly see the occasional price spike. We can also see periodicity in the price.

at this time of the night the demand is low and price spikes rarely occurs. Since the intra-weekly process,  $D_t$ , is deterministic an occasional spike does not influence the estimation much. If we look at the descriptive statistics in table II the price spikes shows up as increased skewness and kurtosis. We can also see from figure 10 that the occurrences of price spikes has increased dramatically the last three years. The descriptive statistics also indicate that the spot price is lower and more volatile in the summer than the rest of the year. The low price is due to the seasonal pattern of electricity consumption, and the high volatility is because of deviations in hydrological balance.

## 5.2 FLC data

To be able to compare our algorithm to real market participants we have managed to get hold of an unique data-set. The data-set consist of historical FLC policies for nine real market participants. The policies are for two kinds of flexible load contracts:

- Summer FLC: With a settlement period from 1. May to 30. September. The flexibility is to exercise in 1667 of 3672 hours (45.4%).
- Winter FLC: With a settlement period from 1. October to 30. April. The flexibility is to exercise in 3333 of 5088 hours (65.5%).

Together these two contracts make up a flexible load contract called “5000 hours FLC with 2/3 of the volume in the winter and 1/3 in the summer.” For three of the participants we have policies from 1. May 1997 to 1. May 2002, and for three other participants we have policies from 1. May 1999. Due to incompatibilities we could only use the summer FLC policies for the remaining three participants.

The FLC data was obtained from Skagerak Energi AS - one of Norway’s leading power companies. To get hold of the data set we had to anonymize the data by scaling the contracts and by naming the participants as  $C1, C2, \dots, C9$ .

### 5.3 Parameter estimation

With the price data we can now begin the estimation of the parameters in the spot price process. As we recall from section 3 it is possible to estimate the spot price parameters by solving the maximization problem given by (3.7) on page 87. To separate the fast mean reversion generated by large and sudden changes in the demand or supply from the more slowly mean reversion generated by the hydrological balance, we used a two stage estimation procedure. First we estimated the parameters in  $X_t$  from hourly prices with a weekly sampling interval. By construction  $D_t$  will start out at zero every week, meaning that  $D_t$  will be zero in the weekly data sample. Assuming an hourly sampling resolution of  $\mathbf{P}$ , we pick every 168’th value and use this data sample to estimate the parameters  $a, \sigma, A_1^X, b_0, A_2^X, B_1^X$  and  $B_2^X$  by solving (3.7) on page 87. The second stage is to estimate the parameters in  $D_t$  from the full data sample  $\mathbf{P}$ . To get an estimate for the parameters in  $D_t$  we insert the parameters estimated from the first stage into (3.6) and solve

the maximization problem given by (3.7). To ensure that  $D_t$  start at zero at the beginning of every week, we set  $d_0$  equal to the value of  $-\varepsilon$  at time  $t_1$ .

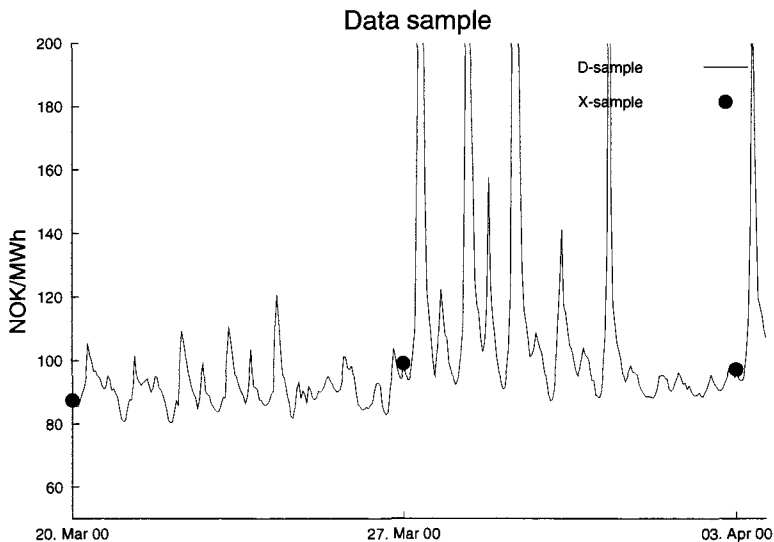


**Figure 11:** We can here see the relationship between the  $D_t$  sample and the  $X_t$  sample. We have in this figure on purpose picked a period with price spikes to show that  $X_t$  is usually not effected by spikes.

To incorporate new spot prices into our sample we re-estimated the parameters 1. May and 1. October each year. The re-estimation of the parameters made it possible to adapt to changes in dynamics of the spot price and use the largest available sample to get more accurate estimates. The results are given in table III. As we can see from the estimated parameters the speed of mean reversion,  $a$ , is equal in all sub samples. This indicates that the mean reversion property of the spot price dynamics is unchanged over the last eight years. This is however not the case for the volatility parameter,  $\sigma$ , which has decreased. The deseasonalised long run mean,  $b_0 + d_0$ , has also decreased during the data period. Since we are operating with nominal prices we expected an increase, but the effect of the deregulation of the electricity market and several years with more than normal precipitation must have counteracted this.

The remaining parameters in the table determines the shape of the seasonal patterns. The day and weekly price patterns are quite stable throughout the sample period. The parameters  $A_1^X, A_2^X, B_1^X$  and  $B_2^X$  which control the yearly price cycle on the other hand seems to be more varying. This may indicate that the yearly price pattern is influenced by other factors than just the deviation from long run mean and the time of the year.

**Table II:** Descriptive statistics

	Nominal prices					
	Avg	Min	Max	SD	Skewness	Kurtosis
1993*	80.04	14.27	193.75	41.10	0.1896	2.1258
1994	182.65	60.81	459.35	68.49	1.0679	7.0252
1995	117.67	25.38	210.89	60.59	-0.5807	2.7852
1996	253.63	102.97	391.62	79.16	0.2880	3.0466
1997	134.99	28.40	377.80	73.61	0.7945	4.4389
1998	116.35	17.97	735.28	70.47	0.5873	17.7840
1999	112.11	39.99	654.98	67.29	1.9075	28.3528
2000	103.33	19.01	1808.66	66.06	12.7962	410.4873
2001*	188.46	31.21	1951.76	67.86	11.6510	218.7751
Full sample	142.42	14.27	1951.76	67.86	2.2028	33.5961
W1	154.56	20.36	1951.76	65.90	5.4542	100.3643
SO	124.54	14.27	391.62	73.05	1.0170	3.7532
W2	157.53	29.45	735.28	51.37	1.1702	6.0739

	Deseasonalized prices					
	Avg	Min	Max	SD	Skewness	Kurtosis
1993*	-34.41	-94.98	90.41	28.15	0.31	2.64
1994	57.05	-51.22	318.14	40.31	1.30	8.77
1995	-7.93	-107.76	75.60	28.87	-0.49	3.23
1996	128.55	-7.91	271.32	53.04	0.03	2.38
1997	9.06	-74.10	234.89	28.50	1.02	5.85
1998	-9.30	-97.56	583.46	27.80	1.99	46.66
1999	-13.48	-61.04	509.17	23.27	3.81	60.41
2000	-22.25	-74.80	1658.95	36.79	19.46	724.19
2001*	66.58	-93.85	1801.81	68.14	10.55	195.98
Full sample	18.35	-107.76	1801.81	63.78	2.74	39.26
W1	14.32	-88.16	1801.81	63.26	5.99	113.10
SO	20.48	-97.56	271.32	70.63	1.09	3.68
W2	20.09	-107.76	583.46	50.44	1.31	6.29

Descriptive statistics conducted on yearly and seasonal subsamples. W1 denotes the period 1. January to 30. April, SO denotes the period 1. May to 30. September and W2 denotes the period 1. October to 31. December. The deseasonalized is performed by subtracting  $E_t[P_s]$ ,  $s = \{1, \dots, 8760\}$  from the prices at the beginning of each year. The main results from the statistics is that the average price has decreased and the skewness and kurtosis has increased. We also see that the skewness and kurtosis is highest in the W1-period, and the S-period has the highest volatility.

\*not all prices for this year is included in the calculation of the statistics

Table III: Estimated parameters

	Sub samples											
	93-97S	93-97W	93-98S	93-98W	93-99S	93-99W	93-00S	93-00W	93-01S	93-01W		
$a$	0.0004	0.0004	0.0004	0.0004	0.0004	0.0004	0.0004	0.0004	0.0004	0.0004	0.0004	
$\sigma$	1.9872	1.9836	1.8991	1.8922	1.8238	1.7819	1.7435	1.7126	1.6674	1.6655	1.6655	
$b_0$	159.97	152.52	150.93	146.04	142.03	141.03	136.05	134.98	138.43	138.39	138.39	
$d_0$	-10.06	-10.12	-10.11	-10.48	-10.65	-10.59	-10.77	-11.06	-12.49	-12.85	-12.85	
$A_1^X$	32.19	31.16	33.80	33.70	34.44	33.70	32.55	32.94	28.87	27.14	27.14	
$A_2^X$	-8.40	-6.41	-5.36	-3.36	-2.68	-2.84	-3.57	-3.40	-5.07	-3.68	-3.68	
$A_1^D$	-3.07	-3.18	-3.16	-3.30	-3.29	-3.27	-3.13	-3.31	-3.42	-3.59	-3.59	
$A_2^D$	-0.24	-0.24	-0.13	-0.13	-0.16	-0.18	0.00	0.02	0.07	0.09	0.09	
$A_3^D$	-5.31	-5.56	-5.54	-5.87	-5.87	-5.93	-6.24	-6.51	-7.39	-7.82	-7.82	
$A_4^D$	1.58	1.96	1.76	2.00	1.80	1.90	1.78	2.01	1.88	2.28	2.28	
$B_1^X$	-3.65	1.44	-2.42	3.66	-0.09	0.94	-2.00	-0.54	2.59	2.99	2.99	
$B_2^X$	12.32	12.99	10.82	7.59	6.63	6.33	5.79	4.50	4.14	4.33	4.33	
$B_1^D$	4.09	4.50	4.44	4.67	4.69	4.73	4.98	5.11	5.49	5.76	5.76	
$B_2^D$	2.78	2.99	2.94	3.00	3.00	2.97	3.13	3.17	3.82	3.93	3.93	
$B_3^D$	-4.75	-5.01	-4.92	-5.17	-5.07	-5.03	-4.88	-4.99	-5.19	-5.56	-5.56	
$B_4^D$	-4.24	-4.25	-4.23	-4.34	-4.34	-4.30	-4.61	-4.72	-5.54	-5.70	-5.70	

This table shows the estimated parameters obtained by solving (3.7). Each column represents a sub sample. "93-97S" represents the period 4. January 1993 to 30. April 1997, "93-97W" represents the period 4. January 1993 to 30. September 1997 and so on. We see a decrease in the long term average price ( $b_0 + d_0$ ) and the volatility ( $\sigma$ ). The parameters determining the daily and weekly price patterns is quite stable, but the parameters determining the yearly patterns is more unstable. In addition we use a risk free interest rate of 5% pro anno in the optimization algorithm.

## 6 Results

The purpose of this paper is to study how a flexible load contract can be exercised optimally when only historical spot price information is used. We divide this chapter into two parts. In the first part we analyze the exercise policy from our algorithm and in the second part we study different properties of a FLC.

### 6.1 Results from the case

In this section we focus on the case contract defined in the first section. This was a FLC for the summer 1997 (from 1. May to 1. October), totally 3672 hours. In our case we paid 958525 NOK for the right to withdraw 8335 MWh, with a maximum of 5 MWh per hour. Therefore our target is to exercise the contract during the 1667 hours with the highest spot price.

In figure 12 we show how our algorithm exercised the contract during the summer period of 1997. The plot shows the accumulated control (i.e. the  $Q$ -variable) at each instant. We compare this with the aposteriori best path which picks exactly the best 1667 hours. We also show how the contract was utilized by a market participant. Even though the historical contract is closer to the aposteriori best, it is not necessarily better than the model. This is because there is no monotonicity in the value of the policies as we get closer to the ex post optimal curve. This can be illustrated by the policy picking the same hours as the optimal, but with a 12 hours lag. This policy will normally perform poorly (because of the low price levels in the night) but it will be very close to the aposteriori optimal curve. In figure 12 we have also plotted the frequency plot of all the prices together with the distribution of the prices for the exercised volume. As we can see, our model managed to exercise most of its volume on the “right side” of the price distribution. This indicates an ability to distinguish a high-price state from a low-price state. The actual performance of the model is difficult to measure from the frequency plot or the accumulated control. Therefore we need to calculate

**Table IV: Value of exercised FLC (Summer-1997)**

	Total revenue from FLC	Revenue excess base load	Excess revenue per MWh
<b>Model:</b>			
1h	1 000 559	98 353	11.80
24h	982 141	79 935	9.59
<b>Competitors:</b>			
C1	1 010 281	108 075	12.97
C2	1 000 506	98 300	11.79
C3	1 007 316	105 110	12.61
C4	986 806	84 600	10.15
C5	<b>1 013 166</b>	<b>110 960</b>	<b>13.31</b>

Value of the exercised FLC obtained by our model and 5 competitors. Since the total revenue mainly consist of the value of the base load, and this base load is often hedged when a FLC is bought, it is common to look at the total or per MWh excess revenue. For this particular FLC we see that competitor C5 managed to obtain the highest revenue, with our model obtaining a 1.2% lower total revenue.

the realized revenue from the different policies. The results are given in table IV. We see that the model based on an hourly update gets a fourth place, but the difference from the other competitors is relatively small. The model has an advantage since the control can use hourly price information. We can adjust for this and use the (possibly<sup>11</sup>) more realistic model where a 24 hours deterministic development of the observed price is used to find the control. We see that the result is worsened, as expected.

It is not possible to conclude how good our model is just by analyzing a single FLC. We must keep in mind that this problem is of a stochastic nature. Therefore even though we knew the real stochastic process (which of course is impossible) the optimal control could give bad results when only one season

<sup>11</sup>The market participants does have good estimates for price development the following days. If we use this information the model with an hourly update may be realistic after all.



(i.e. one replicate) is studied. But since the expected value is maximized, the long run accumulated value should be good. In the next subsection we introduce a new FLC for the winter period and again show how our model performs compared to real life competitors during the 1997 - 2002 period.

### **6.1.1 Results 1997-2002**

To supplement the FLC for the summer period we introduce a new type of FLC for the winter period 1. October to 30. April, totally 5088 hours. The new contract has a total volume of 16665 MWh and a maximum effect of 5 MW. Our goal is therefore to pick the 3333 hours with the highest price. With this contract we are able to show how the model performs over the whole 1997 - 2002 period. Finding a good method to compare different contracts is not straight forward. Contracts with the same degree of flexibility and with equal delivery period must be used. In addition competitors may have different risk attitudes. We decided to focus on the excess revenue obtained for the period 1997-2002.

The results are presented in table V and figures 15 to 23 starting on page 123. We may draw some conclusions from the results. First of all, our model manage to obtain the highest accumulated revenue during the period. The model also demonstrates that it has the courage to pick many hours early if the prices are sufficiently good. Opposite, the model waits for a long time if the prices are poor. This can be seen as a risky behavior, and may be a consequence of the risk neutral model<sup>12</sup> formulation. The results also shows that the results vary substantially from extremely good (as in W2001) to extremely bad (as in W2000), but with a good average performance. This may also be seen as a materialization of risk neutrality. We will in the next subsection take a closer look at the FLC for the winter period 2000, and try to analyze the result.

Another observation is that our model seems to perform better for the winter contracts than for the summer contracts. One reason can be that the

---

<sup>12</sup>On the other hand, we believe that this routine does the correct trade off between the different effects of the model such as interest rate, volatility, reversion and periodicity.

winter contract has a lower degree of flexibility than the summer contract. For the winter contract we have to exercise  $3333/5088 \approx 65.5\%$  of the hours against only  $1667/3672 \approx 45.4\%$  for the summer contract. Another reason may be that the process is best calibrated to the winter data. The reason for this is that since we have only used two trigonometric functions to model the changes through the year, the process can not model the summer vacation and all the holidays in May properly. The low prices in the summer is typically expected to appear 6 months after the highest winter prices. This is not necessarily the case in the real world. Normally the lowest prices appear in the vacation weeks of July. Our spot process does not expect collapse in the July prices, and therefore the routine has a tendency to pick too few hours in May and June. Then, when the really poor prices appear in July these hours cannot be exercised either. Now the routine is basically forced to take all the hours in August and September. This scenario is broken if the early summer prices are sufficiently high as in the summer of 2001. We believe that the performance in the summer contracts could be improved with a more representative process. Several different ideas can be followed.

- We could include more trigonometric functions into the spot process.
- We could estimate separate summer and winter processes.
- We could include a drift term into the process such that the holidays are placed properly.

We feel that we have demonstrated that the model works quite good with this level of precision, and leave the process of refinements for future work.

## RESULTS CASE (SUMMER-1997)

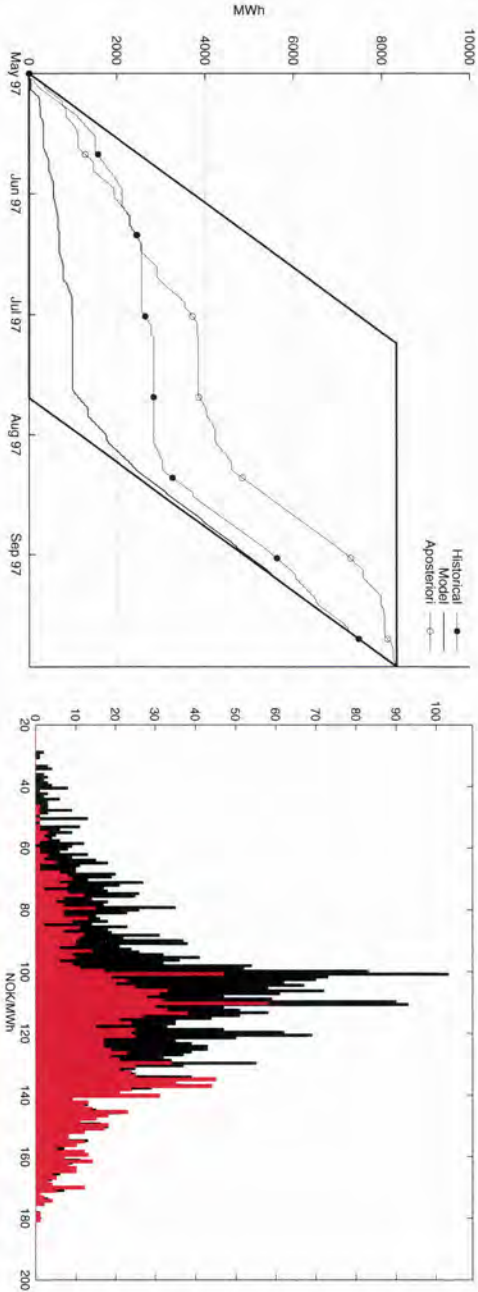


**Figure 12:** On the left hand side we have plotted the algorithm's exercise policy together with a competitor's (denoted as C1 in subsequent tables) exercise program. The a posteriori best exercise is also plotted as a reference. On the right hand side we have a figure of the empirical density function for all spot prices and spot prices for the exercised volume.

Table V: Results for the period 1997 - 2001

	Model		Historical								
	1h	24h	C1	C2	C3	C4	C5	C6	C7	C8	C9
			24h	24h	24h	24h	24h	24h	24h	24h	24h
S-1997	98 353	79 935	108 075	98 300	105 110	84 600	110 960				
W-1997	179 315	<b>185 980</b>	59 595	54 740	38 765						
S-1998	-8 670	-35 590	49 245	<b>133 155</b>	90 620	-25 090	90 605				
W-1998	<b>186 315</b>	185 315	122 885	183 210	51 650						
S-1999	174 035	155 200	177 770	175 450	<b>181 755</b>	165 450	181 735	168 205	171 080	164 520	
W-1999	<b>167 315</b>	157 985	67 340	40 175	7 565			60 740	73 125	69 590	95 935
S-2000	144 195	99 020	157 430	155 425	<b>180 775</b>	141 015	181 655	160 290	160 975	150 685	
W-2000	-75 990	-64 995	<b>125 820</b>	113 525	49 450			113 515	109 030	17 200	107 590
S-2001	<b>173 620</b>	152 530	111 875	101 030	24 870	121 305	44 145	112 755	116 605	71 790	
W-2001	<b>220 645</b>	207 815	162 452	143 243	91 386			82 733	83 271	82 688	82 869
Sum all summer	581 450	451 095	604 395	<b>663 360</b>	583 130	487 280	609 100				
Sum all winter	<b>677 600</b>	672 100	538 092	534 893	238816						
Sum all	<b>1 259 050</b>	1 123 195	1 142 487	1 198 253	821946						
Sum from S-1999	<b>803 820</b>	707 555	802 687	728 848	387400			698 238	714 086	556 473	

This table shows the revenue excess base load for all the FLC for the period 1997 - 2001. The best FLC's are marked in bold.

### **6.1.2 A closer look**

The revenue from the FLC during the winter 2000 period was very low. In fact the revenue was lower than the value of a base load contract. We have two different explanations for this. Firstly, there may be weaknesses in the routine, especially due to the limitations of the movements of the discretized price process from hour to hour. Secondly and more important there are clearly an informational asymmetry since the market has access to information the model does not have.

From figure 21 on page 129 we see that the algorithm starts out with an exercise policy close to maximum. This was a result of the higher-than-normal prices in this period. The degree of exercised volume was later reduced some, and the difference between the competitors policy and ours was reduced. During February our model saw sufficiently high prices to exercise the remaining volume, thereby missing several price spikes in March and April. This is reflected in the density plot on page 129 as the low volume exercised in the 180 - 240 price range. If we had used a price process that was able to model spikes, the algorithm would not have exercised the remaining volume so soon. The forward prices did capture large parts of the price spikes and if incorporated would have helped. On the other hand the FLC for the winter 2001 period did very well since the routine overlooked the predictions given by the forward market. So the effect of information from the forward market is not clear. We therefore believe the main reason for the poor winter 2000 results was the algorithms inability to capture the possible future price spikes.

## **6.2 Analyzing properties of a FLC**

In the remaining part of this section we analyze different properties of the flexible load contract such as pricing, value of flexibility, different update policies and parameter sensitivity.

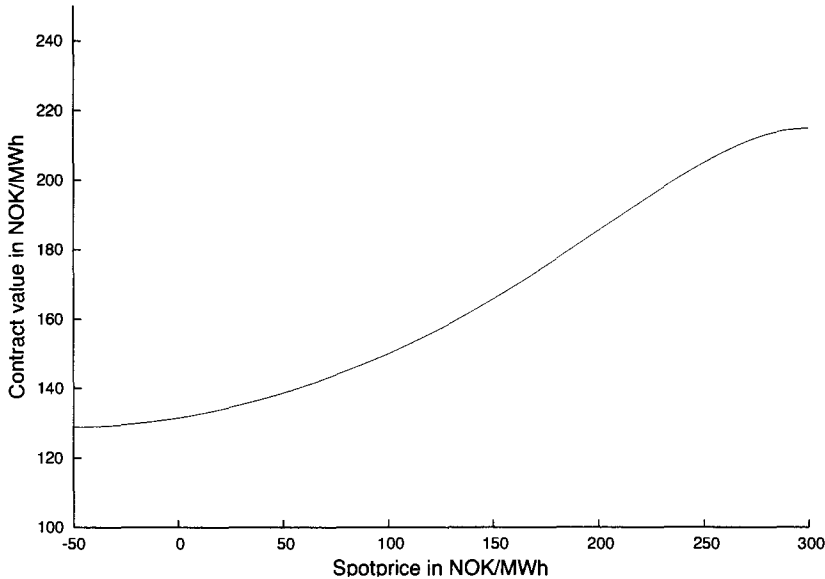


**Figure 13:** *The value in NOK/MWh for a FLC against spotprice pr. 1. May 1997.*

### 6.2.1 Pricing

Until now we have primarily focused on the FLC's exercise policy. We now turn our attention to valuation of the contract.

In our context we have no forward market, so the value of a FLC should be the expected discounted cash flow generated from the optimal exercise policy. If there is a forward market, the FLC price would be influenced by several factors such as the expected value of the exercise policy, risk premium in the forward market and the value of the strategy consisting of using a FLC to hedge forward contracts with the highest price. To illustrate the last part, let us assume there exist a 1667 hours base-load forward contract with a price 125 NOK/MWh and a settlement period within the period 1. May 1997 - 30. September 1997. Then the price of the FLC defined in the introduction section must be greater than  $125 * 5 * 1667 = 1041875$  NOK. If not, we can construct an arbitrage by selling the forward and buying the FLC and choosing an exercise policy corresponding to the settlement period of the forward contract. This would give us a positive present value with no risk.

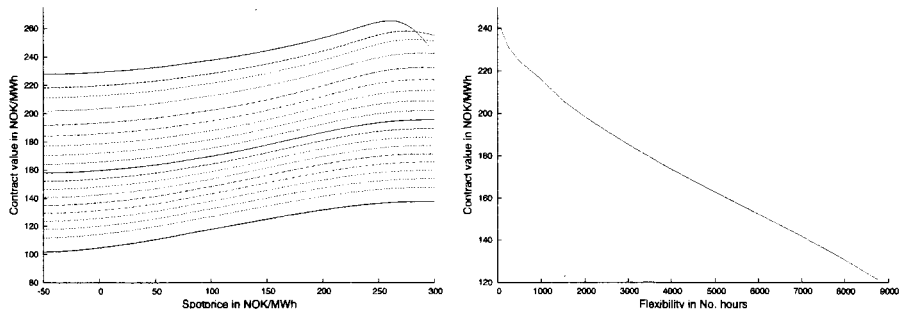


**Figure 14:** The left plot shows the initial value of 20 FLC's with different degrees of flexibility. The right plot presents the price pr. MWh as a function of the flexibility when the spot price is 125.54 NOK. This was the long run price level pr 1. October 2001.

Figure 13 presents the time zero value of the optimal exercise policy for the FLC defined in section 1 on page 70. Clearly the value is increasing with increasing spotprice. The effect of the mean reversion of the spot price can be seen as a slower increase or decrease in the curvature when the spot price moves away from the long term spot price level of 149.91 NOK/MWh. Even with a negative spot price, the contract has a positive value.

### 6.2.2 Flexibility

The flexibility of a flexible load contract can be measured by the percentage of the hours we must exercise. A high percentage implies a low flexibility and vice versa. The FLC's value pr MWh is increasing with increasing flexibility. If we have no flexibility the FLC is basically an ordinary base load contract. To see the value of the flexibility we have valued several contracts with different degrees of flexibilities. The results are given in figure 14. The contracts have a one year settlement period. We used parameters estimated from 1993-2001, given in the right column in table III on page 107. Observe that the value falls close to the upper grid boundary when the flexibility is high. This is a numerical error due to the grid constraints.

### **6.2.3 Sensitivity to the spot volatility and mean reversion**

We will now analyze the sensitivity of the spot volatility and speed of mean reversion. The analyze is conducted by first changing the spot volatility,  $\sigma$ , while keeping all the other parameters constant and then changing the speed of mean reversion. We used the same parameters as used in our case contract. With a spot price of 150 NOK we got a value of 1 352 230 with  $\sigma = 0$ , 1 381 588 with  $\sigma = 2$  and 1 446 230 with  $\sigma = 4$ . This indicates that the value of a FLC increases with an increase in the volatility. By examining the exercise policy we noticed a tendency to wait longer with the exercise when the volatility was high. As we can see from the expression for the spot price process, (3.4) on page 85, the spot diffusion is reduced when the speed of mean reversion is increased. That is,  $a$  has the opposite effect as the spot price volatility  $\sigma$ . With infinite reversion the spot price would be deterministic, and the contract exercised according to the seasonal patterns.

### **6.2.4 Time between updates of the exercise program**

As discussed earlier the market participants use different effort to optimize the utilization of these contracts. The trade off between payoff and effort must be done carefully. The time invested in the optimization must be balanced against the size of the contract. To analyze the sensitivity to the time between updates of exercise program we find exercise revenue for different lengths between policy updates. The idea is to calculate the full optimal control matrix with an hourly resolution. The 24 hours exercise program is then calculated by using the observed spot price once every day, and a deterministic development of the price between these observations. This was repeated with weekly and biweekly observations. From table VI and table VII we see that the largest average decrease occurs from hourly to daily update. Hourly updates may seem unrealistic, but price-conditioned exercise policies exists and are very similar to hourly updates.

The effect of time between updates is less in the summer than in the winter. The difference in revenue from weekly to biweekly is very small,



**Table VI:** *Effect of time between policy-updates, I*

	1h	24h	168h	336h
S-1997	11.79	9.59	9.82	9.82
W-1997	10.76	11.16	10.84	10.95
S-1998	-1.04	-4.27	-5.08	-4.49
W-1998	11.18	11.12	10.77	10.22
S-1999	20.88	18.62	18.30	18.33
W-1999	10.04	9.48	9.10	8.28
S-2000	17.30	11.88	12.74	12.27
W-2000	-4.56	-3.90	-5.59	-4.38
S-2001	20.83	18.30	17.34	17.07
W-2001	13.24	12.47	12.28	12.07
Avg. summer	13.95	10.82	10.62	10.60
Avg. winter	8.13	8.07	7.48	7.43
Avg. all	11.04	9.45	9.05	9.01

The effect of time between policy-updates expressed as excess revenue per MWh.

**Table VII:** *Effect of time between policy-updates, II*

	1h	24h	168h	336h
S-1997	98 353	79 935	81 850	81 850
W-1997	179 315	185 980	180 649	182 482
S-1998	-8 670	-35 590	-42 342	-37 424
W-1998	186 315	185 315	179 482	170 316
S-1999	174 035	155 200	152 531	152 781
W-1999	167 315	157 985	151 652	137 986
S-2000	144 195	99 020	106 188	102 270
W-2000	-75 990	-64 995	-93 157	-72 993
S-2001	173 620	152 530	144 529	142 278
W-2001	220 645	207 815	204 646	201 147
Sum summer	581 450	451 095	442 755	441 755
Sum winter	677 050	672 100	623 271	618 938
Sum all	1 259 050	1 123 195	1 066 026	1 060 693

The effect of time between policy-updates expressed as excess revenue.

indicating that one could use a biweekly update policy for small contracts or if updating the policy is costly.

## 7 Concluding remarks

In this paper we have analyzed flexible load contracts by formulating the contract as a stochastic optimization problem. The value function is expressed as the solution of the Hamilton-Jacobi-Bellman equation in which the optimal control takes only the extreme values. By carefully examining the dynamics of the spot price in the Nordic electricity market we decided to use a time dependent mean reverting Ornstein-Uhlenbeck process. The process modelled daily, weekly and yearly price cycles. In addition it captures mean reversion due to deviations in the hydrological balance. The process has 21 parameters which was estimated from historical price data by a mixture of OLS and maximum likelihood. Estimation was conducted partly on a weekly data sample and partly on an hourly data sample. This to distinguish the short range factors from medium range factors.

To be able to solve the optimization problem we discretized the time and state space and derived an algorithm to find the value function and optimal control in each node. To dampen the effects of a truncated price space we combined absorbing and reflecting boundary conditions.

We implemented the algorithm and calculated the optimal control for the five year period 1. May 1997 to 30. April 2002. The accumulated revenue from this control was compared to the revenue for nine market participants. We find that our algorithm obtains the highest accumulated exercise revenue for this period. The model also demonstrates that it has the “courage” to pick many hours early if the prices are sufficiently good. This can be seen as a more risky behavior, and may be a consequence of the risk neutral assumption. Another observation is that our model seems to perform better for winter contracts than for the summer contracts. We believe the performance for the summer contracts can be improved with a more representative process.

We see several important model extensions for further research:

- The process modelling the spot price should exhibit spikes, i.e. sudden “jumps”. This is especially important in the European market where

price spikes is common. This can be reflected in the model by introducing a nonlinear function of the OU-process. The calibration could be done with maximum likelihood as before.

- The underlying spot price process could be calibrated to the forward and future contracts traded in the market. Since electricity is a non storable commodity, there is no clear connection between the expected future spot price and the value of these financial products. To use the financial market to predict the future spot price one first need to know the market price of risk. If this market price of risk is unknown or stochastic one may be better off calibrating the spot price partially to historical information and partial to the information from the financial market.

In our opinion this model demonstrates a great potential for utilization of contracts of this type. The methods can be developed further to improve the results even more. We stress that the methods are fully operational, and can be implemented by practitioners, for instants for benchmarking or as an aid to improve the exercise policy.

## References

- [1] Bjørgan, R., Song, H. and Liu, C. C., (2000) “Pricing flexible electricity contracts”, *IEEE Transactions on power systems*, vol. 15, pp. 477-482.
- [2] Johnson, B. and Barz, G., (2001), “Energy Modelling and the Management of Uncertainty”, *Risk Books*, Second edition.
- [3] Keppo, J., (2002), “Pricing of electricity swing options”, Working paper University of Michigan.
- [4] Knittel, C. R. and Roberts, M. R., (2001), “An empirical examination of deregulated electricity prices”, Working paper, POWER, University of California Energy Institute.
- [5] Koopmans, T. C. and Hood, W. C., (1953), “The Estimation of Simultaneous Linear Economic Relationships”, *Wiley*.
- [6] Kushner, H. and Dupuis, P., (2001), “Numerical Methods for Control Problems in Continuous Time”, *Springer*, Second edition.
- [7] Lucia, J. and Schwartz, S., (2002), “Electricity prices and power derivatives: Evidence from the Nordic power exchange”, *Review of Derivatives Research*, vol. 5, pp. 5-50.
- [8] Ronn, E. I., Jaillet, P. and Tompaidis, S., (2003), “Valuation of commodity-based swing options” *Management Science*.
- [9] Simchi, M., Lari-Lavassani, A. and Ware, A., (2001), “A discrete valuation of swing options”, *Canadian Applied Mathematics Quarterly*, vol. 9.
- [10] Stage, S. and Larsson, Y., (1961), “Incremental cost of water power”, *AIEE Transactions*, pp. 361-365.
- [11] Thompson, A. C., (1995), “Valuation of path-dependent contingent claims with multiple exercise decisions over time; the case of take-or-

pay”, *Journal of Financial and Quantitative Analysis*, vol. 30, pp. 271-293.

- [12] Øksendal, A., (2001), “Mathematical models for investment under uncertainty”, *Dissertation*, University of Oslo, Faculty of Mathematics and Sciences.

# RESULTS WINTER-1997

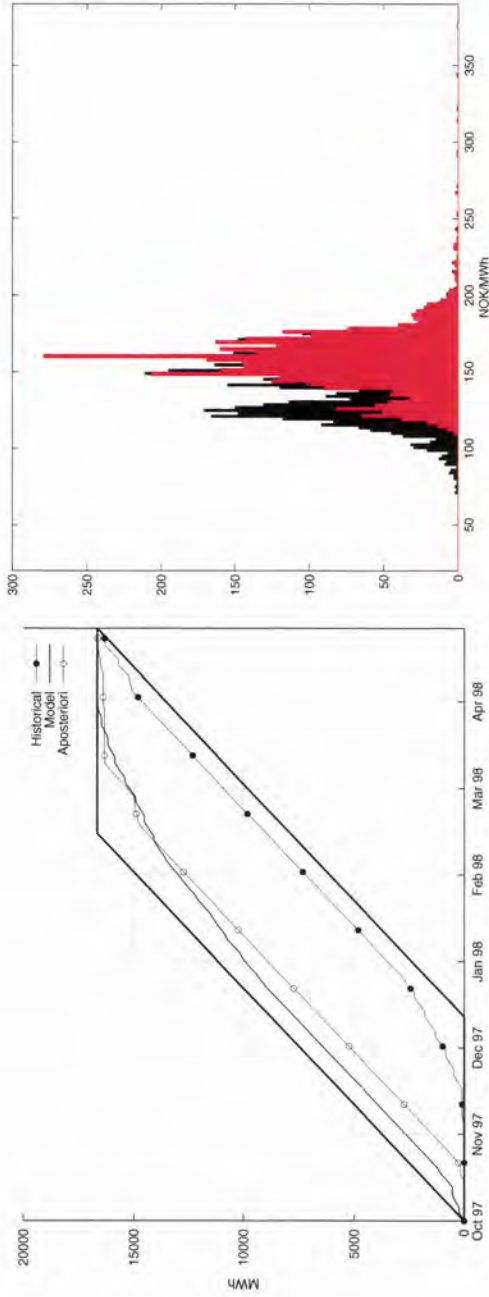


Figure 15: Flexible load contract: Winter 1997

# RESULTS SUMMER-1998

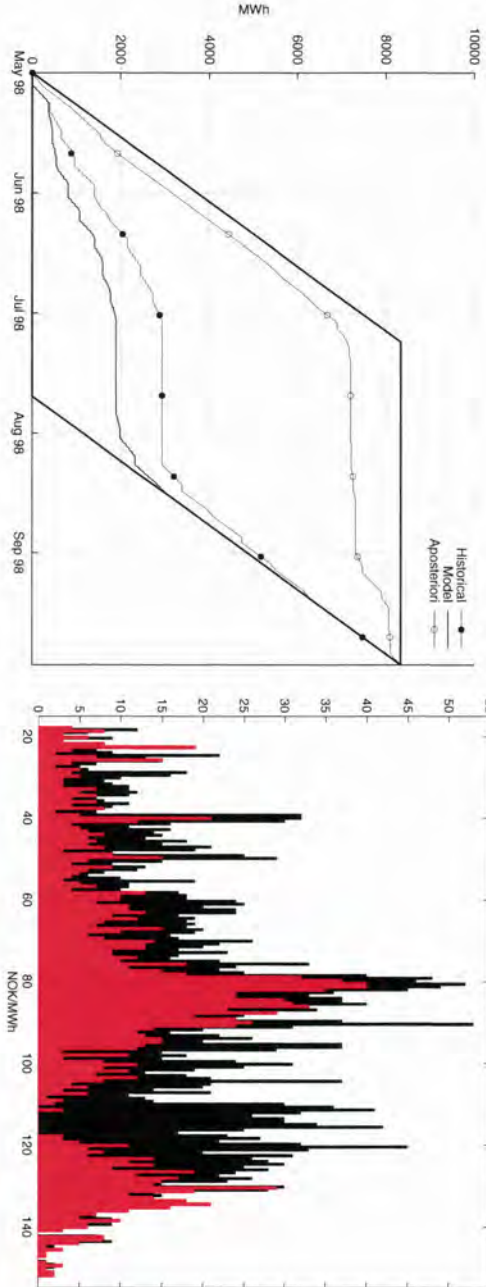


Figure 16: Flexible load contract: Summer 1998

# RESULTS WINTER-1998

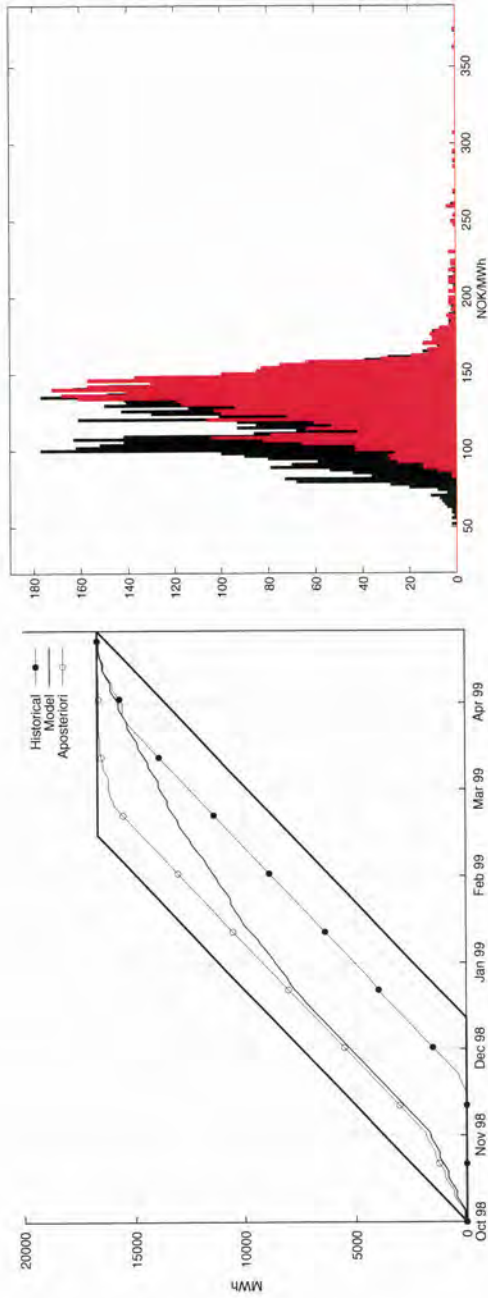


Figure 17: Flexible load contract: Winter 1998



## RESULTS SUMMER-1999

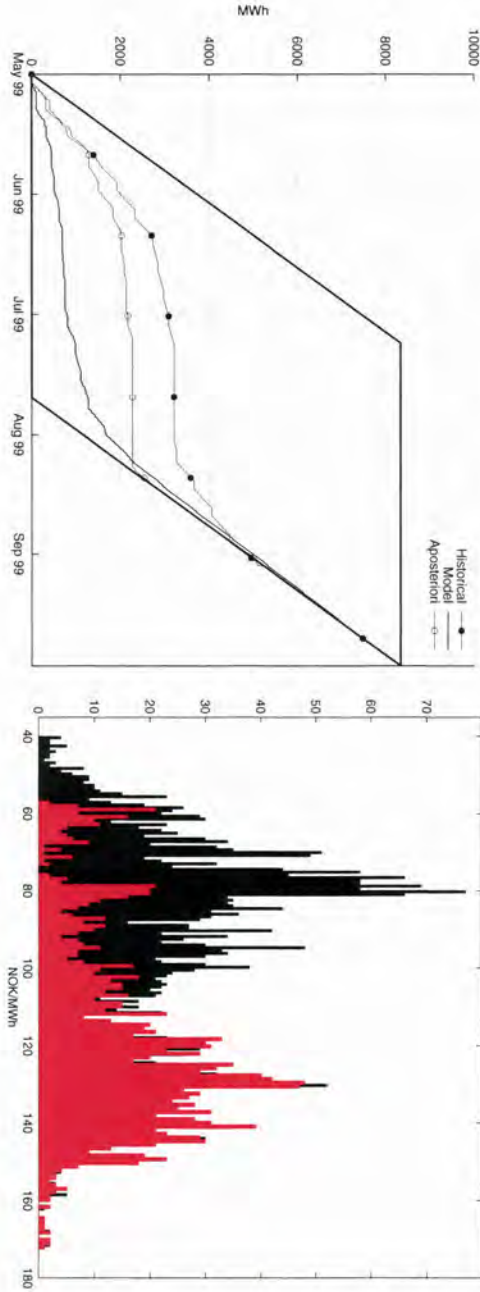


Figure 18: Flexible load contract: Summer 1999

## RESULTS WINTER-1999

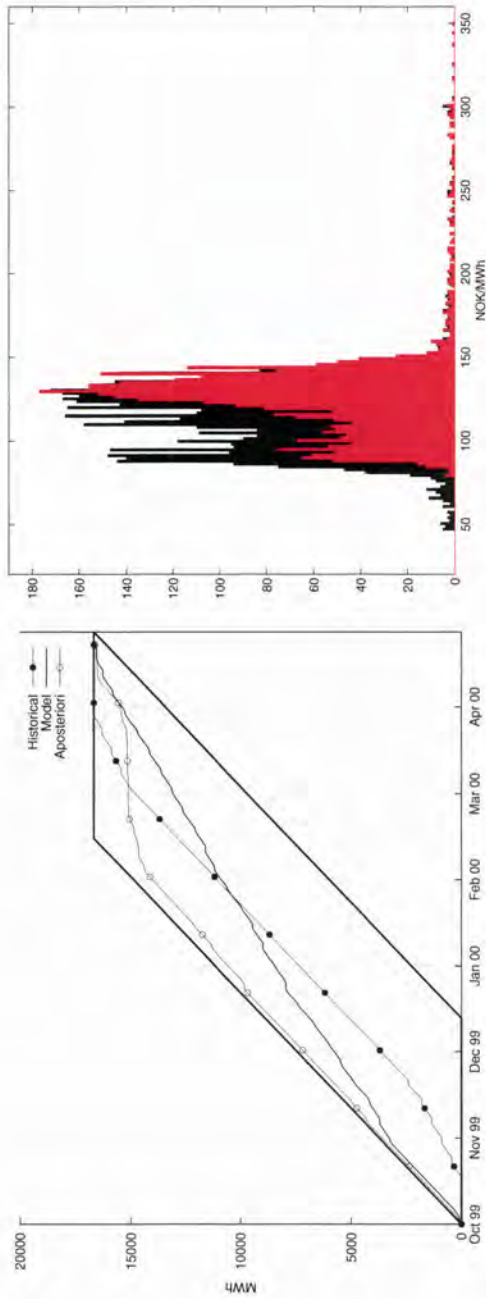


Figure 19: Flexible load contract: Winter 1999

# RESULTS SUMMER-2000

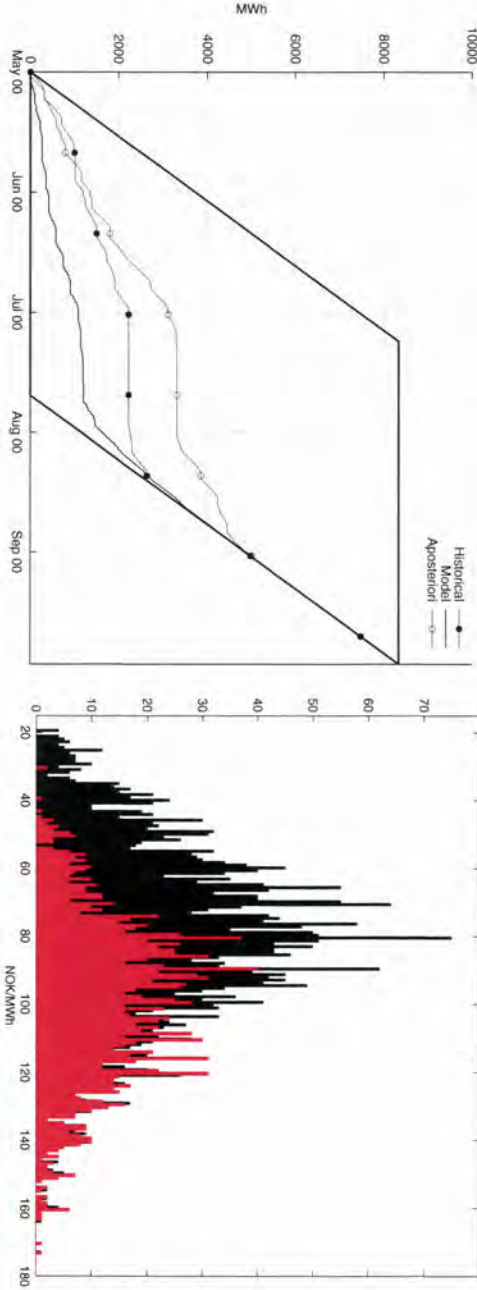


Figure 20: Flexible load contract: Summer 2000

## RESULTS WINTER-2000

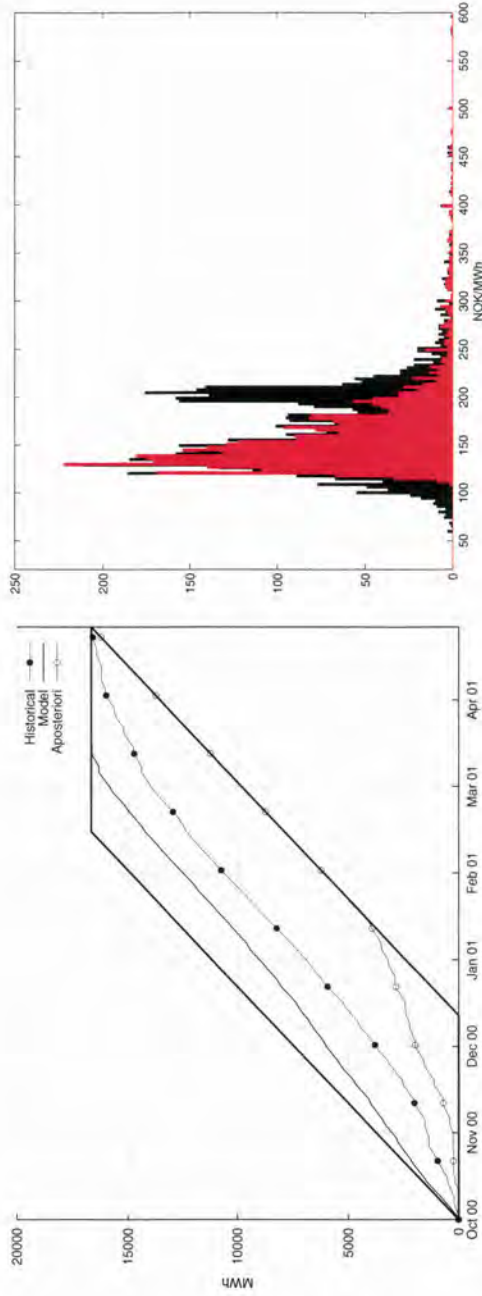


Figure 21: Flexible load contract: Winter 2000

## RESULTS SUMMER-2001

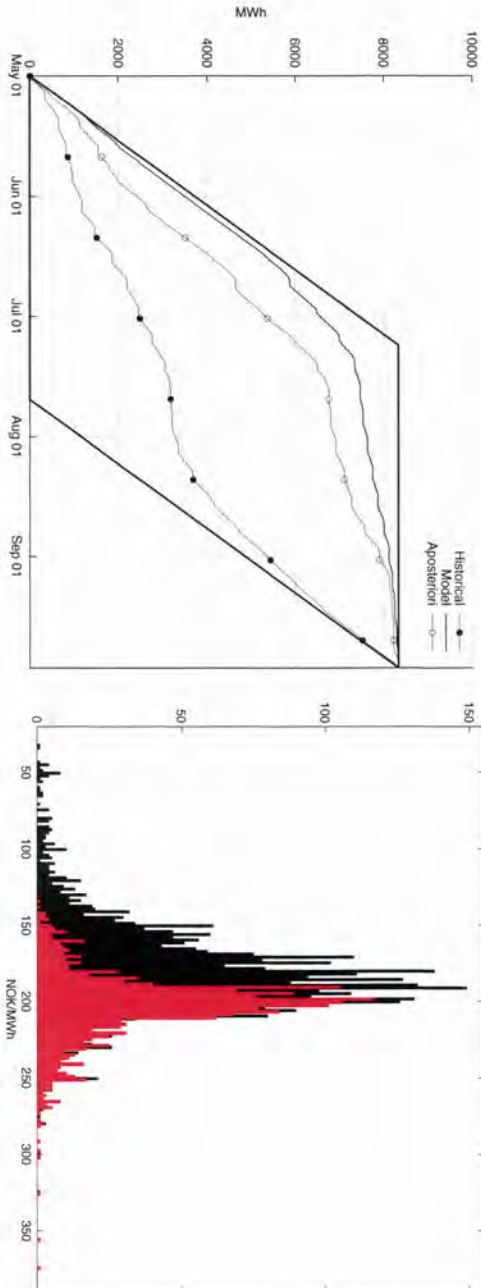


Figure 22: Flexible load contract: Summer 2001

# RESULTS WINTER-2001

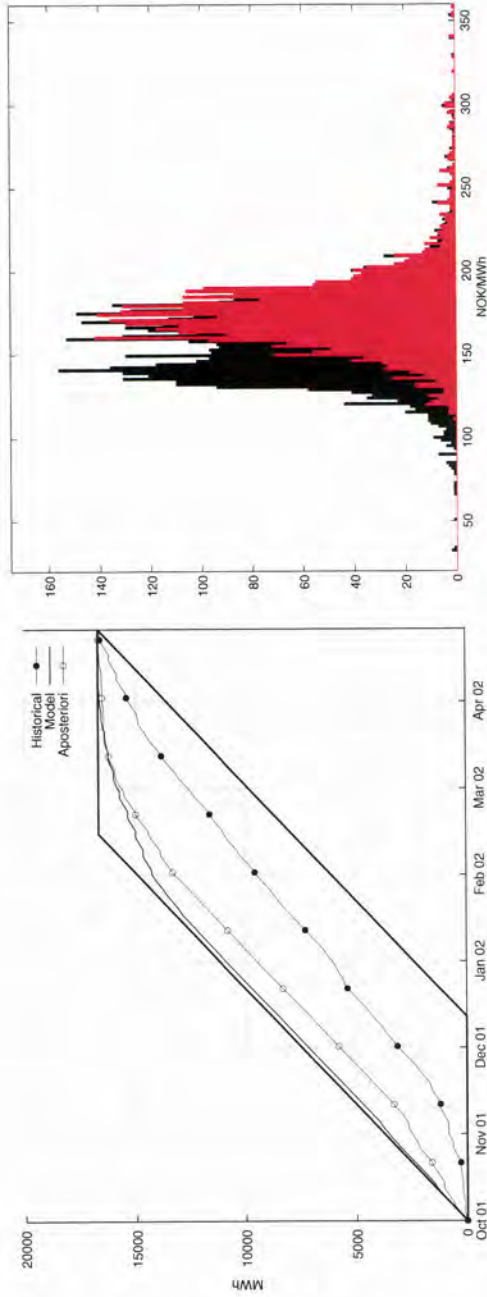


Figure 23: Flexible load contract: Winter 2001



# Empirical study of the risk premium in an electricity market \*

Fridthjof Ollmar

## Abstract

We conduct an explorative analysis of the risk premium in the Nordic power market. From our theoretical model of an electricity market, we define the risk premium as the conditional expected return pr unit risk. The discretized version of the risk premium is estimated by a Nadaraya-Watson estimator, obtaining a nonparametric estimate. From forward and future data from 1995 to 2002 we find: A negative risk premium (implying that the market on average can be described by contango), increased volatility with increased forward price and clear seasonal patterns. We argue that the large dependency on hydroelectric power in the Nordic power market is the main reasons for the structure of the risk premium.

*Key words:* Risk premium, electricity market, nonparametric

---

\*I would like to thank Gunnar Stensland, Arne-Christian Lund and Jostein Lillestøl for helpful comments. I would also like to acknowledge helpful suggestions from the participants at the Statkraft alliance meeting in Amsterdam 2003.



## 1 Introduction

With *risk premium* we mean expected return pr unit risk. The risk premium is important for producers and consumers wanting to hedge their exposure. It is also essential for traders wanting to maximize their return / risk ratio. For financial engineering purposes, knowing the risk premium enable us to risk-adjust cash flows.

A positive risk premium means that the commodity forward prices are backwardated. Backwardation implies that immediate ownership of the physical commodity entails some benefit or convenience which deferred ownership via a long forward position does not have. The reverse situation is called contango. The benefit or disadvantage expressed as a rate is usually called the convenience yield. For commodities that sustain over time (i.e. they are storable), convenience yield is a naturally concept. The classical theory of convenience yield is often referred to as “the theory of storage” and is based on work by Kaldor (1939), Working (1948 and 1949) and Telser (1958). The theory explains convenience yield as a timing option, and the main idea is that the holder of a storable commodity can decide when to consume it. If it is optimal to store a commodity for future consumption, then it is priced like an asset, but if it is optimal to consume it immediately, it is priced as a consumption good. The spot price of a storable commodity is thus the maximum of its current consumption and asset value, and the forward prices is derived from the asset value of the deferred right to consume after delivery. With nonstorable commodities like electricity we must price them as pure consumption goods.

The value of a consumption good depends on the relative bargaining powers amongst the market participants. In a power market we have: Producers (who wants to sell), consumers (who wants to buy) and traders (who buy or sell depending on the expected profit they get).

In this paper we examine the risk premium in an electricity forward market. The nonstorable property of electricity renders the cost-of-carry relationship between the spot price and the forward price useless. Since it is possible to store the good that is used to produce electricity (e.g. in an hydro-power electricity market it is possible to store the water that is used to produce the electricity), one could argue that the traditional methods of cost of carry can partially be used in an electricity market. In our study we will not use the cost-of-carry relationship. Instead we will model a single electricity forward contract and use the expected return and volatility of this contract to find the risk premium.

The paper is organized as follows. We start by deriving a model of an electricity market in section 2. Then in section 3 the model is discretized and estimators are derived. The estimators are then in section 4 used on several data samples to analyze the risk premium. The paper concludes with some remarks.

## **2 The model**

In this explorative study of the risk premium, we start by constructing a model of a single future contract in an electricity market. We apply a similarly notation / setting as Duffie in “Dynamic asset pricing theory” (1996). Fix a measurable space  $(\Omega, \mathcal{F})$ , where  $\Omega$  is to be thought of as states of the world and the elements of  $\mathcal{F}$  as events. On this measurable space we will construct the real world probability measure,  $P$ , and one or more equivalent martingale probability measures,  $Q$ . The first object we need to define is the source of unexpected information i.e. noise. To model new information we use a single Brownian motion  $B \in \mathbb{R}$ , restricted to some time interval  $[0, T]$ , on a given probability space  $(\Omega, \mathcal{F}, P)$ . In addition we fix the standard filtration  $\mathbb{F} = \{\mathcal{F}_t : t \in [0, T]\}$  of  $B$ .

In our model the noise will be related to the spot price,  $S_t$ , of electricity. Due to lack of storability and price inelastic demand, we expect a high spot

price volatility. We argue that this high volatility will make the dynamics of the spot price dominant to the dynamics of the short term interest rate. We will therefore assume a deterministic interest rate,  $r_t$ . By assuming a deterministic interest rate forward prices will evolve in the same manner as future prices. See Cox et. al. 1981. The first asset we introduce is the spot price,  $S$  of electricity

$$dS_t = \mu_s dt + \sigma_s dB_t; \quad S_0 = s$$

where  $\mu_s : \mathbb{R} \times [0, T] \rightarrow \mathbb{R}$ ,  $\sigma_s : \mathbb{R} \times [0, T] \rightarrow \mathbb{R}$  and  $s \in \mathbb{R}$ . We can think of  $S_t$  as the price at time  $t$  for one MWh (Mega Watt hour). We assume that it is possible to trade in  $S$ . But since storing electricity is not economical feasible we will not assume that it is possible to purchase electricity today at the spot price and store it for subsequent sale, i.e. we will not be able to make use of the cost of carry principle. The lack of storability is one of the most important features that distinguishes the electricity market from most other commodity markets.

Next we introduce a forward market into our model. Due to the non-storability of electricity, the forward contract has a settlement *period* instead of a fixed settlement date. We define a forward in an electricity market as a security that pays the difference between the forward price and spot for a given settlement period. The next asset we introduce in our model is a period based base-load forward contract. The name *base load* refers to the distribution of the delivered quantum and means that the delivered quantum is evenly distributed in the delivery period. Let  $F(t, T^s, T^e)$  denote the price at time  $t$  for one MWh delivered evenly distributed in the time period  $[T^s, T^e]$ . Where  $T^s$  is the start of the settlement period and  $T^e$  is the end of the settlement period. Since the true price of a forward contract is zero we

have

$$\begin{aligned}
 0 &= E_t^Q \left[ \int_{T^s}^{T^e} \left( S_u - F(t, T^s, T^e) \right) e^{-\int_0^u r(v) dv} du \right] \\
 &\Downarrow \\
 F(t, T^s, T^e) &= \frac{1}{\int_{T^s}^{T^e} e^{-\int_0^u r(v) dv} du} \int_{T^s}^{T^e} E_t^Q [S_u] e^{-\int_0^u r(v) dv} du \quad (1)
 \end{aligned}$$

where  $E_t^Q[ \ ]$  denotes the conditional expectation (condition on  $\mathcal{F}_t$ ) with respect to a probability measure  $Q$  which is defined by the density process

$$\xi_t = \exp \left\{ - \int_0^t \lambda_u dB_u - \frac{1}{2} \int_0^t \lambda_u \cdot \lambda_u du \right\}$$

where  $\lambda : \Omega \times [0, T] \rightarrow \mathbb{R}$  and can be interpreted as the *market price of risk* process. At this stage we have not assumed any functional form for  $\lambda$ . From Girsanov's theorem and the assumptions leading to the martingale property of the forward price w.r.t  $Q$ -measure, we can write (1) in the following stochastic differential equation form

$$dF(t, T^s, T^e) = \lambda \sigma_F(t, T^s, T^e) dt + \sigma_F(t, T^s, T^e) dB_t \quad (2)$$

The above equation is of course under the real probability measure  $P$ , and the real world drift term  $\mu_F$  must therefore be equal to  $\lambda \sigma_F$ . We will later use this relation to estimate the risk premium connected to the electricity forward.

### 3 Estimation

In the previous section we defined a general model of the price movements of a single forward contract in an electricity market. We will in this section discretize and estimate the drift and diffusion of this contract.

### 3.1 Discrete approximations

Before estimating the risk premium, we discretize the forward process. Let  $F(t, T^s, T^e)$  be a time homogeneous Ito diffusion of the form

$$dF_t = \mu_F(F_t) dt + \sigma_F(F_t) dB_t$$

For a twice differentiable function  $f : \mathbb{R} \times [0, T] \rightarrow \mathbb{R}$  the infinitesimal generator  $\mathcal{A}$  of  $f(x, t)$  is defined as

$$\begin{aligned} \mathcal{A}f(x, t) &= \lim_{u \downarrow t} \frac{E[f(F_u, u) \mid F_t = x] - f(x, t)}{u - t} \\ &= \frac{\partial}{\partial t} f(x, t) + \frac{\partial}{\partial x} f(x, t) \mu_F(F_t) + \frac{1}{2} \sigma_F(F_t)^2 \frac{\partial^2}{\partial x^2} f(x, t) \end{aligned} \quad (3)$$

We can think of the generator  $\mathcal{A}$  as the infinitesimal expected change in a function of a stochastic variable. It is possible to write the conditional expectation  $E_t[f(F_{t+\Delta}, t + \Delta)]$  in the form of a Taylor series expansion, (see Stanton 1997 for details),

$$\begin{aligned} E_t[f(F_{t+\Delta}, t + \Delta)] &= f(F_t, t) + \mathcal{A}f(F_t, t)\Delta + \sum_{n=2}^{\infty} \frac{1}{n!} \mathcal{A}^n f(F_t, t) \Delta^n \quad (4) \\ &\Updownarrow \\ \mathcal{A}f(F_t, t) &= \frac{1}{\Delta} E_t[f(F_{t+\Delta}, t + \Delta) - f(F_t, t)] + \sum_{n=2}^{\infty} \frac{1}{n!} \mathcal{A}^n f(F_t, t) \Delta^{n-1} \end{aligned}$$

where  $\Delta \equiv u - t$  and  $\mathcal{A}^n f$  means  $\mathcal{A}$  operated on  $f$   $n$  times. To derive an approximation to the drift  $\mu_F(F_t)$  and the diffusion  $\sigma_F(F_t)$  we consider the following functions

$$u(x, t) = x$$

and

$$v(x, t) = (x - F_t)^2$$

From (3), the definition of the infinitesimal generator  $\mathcal{A}$ , we get

$$\mathcal{A}u(x, t) = \mu_F(x)$$

and

$$\mathcal{A}v(x, t) = 2(x - F_t)\mu_F(x) + \sigma_F^2(x)$$

and with  $x = F_t$  we get

$$\mathcal{A}v(F_t, t) = \sigma_F^2(F_t)$$

From equation 4 we get the following  $N$ 'th order Taylor approximation for  $\mu_F(F_t)$  and  $\sigma_F^2(F_t)$

$$\begin{aligned}\mu_F(F_t) &= \frac{1}{\Delta}E_t[F_{t+\Delta} - F_t] + \sum_{n=2}^N \frac{1}{n!}\mathcal{A}^n u(F_t, t)\Delta^{n-1} + O(\Delta^N) \\ \sigma_F^2(F_t) &= \frac{1}{\Delta}E_t[(F_{t+\Delta} - F_t)^2] + \sum_{n=2}^N \frac{1}{n!}\mathcal{A}^n v(F_t, t)\Delta^{n-1} + O(\Delta^N)\end{aligned}$$

If we choose  $N = 1$  we get the following first order approximations

$$\begin{aligned}\mu_F(F_t) &= \frac{1}{\Delta}E_t[F_{t+\Delta} - F_t] + O(\Delta) \\ \sigma_F^2(F_t) &= \frac{1}{\Delta}E_t[(F_{t+\Delta} - F_t)^2] + O(\Delta)\end{aligned}\tag{5}$$

We can now use these approximations to find an approximation to the risk premium. From equation 2 on page 137 we have that the forward drift term,  $\mu_F$ , must be equal to  $\lambda \sigma_F$ , implying (for a positive  $\sigma_F$ )

$$\lambda(F_t) = \frac{\mu_F(F_t)}{\sigma_F(F_t)}$$

and together with equation 5 we have the following first order Taylor approximation of the risk premium

$$\lambda(F_t) = \frac{E_t[F_{t+\Delta} - F_t]}{\sqrt{\Delta} E_t[(F_{t+\Delta} - F_t)^2]} + O(\Delta)$$

This equation will be the basis for our estimation procedures.

### **3.2 The estimator**

We will derive an estimator for the drift and diffusion term of our period based forward. A nonparametric estimation method is preferred since we know little

about the functions we want to estimate. Common nonparametric regression estimators are Nadaraya-Watson (Nadaraya 1964, Watson 1964), smoothing splines (Schoenberg 1964, Reinsch 1967), and local polynomials (Stone 1977, Cleveland 1979). We choose to use the Nadaraya-Watson estimator since it is intuitive, flexible and can easily be extended to handle our data. Let  $(X_1, \Delta F_1), \dots, (X_n, \Delta F_n)$  be a set of independent and identically distributed pairs of random variables where  $X_i$  are scalar predictors and the  $\Delta F_i$  scalar responses. In regression analysis, a functional relationship between predictor and response is assumed as

$$\Delta F_i = m(X_i) + \epsilon_i \quad (6)$$

where the  $\epsilon_i$  are independent and satisfy  $E(\epsilon_i) = 0$  and  $V(\epsilon_i) = \sigma^2(X_i)$ . The goal is to estimate  $m(x_0)$ . The Nadaraya-Watson estimator is based on a local approximation of  $m(x)$  by a constant  $m(x_0)$ ; provided that  $x$  is close to  $x_0$ . The estimator of  $m(x)$  can be represented by the weighted local mean

$$\hat{m}(x_0) = \frac{\sum_{i=1}^n K\left(\frac{x_i - x_0}{h}\right) \Delta F_i}{\sum_{i=1}^n K\left(\frac{x_i - x_0}{h}\right)} \quad (7)$$

where  $h$  is the bandwidth and  $K(\cdot)$  is the kernel density which is used to weight each observation. In the above regression analysis, the functional relationship between predictor and response is one dimensional, while our observed data depend on several variables (observation time, start of settlement period and end of settlement period). We must therefore transform the observations into data that can be used by the Nadaraya-Watson estimator. The transformation is performed by introducing a variable bandwidth and organizing the observations by: Average time to delivery, observation seasonal date and delivery seasonal date.

The use of a variable bandwidth has been advocated for various reasons. Such a local bandwidth should e.g. adopt to: Local curvature of  $m$ , local variance in case of heteroscedasticity or local density of design points. Our

reason for wanting to have a variable bandwidth is to adjust for variable length of settlement period in our data sample. The idea is to have a narrow bandwidth for forward contracts with a short settlement period and a wider bandwidth for forward contracts with a longer settlement period. The variable bandwidth,  $h$ , is heuristically defined as the solution to

$$\int_{-\frac{T^e - T^s}{2}}^{+\frac{T^e - T^s}{2}} K\left(\frac{x}{h}\right) dx = g \quad (8)$$

where  $g$  is the percentage of the total weight the settlement period is given. Meaning that  $g = 0.8$  gives the observations in the settlement period a total weight of 80%. The effect this smoothing percentage is illustrated in figure 1.  $K()$  is the kernel density and is used to weight each observation. There are many types of kernels to choose from and we have chosen the standard normal probability kernel.

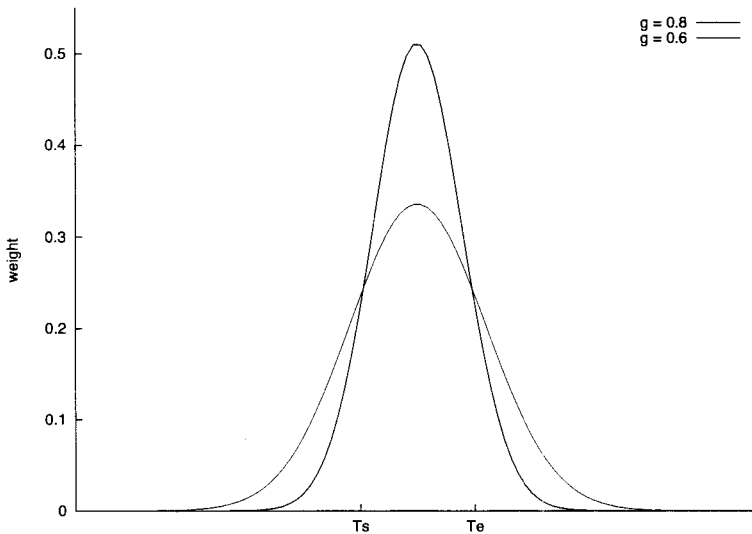


**Figure 1:** *Two weight functions with different smoothness parameters. The area under the two functions are 0.8 and 0.6. With  $T^e - T^s = 2$  the  $h$ -value for  $g = 0.8$  is 1.040 and the  $h$ -value for  $g = 0.6$  is 1.0625. Meaning that a large  $g$  implies a narrow bandwidth.*



The notation we will use for the data sample is as follows: Each observation of a forward or a future contract is defined by an observation date, a closing price, a start of settlement and an end of settlement date. Let  $i \in \{1, \dots, n\}$  denote a time index and  $t_i$  the observation date. For each observation date we can have several contracts with different settlement periods. By letting  $j$  be an index of all the different settlement periods we can write the start of settlement as  $T_j^s$  and the end of settlement as  $T_j^e$ . So the observed closing price at time  $t_i$  for a contract with the settlement period  $[T_j^s, T_j^e]$  can be represented by  $F(t_i, T_j^s, T_j^e)$ .

The second step of transforming the observation into data which can be used by the Nadaraya-Watson estimator is to organizing the observations by

- $\tau$  - average time to delivery.
- $\kappa$  - observation seasonal date.
- $\delta$  - delivery seasonal date.

Since we are working with a delivery period instead of a fixed delivery date we approximate time to maturity by *average* time to maturity defined by

$$\tau_{i,j} \equiv \frac{T_j^s + T_j^e}{2} - \frac{t_{i-1} + t_i}{2} \quad (9)$$

Observation seasonal date,  $\kappa$ , is defined as the number of days from 1. January to the observation date  $t$ . Similarly the delivery seasonal date,  $\delta$ , is defined as the number of days from 1. January to the average settlement

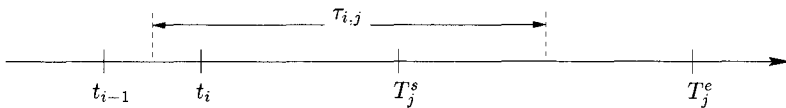


**Figure 2:** Illustration of the average time to maturity,  $\tau$ .  $t_i$  is observation date number  $i$ ,  $T_j^s$  start of settlement period for contract number  $j$  and  $T_j^e$  is the end of settlement period for contract number  $j$ .

date  $t + \tau$ . For each of the variables stated above we will estimate two versions of  $\mu_F(F_t)$ ,  $\sigma_F(F_t)$  and  $\lambda(F_t)$ . One version that depends on  $F_t$  and one that does not depend on  $F_t$  (i.e. a constant).

Using the variable bandwidth in (8) together with the Nadaraya-Watson estimator in (7) we can now estimate  $\mu_F$  and  $\sigma_F$  by the following estimators

**One dimensional version:**

$$\hat{\mu}_F(\alpha) = \frac{\sum_{i,j} K\left(\gamma_j(x_{i,j}, \alpha, g^x)\right) z_{i,j}}{\sum_{i,j} K\left(\gamma_j(x_{i,j}, \alpha, g^x)\right)} \quad (10)$$

$$\hat{\sigma}_F^2(\alpha) = \frac{\sum_{i,j} K\left(\gamma_j(x_{i,j}, \alpha, g^x)\right) \{z_{i,j} - \hat{\mu}_F(x)\}^2}{\sum_{i,j} K\left(\gamma_j(x_{i,j}, \alpha, g^x)\right)} \quad (11)$$

$$z_{i,j} = F(t_i, T_j^s, T_j^e) - F(t_{i-1}, T_j^s, T_j^e)$$

$$\gamma_j(x, \alpha, g^x) = (x - \alpha)/h(T_j^s - T_j^e, g^x)$$

**Two dimensional version:**

$$\hat{\mu}_F(\alpha, \beta) = \frac{\sum_{i,j} K\left(\gamma_j(x_{i,j}, \alpha, g^x), \gamma_j(y_{i,j}, \beta, g^y)\right) z_{i,j}}{\sum_{i,j} K\left(\gamma_j(x_{i,j}, \alpha, g^x), \gamma_j(y_{i,j}, \beta, g^y)\right)} \quad (12)$$

$$\hat{\sigma}_F^2(\alpha, \beta) = \frac{\sum_{i,j} K\left(\gamma_j(x_{i,j}, \alpha, g^x), \gamma_j(y_{i,j}, \beta, g^y)\right) \{z_{i,j} - \hat{\mu}_F(x, y)\}^2}{\sum_{i,j} K\left(\gamma_j(x_{i,j}, \alpha, g^x), \gamma_j(y_{i,j}, \beta, g^y)\right)} \quad (13)$$

$$z_{i,j} = F(t_i, T_j^s, T_j^e) - F(t_{i-1}, T_j^s, T_j^e)$$

$$\gamma_j(x, \alpha, g^x) = (x - \alpha)/h(T_j^s - T_j^e, g^x)$$

$$\gamma_j(y, \beta, g^y) = (y - \beta)/h(T_j^s - T_j^e, g^y)$$

We have data sampled at  $x_{i,j}$  and  $(x_{i,j}, y_{i,j})$  for the two dimensional case.  $\gamma$  can be interpreted as scaled observations.  $h()$  is the bandwidth and  $g^x$  and

$g^y$  are smoothness parameters.  $g^x$  determines the bandwidth with respect to the  $x$ -dimension and  $g^y$  determines the bandwidth with respect to the  $y$ -dimension.  $K()$  is the kernel density and is given by

1.  $\dim K(x) = (2\pi)^{-1/2} \exp\{-\frac{1}{2}x^2\}$
2.  $\dim K(x, y) = (2\pi)^{-1} \exp\{-\frac{1}{2}(x^2 + y^2)\}$

### 3.3 Testing the estimator

It is beyond the scope of this paper to derive the properties of the estimator we are going to use in this paper. Instead we will test the estimator on simulated data. Let the price dynamics of a forward contract,  $F$ , with an average time to maturity of  $\tau$  days be determined by

$$dF_t = \mu(\tau)dt + \sigma(\tau)dB_t, \quad F_0 = x$$

where the drift term is

$$\mu(\tau) = \begin{cases} 0 & \tau \in [0, 50] \\ -0.5(\tau - 50)/50 & \tau \in [50, 100] \\ -0.5 & \tau \in [100, 150] \\ 0.15(\tau - 150)/215 - 0.05 & \tau \in [150, 365] \end{cases}$$

and the diffusion term is

$$\sigma(\tau) = \frac{a}{\tau/7 + b} + c, \quad \tau > 0$$

$$a = 2.180$$

$$b = 4.475$$

$$c = 0.193$$

The parameters for the diffusion term is estimated from the full sample volatility function in Koekebakker and Ollmar (2003) “Forward curve dynamics in the Nordic electricity market<sup>1</sup>”.

---

<sup>1</sup>This paper is part of this thesis, and the data is visualized in figure 4 in the paper.

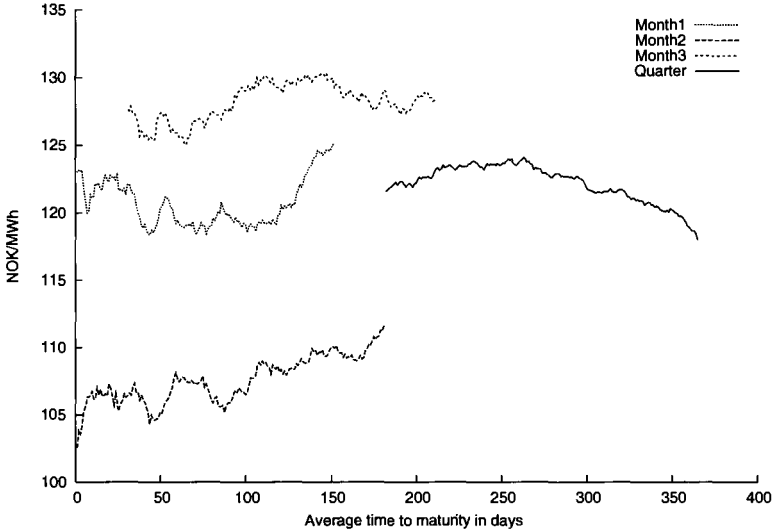


**Figure 3:** *Simulated price data for four forward contracts.*

The data used for estimation is prices from a forward with a quarter of a year settlement period. This forward is split into three monthly contracts when the average time to delivery reaches 182 days. This is visualized in figure 3. This means we simulated 365 daily prices for the three forwards with a one month settlement period. The price of the forward with a quarter of a year settlement period is calculated from the average of the three monthly forwards<sup>2</sup>.

The data sample of the simulated prices is made up of 184 daily prices from the quarterly forward, 151 daily prices from the monthly forward closest to delivery and 181 daily prices from the second closest contract to delivery and 211 daily prices for the last contract. The total data sample consist of 727 prices.

We estimate the drift and diffusion by using the estimators (10) and (11). The estimated functions together with the real functions are given in figure 4. We see that the estimated drift is close to the real drift. The splitting of the

---

<sup>2</sup>We have used a zero interest rate in this example

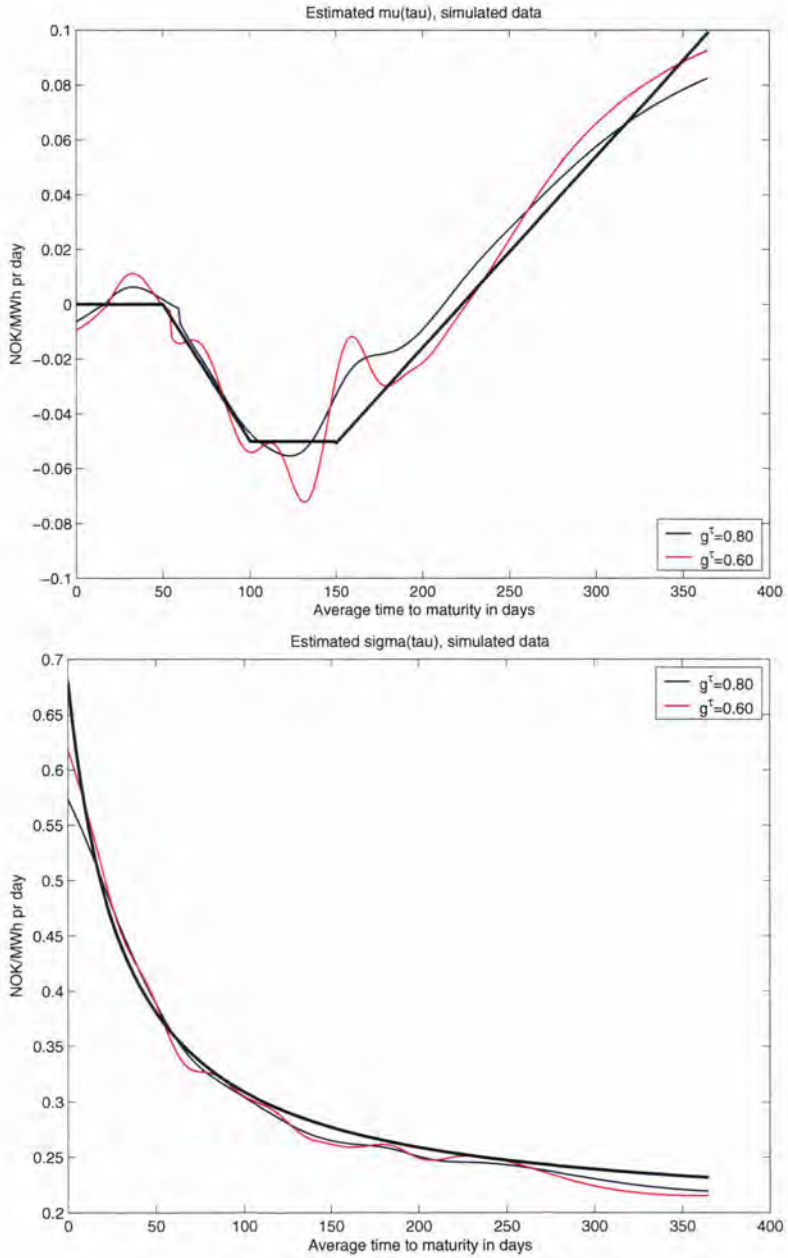


Figure 4: Estimated  $\mu(\tau)$  and  $\sigma(\tau)$  on simulated data.

quarterly forward into monthly contracts at  $\tau = 182$  did not influence the estimated function much. The estimated volatility function is very close to the real volatility function.

To get an impression of the estimators inference properties we repeated the simulation several times. The overall impression was that the estimators can be regarded as accurate and the results can be trusted.

### **3.4 Data**

To conduct our empirical study of the risk premium in an electricity market we chose to use data from one of the oldest and most liquid electricity markets in the world - Nord Pool. Nord Pool was the first international electricity market and was established in 1996. At the present time the power exchange area consists of Norway, Sweden, Finland and Denmark. Nord Pool organizes and operates the physical market Elspot and the financial market Eltermin.

Financial contracts traded on Eltermin are written on the arithmetic average of the system price at a given time interval. This time interval is termed the delivery period. The time period prior to delivery is called the trading period. Both futures and forward contracts are traded at Eltermin. The contract types differ as to how settlement is carried out during the trading period. For futures contracts, the value is calculated daily, reflecting changes in the market price of the contracts. These changes are settled financially at each participant's margin account. For forward contracts there is no cash settlement until the start of the delivery period.

The contracts with the shortest delivery periods are futures contracts. Daily futures contracts with delivery period of 24 hours are available for trading within the nearest week. Weekly futures contracts with delivery periods of 168 hours can be traded 4-8 weeks prior to delivery. Futures contracts with 4 weeks delivery period, are termed block contracts. The forward contracts have longer delivery periods. Each year is divided into three seasons: V1 - late winter (January 1- April 30), S0 - summer (May 1 - September 30) and V2 - early winter (October 1 - December 31). Seasonal

contracts are written on each of these seasonal delivery periods. In January each year, seasonal contracts on S0 and V2 the coming year and all three seasonal contracts for the next two years are available. Furthermore, yearly forward contracts are available for the next three years. In other words, the (average based) term structure goes 3 to 4 years into the future, depending on current time of year.

From Nord Pool we obtained closing prices for all contracts traded from 25. September 1995 to 27. July 2002 a total of 44 385 contracts<sup>3</sup>. Information regarding settlement periods were also obtained from Nord Pools database. To get a better understanding of the format of the dataset a short sample is reproduced in table I.

**Table I:** *Sample of the contract-data*

$i$	$j$	$t_i$	Ticker	$F_{i,j}$	$T_j^s$	$T_j^e$	$\tau_{i,j}$	$\delta_{i,j}$	$\kappa_{i,j}$
1	1	25.Sep 95	GU40-95	144.50	02.Oct 95	09.Oct 95	12.0	279.0	267
1	2	25.Sep 95	GU41-95	146.81	09.Oct 95	16.Oct 95	19.0	286.0	267
1	3	25.Sep 95	GU42-95	149.50	16.Oct 95	23.Oct 95	26.0	293.0	267
2	1	27.Sep 95	GU40-95	147.00	02.Oct 95	09.Oct 95	9.5	278.5	269
2	2	27.Sep 95	GU41-95	148.00	09.Oct 95	16.Oct 95	16.5	285.5	269
2	3	27.Sep 95	GU42-95	150.00	16.Oct 95	23.Oct 95	23.5	292.5	269
3	1	28.Sep 95	GU40-95	147.00	02.Oct 95	09.Oct 95	8.0	278.0	270
3	2	28.Sep 95	GU41-95	148.00	09.Oct 95	16.Oct 95	15.0	285.0	270
3	3	28.Sep 95	GU42-95	149.00	16.Oct 95	23.Oct 95	22.0	292.0	270

This is a sample of the contract data obtained from Nord Pool.  $i$  is the day index and  $t_i$  is the observation date.  $j$  is the period index and in this table consist of three periods i.e.  $j = 1, 2, 3$ . Ticker is the Nord Pools ticker for the observed contract. Where 'G' stands for base-load, 'U' indicates that the contract has a one week long settlement period and '40-95' tells us that the settlement period is week number 40 of year 1995. Since 25. September 1995 was a Monday  $\tau_{1,1} = "5.5 Oct - 23.5 Sep" = 12$  days.  $\kappa_{3,3} = 270$  is the number of days from 1. Jan 1995 to 28. Sep 1995, and  $\delta_{i,j}$  is  $\kappa_{i,j} + \tau_{i,j}$ .

<sup>3</sup>Some of the contracts were left out due to some minor errors in the datafiles.

## 4 Empirical results

By using the estimators given by equations 10 - 13 on the price data we have estimated several versions of  $\mu_F$ ,  $\sigma_F$  and  $\lambda$ .

### 4.1 Functions of $\tau$

The first variable we decided  $\mu_F$ ,  $\sigma_F$  and  $\lambda$  might depend on was the average time to maturity,  $\tau$ . By talking to market participants we got the impression that contracts with a maturity less than three months were mainly bought by retail companies to hedge their procurement costs. We therefore expect a negative risk premium for this period (i.e. we expect  $\hat{\mu}(\tau)$  to be negative for  $\tau \in [0, 100]$ ). There was also a common opinion among market participants that future contracts with a 3 to 36 months horizon were mainly used to take pure speculative positions or to hedge the power producers production revenue. If this is the case, we expect to find a positive risk premium (i.e. you get a positive return by owning a future contract). For contracts with more than three years to maturity liquidity issues plays an important role. Since power producers rarely hedge their long term risk, we believe this will result in a negative risk premium.

The estimated empirical functions for  $\mu_F(\tau)$ ,  $\sigma_F(\tau)$  and  $\lambda(\tau)$  are given in figure 5, 6 and 7 respectively. The first thing we observe from the estimated drift term is that it is negative and increases with time to maturity. For  $\tau = 5$  the estimated drift is -0.50 NOK/MWh, meaning that future contracts with an average time to delivery of 5 days have an expected daily price change of -0.50 NOK/MWh. The negative drift increases toward -0.1 NOK/MWh as average time to maturity increases to 100 days. The relative strong negative drift for contracts with a maturity date less than three months is consistent with the conjecture that retail companies pay a premium to hedge their procurement costs. Contracts with a maturity date from 3 months to 3 years also have a negative drift. This is not in line with our prior belief about a positive premium for future contracts with this maturity horizon. It may



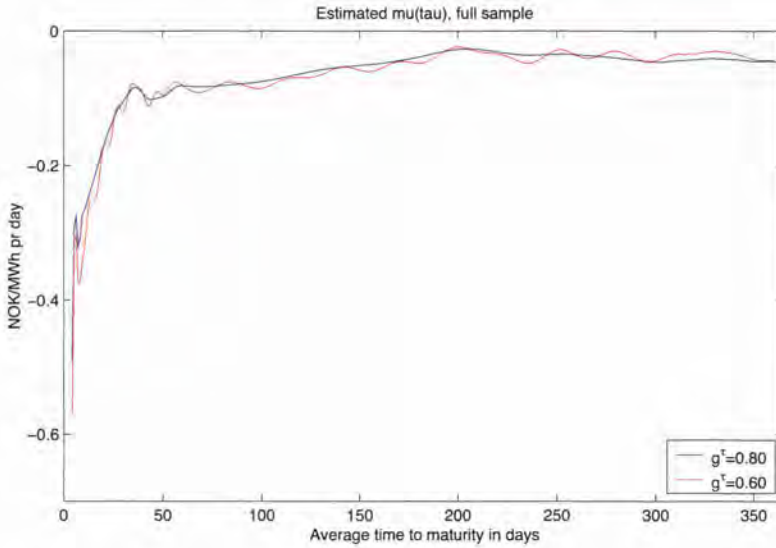


**Figure 5:** Estimated  $\mu(\tau)$  on the full sample. The figure shows conditional expected return on a future contract with an average time to maturity equal to  $\tau$ . We see that the owner of a future contract on average has a negative return. Implying a negative risk premium. The red line is calculated with a narrow bandwidth and the blue line is calculated with larger bandwidth.

be a result of many years with more than normal precipitation and thereby giving a somewhat biased estimate. It may also be due to the so-called “peso” problem<sup>4</sup>. In the Nordic electricity market the peso problem can be viewed as the possibility of a “dry year” with a huge profit for the owner of a future contract. Since this scenario is not in our historical data sample we estimate a negative risk premium despite the possibility that it may be positive. From the same figure we see that contracts with a maturity date of more than three years have a negative drift, supporting the liquidity conjecture.

If we inspect the estimated drift term in figure 5, or the risk premium in

<sup>4</sup>This term goes back to Milton Friedman in his analysis of the Mexican peso during the early 70’s. The Mexican interest rate remained significantly above the US interest rate, although the peso was pegged at 0.08 dollars per peso. Friedman argued that the interest rates reflected an expectation about a future devaluation of the peso. In August 1976, the peso was devaluated by 37.5% to a new rate of 0.05 dollar per peso, thus validating the previous interest rate differential.

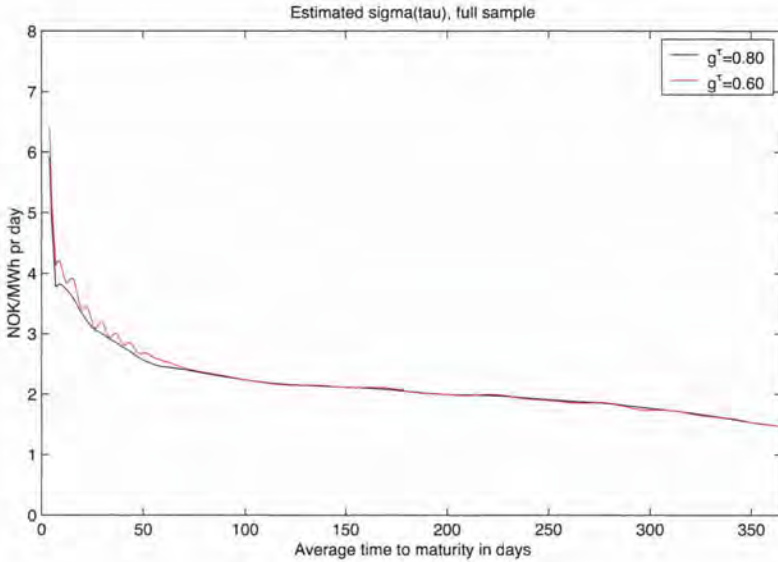
figure 7 with an average time to maturity equal to 7 and 35 days we see a short decrease. We believe this is related to  $\tau = 7$  marks where future contracts with a one day settlement period converges to futures with a one week settlement period, and  $\tau = 35$  marks approximately where future contracts with a one week settlement period converges to futures with a four week settlement period. This may indicate that the risk premium is linked to the type of future contract. This would be the case if the market participants regarded futures with  $\tau \in [0, 7)$ ,  $\tau \in [7, 35)$  and  $\tau > 35$  as three distinct markets.

Another feature of the estimated drift term is that it does not converge to zero as time to maturity decrease. This implies some sort of a “delivery arbitrage”<sup>5</sup>. Since the liquidity for future contracts with a daily settlement period is low, the negative drift term for the very short end may be a result of a liquidity premium.

The estimated volatility functions are as expected decreasing with time to maturity. This is known as the “Samuelson effect”. The empirical volatility function based on the full sample starts out at 8 NOK ( $\tau = 0$ ) and decrease rapidly for the next 100 days to approximately 2 NOK ( $\tau = 100$ ). For the next 1000 days the volatility function converges to approximately 1 NOK. We can interpret the volatility function  $\sigma(\tau)$  as the rate of change of the conditional standard deviation of  $F$ . Thus a value of 5 NOK for  $\tau = 10$  tells us the expected standard deviation for the daily price change of a future contract with approximately the next week as settlement period.

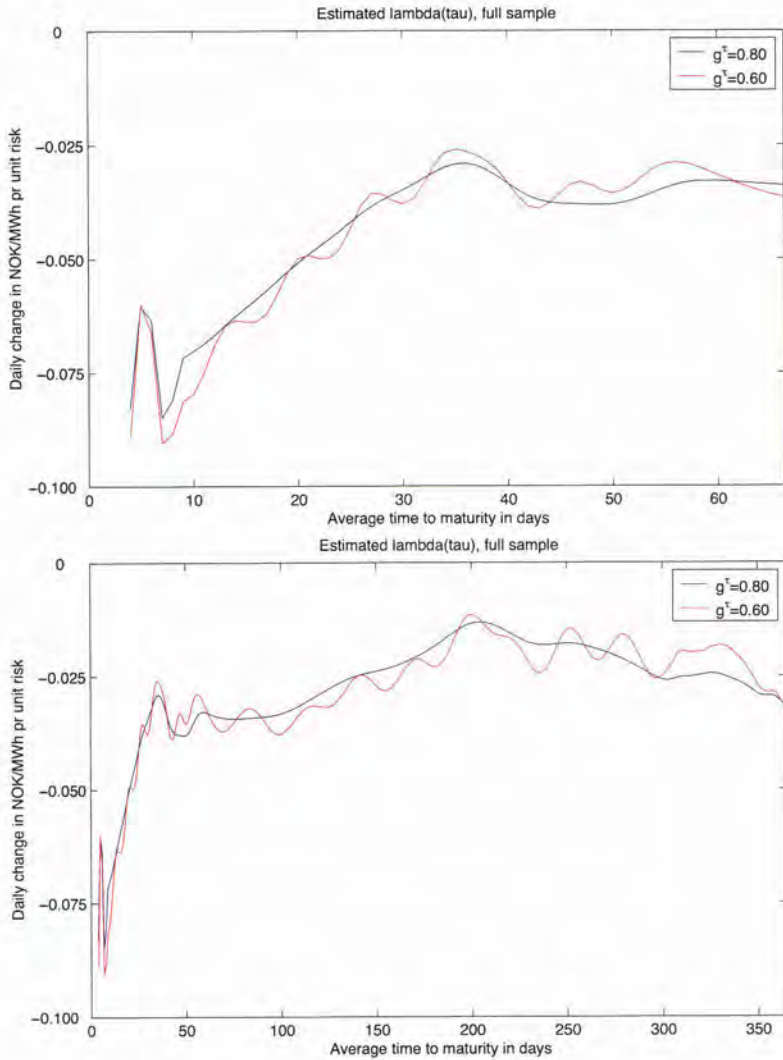
Figure 7 shows the estimated  $\lambda(\tau)$  expressed as the expected daily future price change in NOK/MWh pr unit risk. The risk premium has much of the same characteristic of the estimated drift term. It is negative and is lowest in the short end. The function starts with a value of -0.08 for  $\tau = 0$  and rapidly increases to -0.03 for  $\tau = 35$ . Then increases more slowly to its maximum of -0.02 for  $\tau = 200$ . After that it decreases, reaching -0.05 for  $\tau = 1000$ . A

<sup>5</sup>Since we can not economical store electricity this is only an arbitrage in an expectation sense.

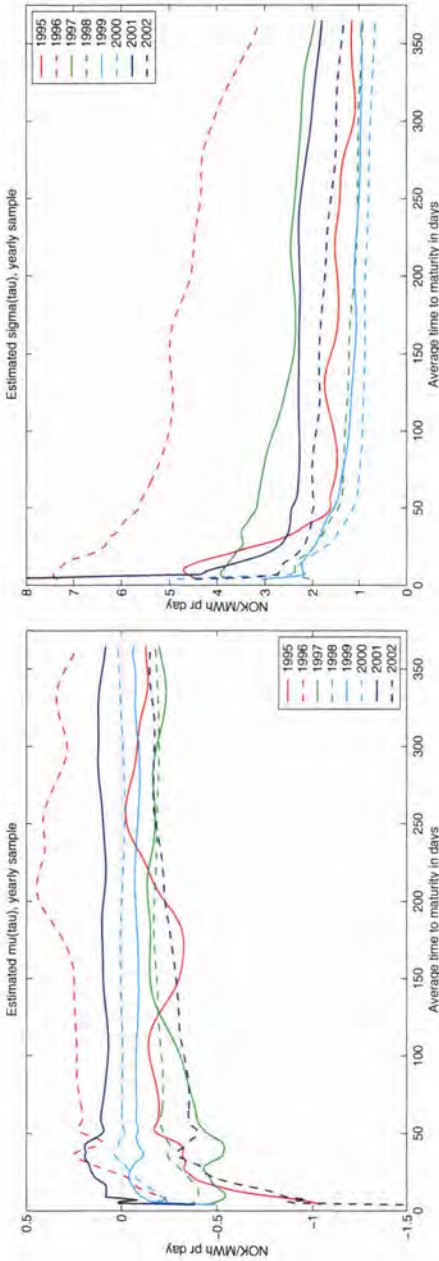


**Figure 6:** Estimated  $\sigma(\tau)$  based on the full sample. The volatility-function starts at 6-7 NOK/MWh pr day and after 100 days falls down to approximately 2 NOK/MWh. For future contracts with an average time to maturity of one to three years the volatility is approximately 1 NOK/MWh.

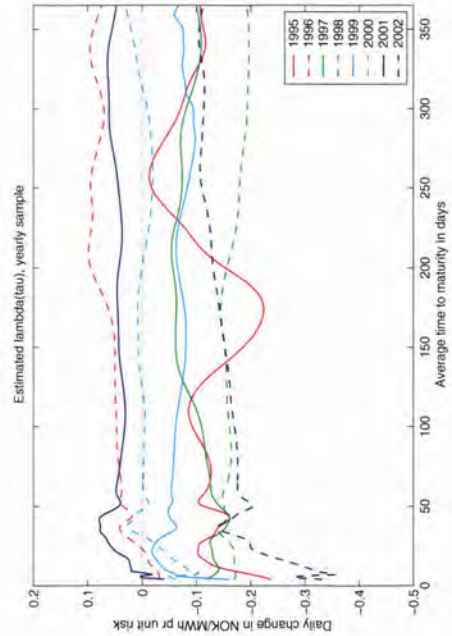
possible explanation for the low premium for contracts with a average time to maturity of 200 days is that these futures are the most heavily traded contracts and are often used to take speculative positions.



**Figure 7:** Estimated risk premium,  $\lambda(\tau)$ , based on the full sample. The risk premium is defined as the conditional expected return pr unit risk,  $\mu(\tau)/\sigma(\tau)$ . We see a top at  $\tau = 35$  days. This is approximately the time when block-contracts are split into weekly contracts. Lambda with an average time to maturity with less than 10 days are estimated on futures contracts with a one day settlement period. These contracts have a low liquidity and this may explain the peak for  $\tau = 5$ . The highest value,  $-0.02$  for the risk premium is for an average time to delivery of 200 days.



**Figure 8:** Estimated  $\mu$ ,  $\sigma$  and  $\lambda$  (yearly sample). In the top-left figure we have plotted the estimated conditional expected return for each of the years in our sample. In the top-right figure we have plotted the estimated volatility function for each year, and in the bottom-left figure the estimated risk premium is plotted. The figures varies from each year. This may be due to a long term effect such as the hydrological balance.



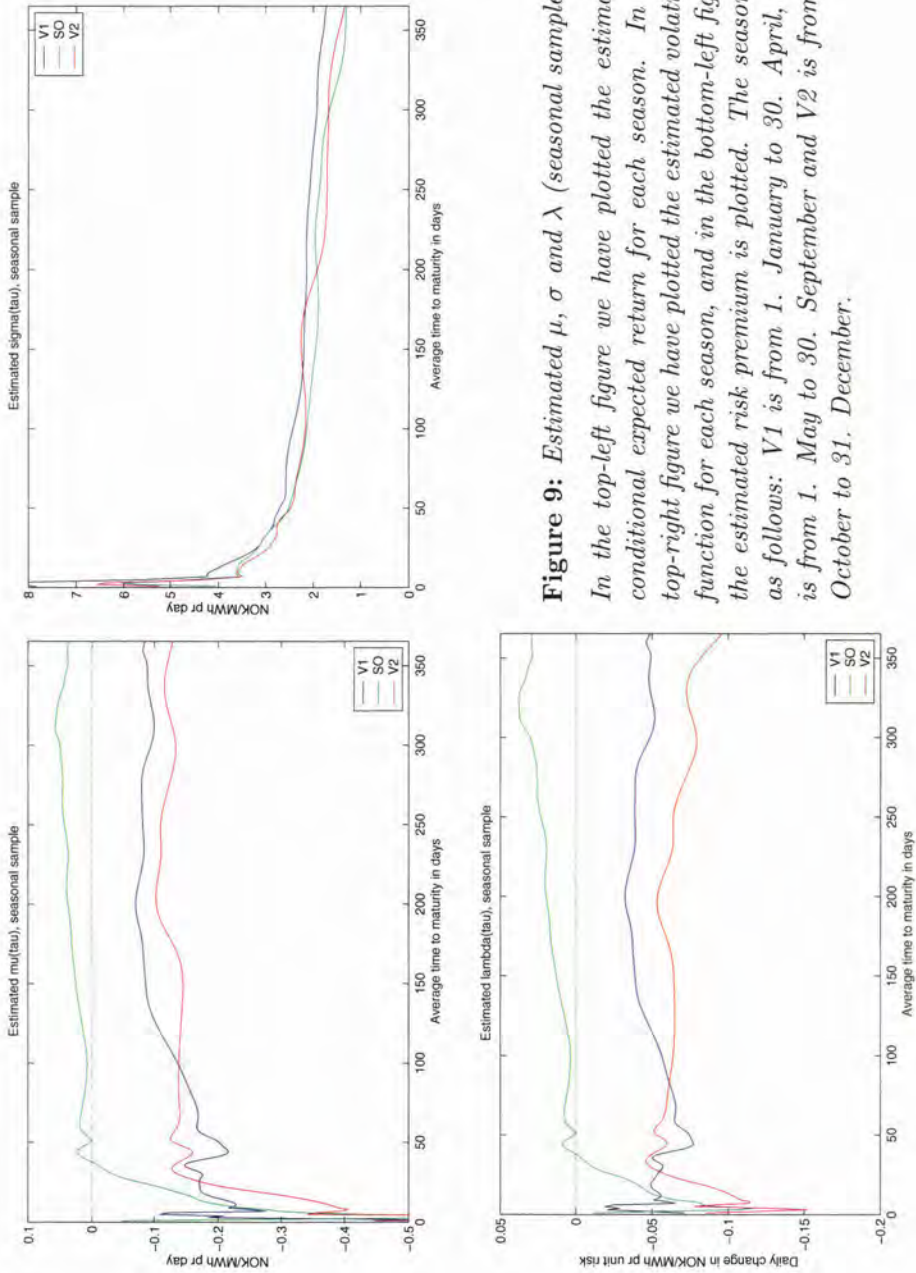


**Figure 9:** Estimated  $\mu$ ,  $\sigma$  and  $\lambda$  (seasonal sample).

In the top-left figure we have plotted the estimated conditional expected return for each season. In the top-right figure we have plotted the estimated volatility function for each season, and in the bottom-left figure the estimated risk premium is plotted. The season is as follows: V1 is from 1. January to 30. April, SO is from 1. May to 30. September and V2 is from 1. October to 31. December.

## 4.2 Functions of $\tau$ and $F$

In this section we assume that  $\mu_F$ ,  $\sigma_F$  and  $\lambda$  are functions of  $\tau$  and  $F$ . To estimate the two-dimensional functions we use (12) - (13). The results are given in figure 10 to 12. To visualize the functions we have plotted the domain of its input variables and represented the values of the functions by color. Red colors represents high values and blue colors represents lower values. To emphasize where the functions are zero we have marked the places with a black line. Further we have masked parts of the figures. The masked parts are areas with few data observations and therefore contains less significant estimates.

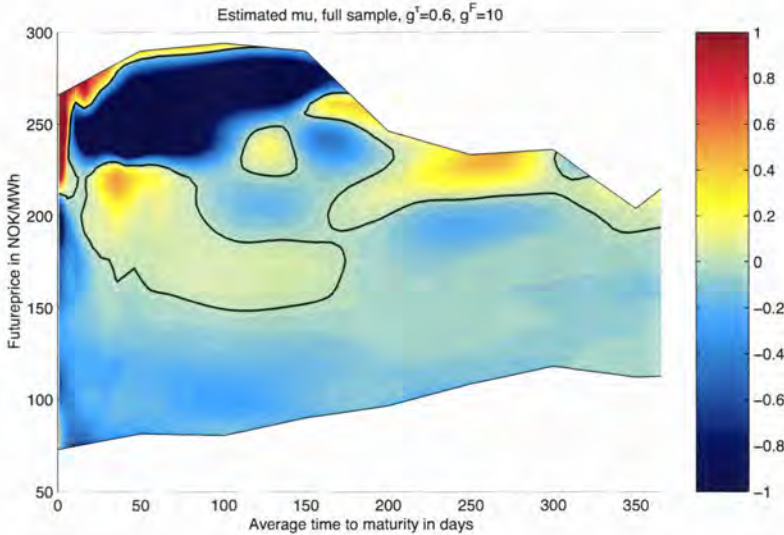


**Figure 10:** Estimated  $\mu(\tau, F)$  based on full sample. The value of the estimated drift is given by the color of the figure. Red colors indicates positive values and blue colors indicates negative values. The black line indicates a zero drift. From the figure we see a mean reverting pattern around the price level  $220 + / - 50$  NOK/MWh level.

From the estimated drift,  $\hat{\mu}(\tau, F)$ , visualized in figure 10, we see signs of mean reversion. The mean reversion show up in the figure as blue values in the area  $(\tau = 75, F = 250)$  and red / yellow values in the area  $(\tau = 75, F =$

175). Since there are few observations of futures with a price of more than 250 and an average time to maturity of more than 200 days, we can not tell if the mean reversion exists for the more long term contracts. However we see that the futures price has a negative drift if the price gets below 150 NOK/MWh and a positive drift if the price gets above 275 NOK/MWh. This indicates that the future price is mean reverting around the price level 220 +/- 50 NOK/MWh, and has a momentum around this band.

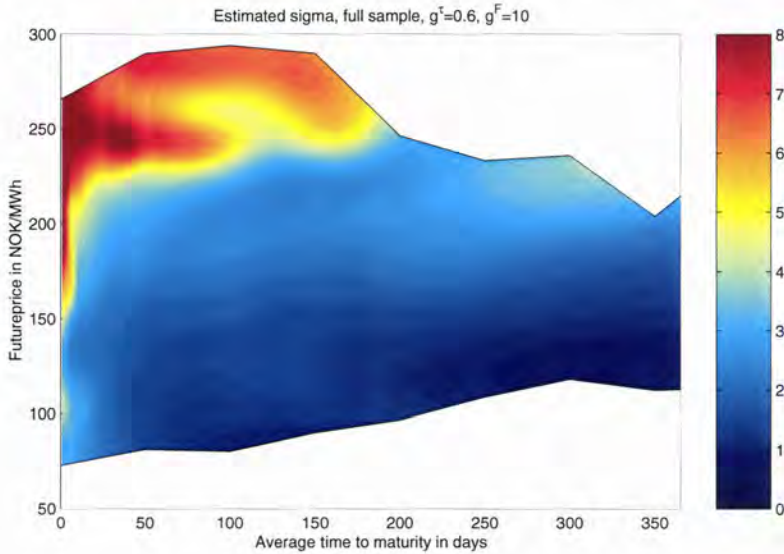


**Figure 11:** *Estimated  $\sigma(\tau, F)$  based on full sample. From the figure we see a that the volatility increases with the price of the future.*

The estimated diffusion in figure 11 shows a clear connection between the future price and the volatility. As the future price increase so does the volatility. This is consistent with a geometric-like diffusion process. For futures with an average time to maturity of more than 20 days the volatility is more sharply falling as the future price decreases.

The estimated risk premium  $\hat{\lambda}(\tau, F)$ , in figure 12, shows both the mean reversion pattern of the drift term and the geometric properties of the diffusion term.

By observing the spot price dynamics and the futures curve we see a clear



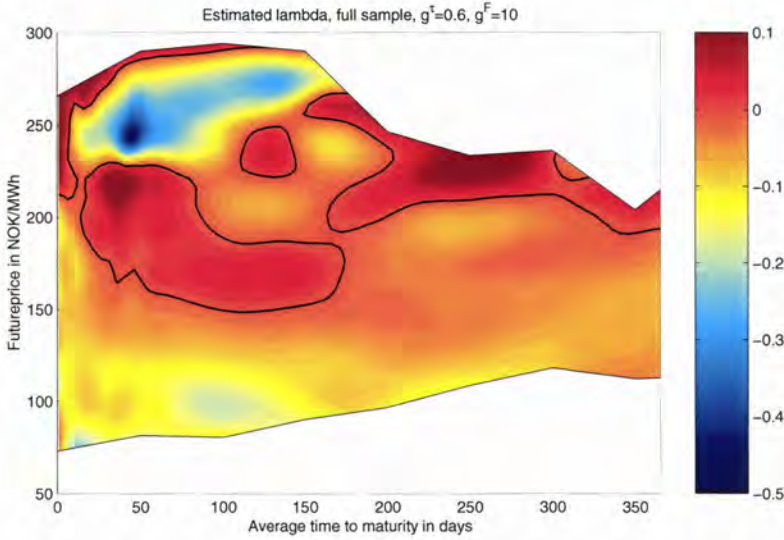


**Figure 12:** *Estimated  $\lambda(\tau, F)$  based on full sample. The risk premium is defined as the conditional expected return pr unit risk. We see that the mean reversion pattern in the estimated return is present in the risk premium.*

seasonal pattern. This pattern is a result of a higher demand for electricity in the winter than in the summer. Since the seasonal variations can be considerable, we divide our future prices into six samples:

- 1 Futures observed in the V1-period (1. January - 30. April).
- 2 Futures observed in the SO-period (1. May - 30. September).
- 3 Futures observed in the V2-period (1. October - 31. December).
- 4 Futures delivered in the V1-period (1. January - 30. April).
- 5 Futures delivered in the SO-period (1. May - 30. September).
- 6 Futures delivered in the V2-period (1. October - 31. December).

The estimated functions  $\hat{\mu}_F(\tau, F)$ ,  $\hat{\sigma}_F(\tau, F)$  and  $\hat{\lambda}(\tau, F)$  for the six samples are given in figure 15 to 20 starting on page 167 in the Appendix.

For sample 2, 3 and 4 we see the same mean reversion patterns for  $\hat{\mu}_F(\tau, F)$  as we found for the full sample estimates. For the other samples the reversion pattern is not so clear. Although it is difficult to see any clear seasonal patterns in the functions, we note that the functions indeed have seasonal variations. Dividing the data sample into several smaller seasonal samples is a crude way of examining seasonal patterns. A better way of examining the seasonal patterns is to organize the observation according to seasonal observation date,  $\kappa$ , or seasonal delivery date,  $\delta$ , and use a two dimensional estimator.

### **4.3 Functions of $\tau$ and $\delta$**

To see if the seasonal delivery date,  $\delta$ , influence the drift, diffusion or the risk premium we estimate the functions using the two dimensional Nadaraya-Watson estimator. The results are given in figure 13. Surprisingly all three figures show clear signs of diagonal stripes. Since we have time to maturity on one axis and seasonal delivery date on the other, the diagonal patterns represent something that is specific to the seasonal observation date,  $\kappa$ .

### **4.4 Functions of $\tau$ and $\kappa$**

To better understand the diagonal patterns of the previous estimation, we again use the two dimensional Nadaraya-Watson estimator to estimate the functions of average time to delivery and seasonal observation time. Results are given in figure 14. Diagonal patterns are now horizontal patterns and suggest that expected return, volatility and risk premium all have seasonal patterns.

The estimated drift term,  $\hat{\mu}_F(\tau, \kappa)$ , is positive in March, May, September and medio December. In all other periods it is negative. We also note that the sign of the drift is nearly independent of the average time to maturity. The most negative areas are in January, February, medio June to medio July and October, for forwards with less than 50 days to delivery.

Seasonal patterns are also present in the estimated volatility function.

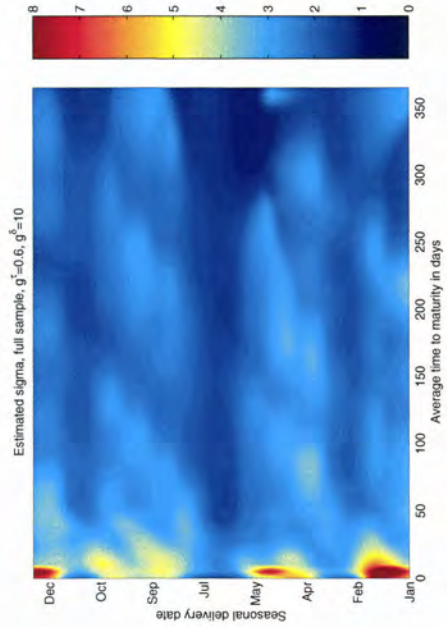
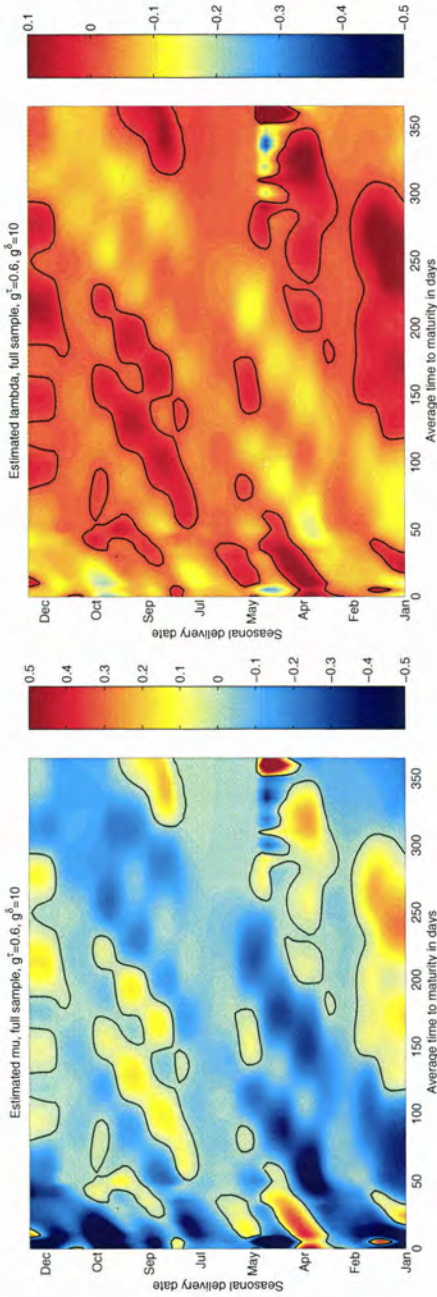


**Figure 13:** Estimated  $\mu(\tau, \delta)$ ,  $\sigma(\tau, \delta)$  and  $\lambda(\tau, \delta)$ .  $\tau$  is the average time to maturity and  $\delta$  is the seasonal delivery date. We see diagonal stripes on all figures. This indicates that we have patterns that depends on the seasonal observation date.

We see that contracts with less than 30 days to delivery traded in January, February, May and December has the highest volatility. The seasonal patterns of the volatility does not coincide with the seasonal patterns of the drift term. From figure 14 we see a high volatility for contracts with an average time to maturity exceeding 50 days and a delivery date in January, March, June, August or October.

From the figure of the risk premium we see that buying a forward in March, May and September gives a high conditional expected return pr unit risk. Equivalent selling a forward in February or a forward with less than 50 days to delivery in June-July and October will give a high expected return pr unit risk.

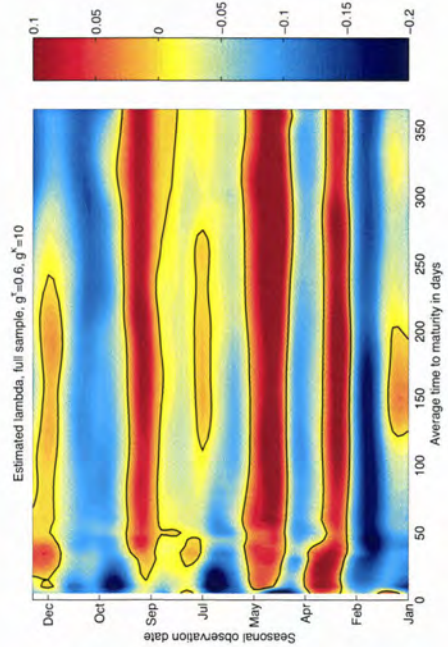
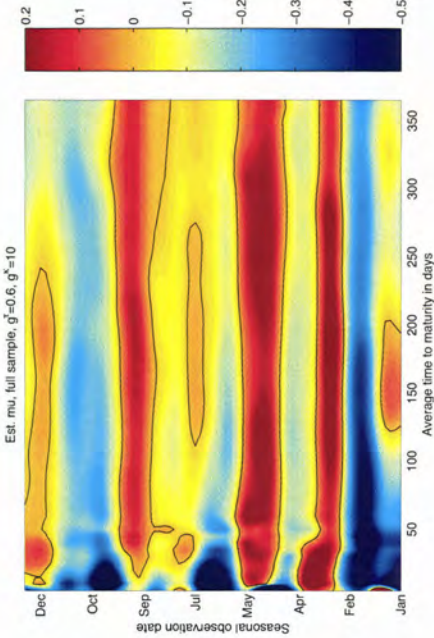
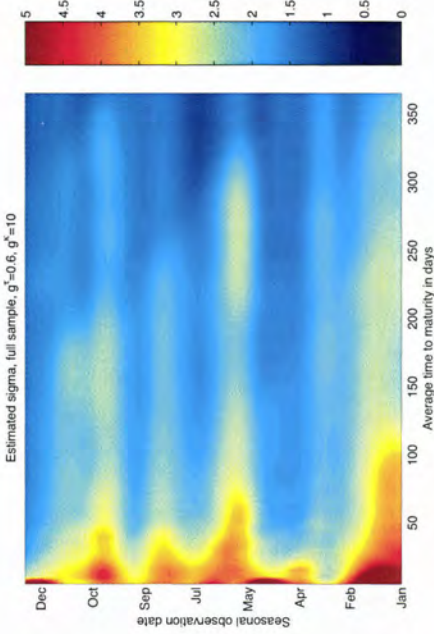


**Figure 14:** Estimated  $\mu(\tau, \kappa)$ ,  $\sigma(\tau, \kappa)$  and  $\lambda(\tau, \kappa)$ .

$\tau$  is the average time to maturity and  $\kappa$  is the seasonal observation date. The patterns are now horizontal, indicating that the patterns are independent of the settlement date.

## 5 Concluding remarks

We have in this paper conducted an empirical analysis of the risk premium in a power market. In context of our model of an electricity market the risk premium is defined as the conditional expected forward price changes per unit risk. The discretized version of the risk premium was estimated by a Nadaraya-Watson estimator, obtaining a nonparametric estimate. We used a variable bandwidth to compensate for varying settlement period lengths in our data. The bandwidth function was heuristically defined, but as the simulation example shows, it seems to handle different lengths of settlement periods good. By organizing the data sample with respect to  $\tau$ ,  $\delta$ ,  $\kappa$  and  $F$  we estimated several versions of the risk premium. Our main findings were:

- Negative risk premium for all maturity dates (i.e. a contango market)
- Increasing volatility with increasing future price
- Expected return is mean reverting with respect to future price in the price range 170 NOK/MWh to 270 NOK/MWh. Outside this range the price is driven by some sort of momentum process.
- Clear seasonal patterns. The time of the year the forward is traded has a major impact on the expected return, volatility and risk premium.

We believe that the complex nature of the risk premium in the Nordic electricity market is related to the large degree of hydro-electric power production. Especially the seasonal patterns and the mean reversion properties can be linked to hydrological phenomena. Although many of our findings coincide with statements from practitioners, we can not be certain that our findings are not influenced by the estimation method. Further research should therefore focus on the estimators small and large sample properties. It would also be interesting to see if the results are changed if we extend our datasample to include the high price period that started autumn 2002.

This paper gives new insights of the forward price dynamics in the Nordic power market. Knowing the drift, volatility and thereby the risk premium,

more precisely is helpful in financial engineering work. We also believe many of the results will help producers and consumers in their hedging decisions - at least it will guide the traders toward the forward contracts with the highest return / risk ration.

## References

- [1] Cox, J. C., Ingersoll, J. E. and S. A. Ross (1981), "The relation between forward prices and futures prices", *Journal of Financial Economics*, vol. 9, pp. 321-346.
- [2] Duffie D., (1996), "Dynamic Asset Pricing Theory", *Princeton University Press*, second edition.
- [3] Kaldor, N., (1939), "Speculation and economic stability", *Review of Economic Studies*, vol. 7, pp. 1-7.
- [4] Koekebakker, S. and Ollmar, F. (2003), "Forward curve dynamics in the Nordic electricity market", Soon to be published in *Managerial Finance*.
- [5] Nadaraya, E. A., (1964), "On estimating regression", *Theory Probab. Appl.*, vol. 9, pp. 141-142.
- [6] Reinsch, C. H., (1967), "Smoothing by spline functions", *Numer. Math.*, vol. 10, pp. 177-183.
- [7] Schoenberg, I. J., (1964), "Spline functions and the problem of graduation", *Proc. Nat. Acad. Sci. USA*, vol. 52, pp. 947-950.
- [8] Silverman, B. W., (1986), "Density Estimation", *Monographs on Statistics and Applied Probability*, vol. 26.
- [9] Stanton, R., (1997), "A nonparametric model of term structure dynamics and the market price of interest risk", *Journal of Finance*, vol. 52-5, pp. 1973-2002.
- [10] Telser, (1958), "Futures trading and the storage of cotton and wheat", *Journal of Political Economy*, vol. 66, pp. 233-244.
- [11] Wand, M. P. and Jones, M. C., (1995), "Kernel Smoothing", *Monographs on Statistics and Applied Probability*. vol. 60.



- [12] Watson, G. S., (1964), "Smooth regression analysis", *Sankhyā Ser. A*, vol. 26, pp. 359-372.
- [13] Working, H., (1948), "Theory of the inverse carrying charge in futures markets", *Journal of Farm Economics*, vol. 30, pp. 1-28.
- [14] Working, H., (1949), "Theory of the price of storage", *American Economic Review*, vol. 39, pp. 1254-1262.

# A Appendix

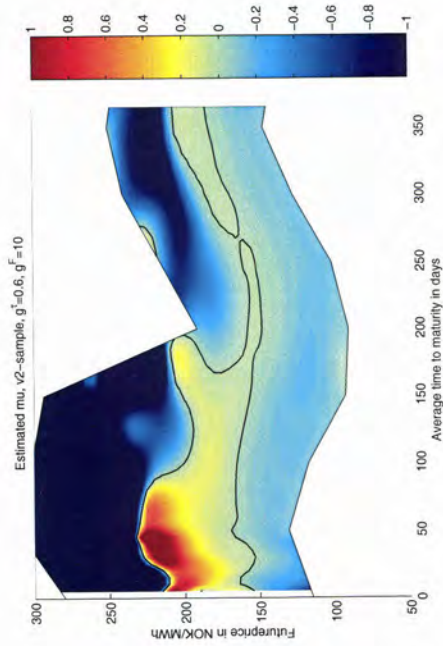
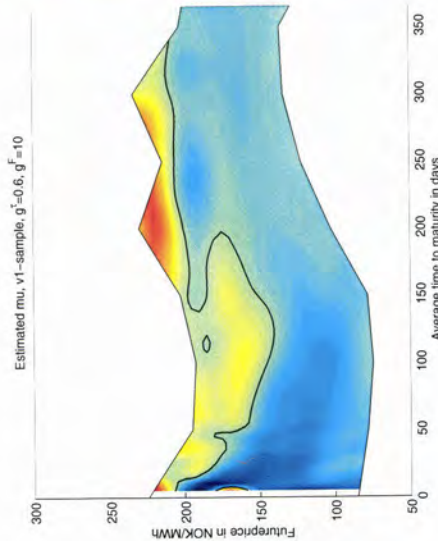
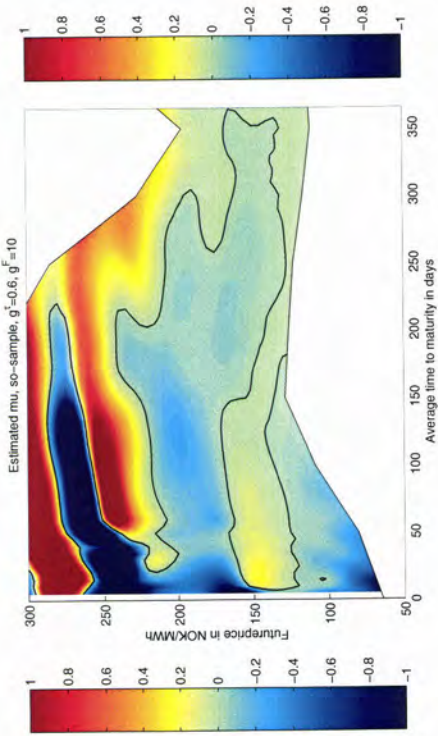


**Figure 15:** Estimated  $\mu(\tau, F)$  (seasonal sample).  
 In this figure we have plotted  $\mu(\tau, F)$  for the three seasons: V1 (from 1. January to 30. April), SO (1. May to 30. September) and V2 (1. October to 31. December). Mean reversion can be seen in the top-right and in the bottom-left figures.

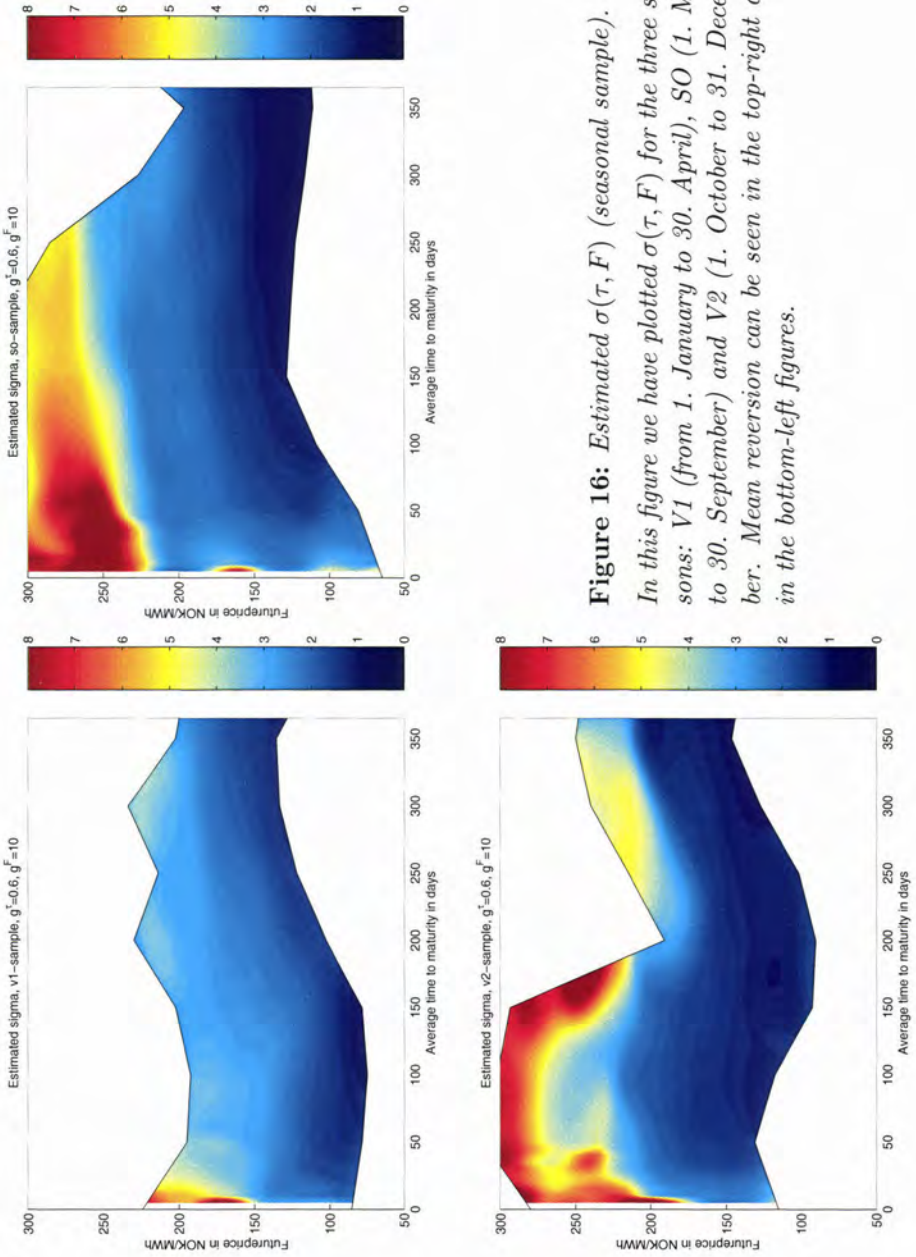


**Figure 16:** Estimated  $\sigma(\tau, F)$  (seasonal sample).  
 In this figure we have plotted  $\sigma(\tau, F)$  for the three seasons: V1 (from 1. January to 30. April), SO (1. May to 30. September) and V2 (1. October to 31. December). Mean reversion can be seen in the top-right and in the bottom-left figures.

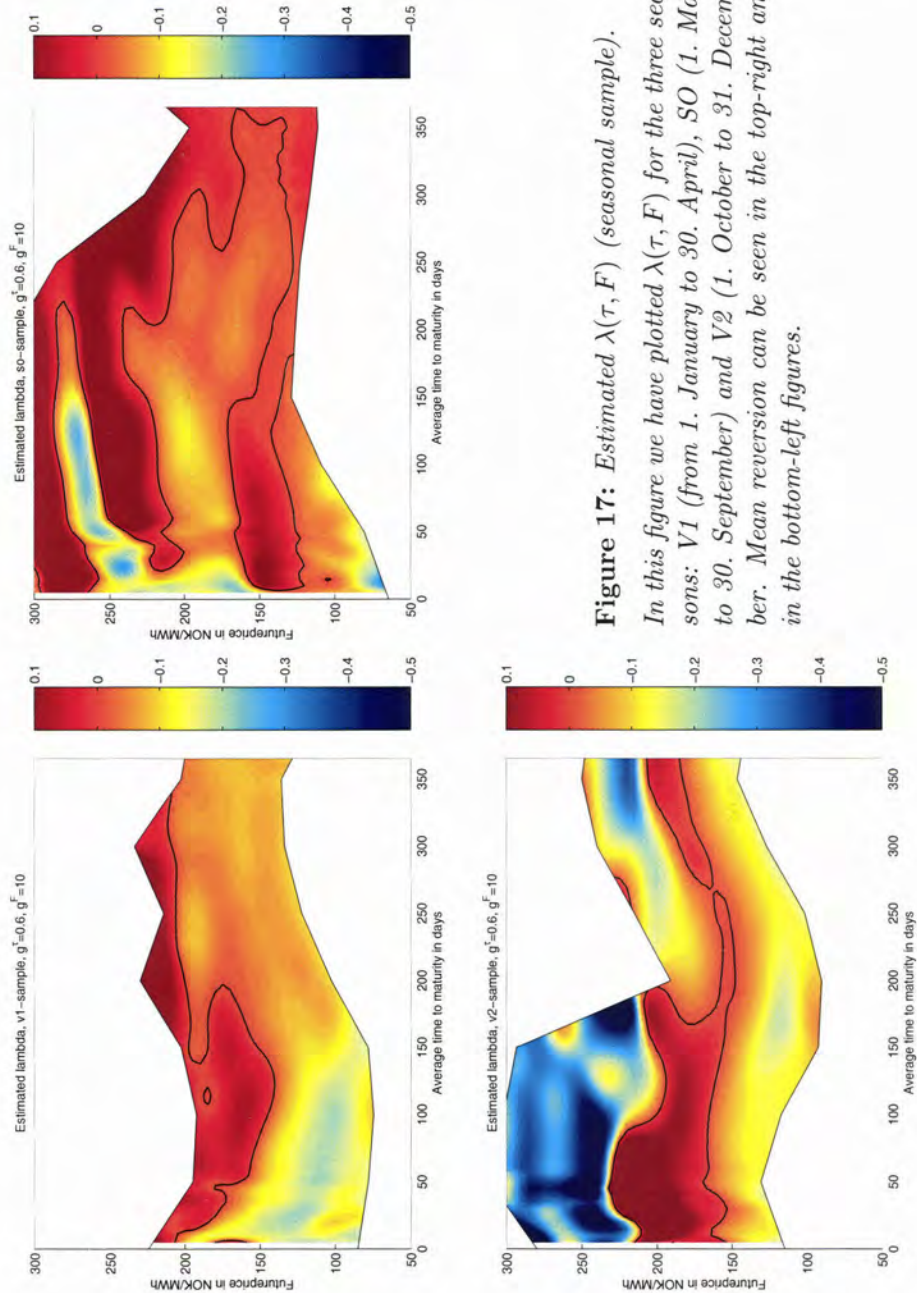


**Figure 17:** Estimated  $\lambda(\tau, F)$  (seasonal sample).  
 In this figure we have plotted  $\lambda(\tau, F)$  for the three seasons: V1 (from 1. January to 30. April), SO (1. May to 30. September) and V2 (1. October to 31. December). Mean reversion can be seen in the top-right and in the bottom-left figures.

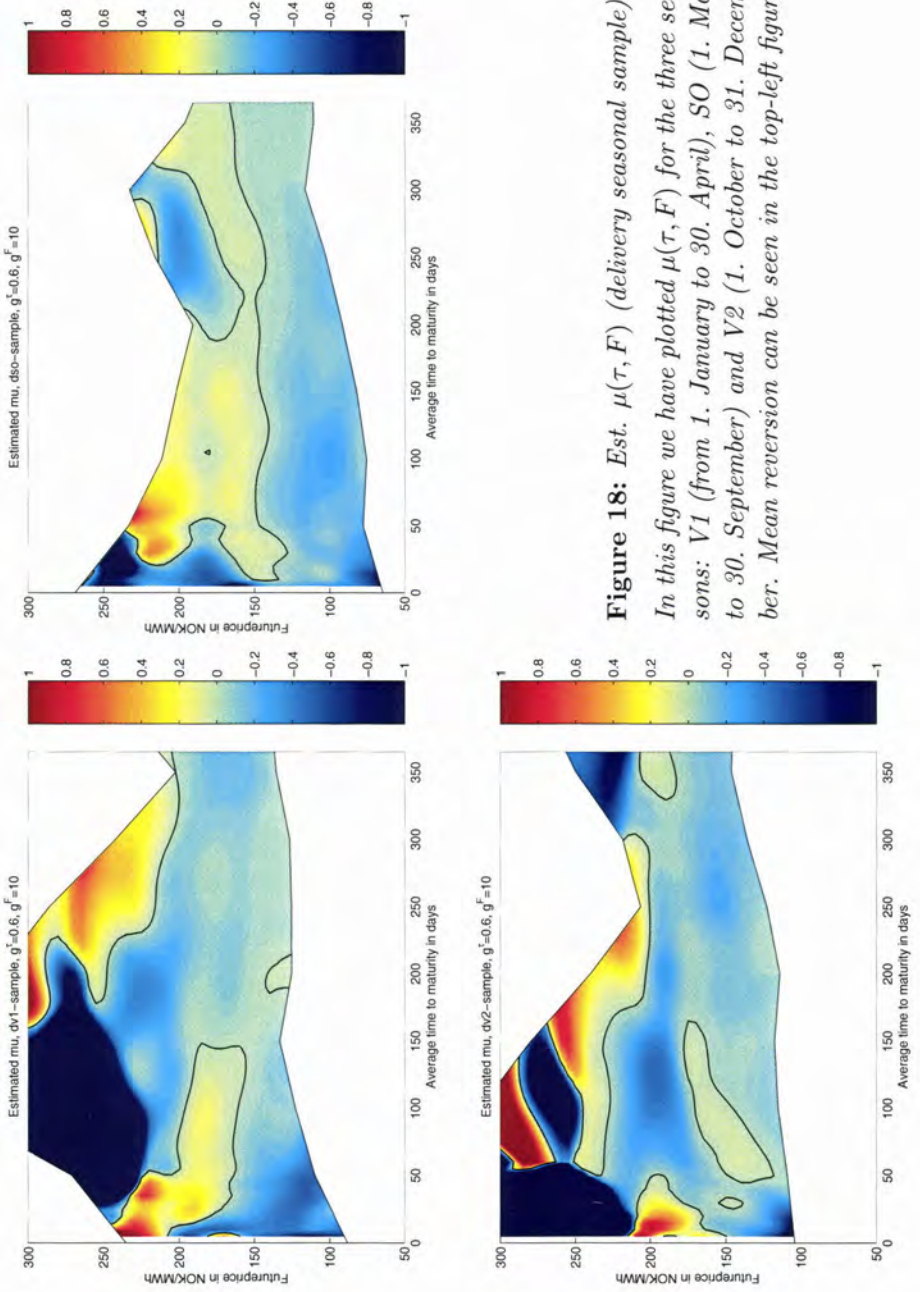


**Figure 18:** Est.  $\mu(\tau, F)$  (delivery seasonal sample).  
 In this figure we have plotted  $\mu(\tau, F)$  for the three seasons: V1 (from 1. January to 30. April), SO (1. May to 30. September) and V2 (1. October to 31. December). Mean reversion can be seen in the top-left figure.

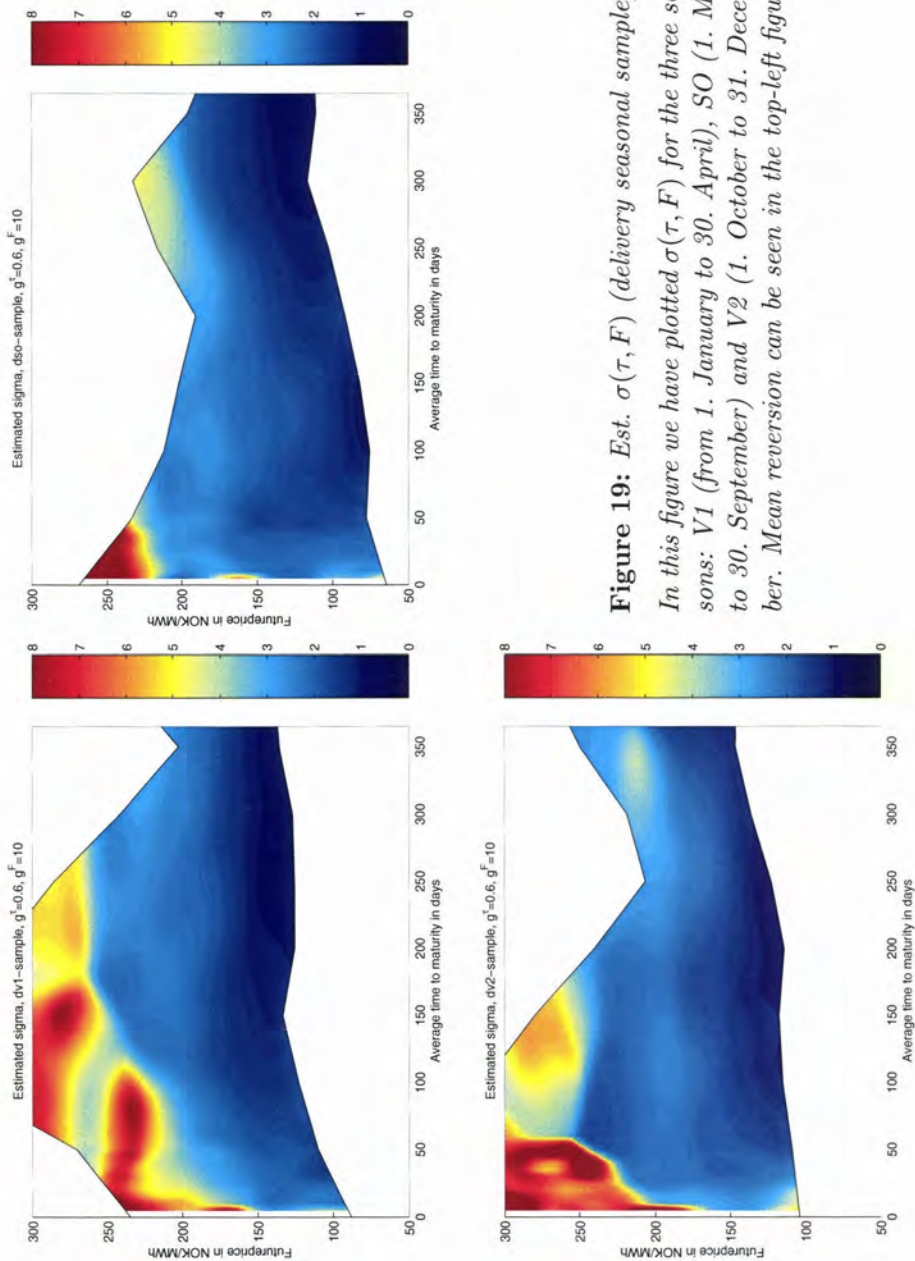


**Figure 19:** Est.  $\sigma(\tau, F)$  (delivery seasonal sample).  
 In this figure we have plotted  $\sigma(\tau, F)$  for the three seasons: V1 (from 1. January to 30. April), SO (1. May to 30. September) and V2 (1. October to 31. December). Mean reversion can be seen in the top-left figure.

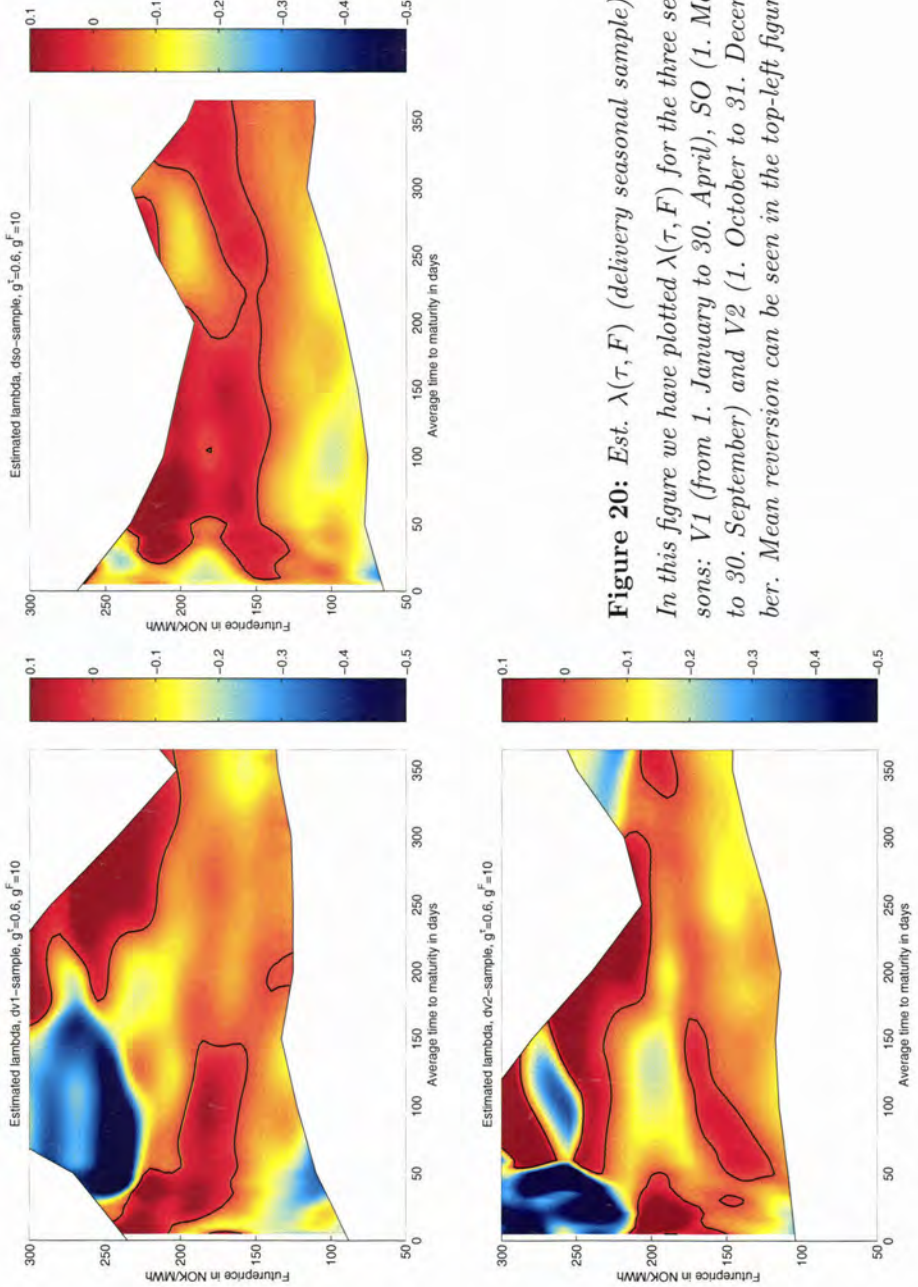


**Figure 20:** Est.  $\lambda(\tau, F)$  (delivery seasonal sample).  
 In this figure we have plotted  $\lambda(\tau, F)$  for the three seasons: V1 (from 1. January to 30. April), SO (1. May to 30. September) and V2 (1. October to 31. December). Mean reversion can be seen in the top-left figure.